Durham E-Theses

The role of phosphorylation of Ire1 in its activation loop in regulation of its RNase activity

ARMSTRONG, MICHAEL,CRAIG

Masters by Research (M.Res) Thesis

Durham University, Department of Biosciences, Durham DH1 3LE, United Kingdom.

The role of phosphorylation of Ire1 in its activation loop in regulation of its RNase activity

Student: Mr Michael C. Armstrong
Supervisor: Dr Martin Schröder

Wednesday 21st December 2016

1.0 **Abstract**

Ire1 is a protein kinase endoribonuclease (RNase) and a resident protein of the endoplasmic reticulum (ER) of *Saccharomyces cerevisiae* and a homologue to the Ire1α ER protein found in humans. Ire1 activates splicing of the mRNA of the unfolded protein response (UPR) gene *HAC1*. This splicing is a response to the accumulation of unfolded or misfolded proteins in the ER lumen. Splicing of *HAC1* mRNA results in the translation of the Hac1 protein Hac1[i] which contains a bZIP transcription factor which promotes the expression of UPR-associated genes which ultimately leads to the alleviation of ER stress. The activation of Ire1 was previously thought to be dependent on phosphorylation within the Ire1 activation loop (a-loop). Here it is shown that in "phospho-dead" mutants, some level of splicing and UPR-activity is retained and that the aspartic acid residue (D836) within the a-loop allows for this retention. Furthermore, it was confirmed that mutation of D836 to alanine completely eliminates *HAC1* mRNA splicing. This work suggests that phosphorylation of the a-loop is critical but not essential to RNase activation and the UPR.

Table of contents

2.0 List of figures and tables

2.1 Figures

3.0 Commonly used abbreviations

a-loop	Activation loop
ADP	Adenosine diphosphate
ATP	Adenosine triphosphate
bZIP	Basic leucine zipper
DNA	Deoxyribonucleic acid
DTT	Dithiothreitol / 1,4-dithio-DL-threitol
ER	Endoplasmic reticulum
ERAD	Endoplasmic reticulum associated degradation
Hac1[i]	Hac1 protein
HLE	Helix response element
IF1[c]/ IF2[c]/ IF3[c]	Interface 1 / Interface 2 / Interface 3
Ire1	Inositol-requiring 1
NBP	Nucleotide binding pocket
mRNA	Messenger RNA
RNA	Ribonucleic acid
Tn	Tunicamycin
UPR	Unfolded protein response
UPRE	Unfolded protein response element
WT	Wild type

4.0 **Acknowledgments**

I would like to thank Dr. Martin Schröder for his support and guidance throughout this Masters project. Additionally, I would like to thank Dr. Max Mushens-Brown for his assistance and advice throughout my time at Durham and the other Masters students in the laboratory, Donata Janickaite and Joseph Nelson, for making my time at Durham an enjoyable one.

I would like to acknowledge the support of all the School of Biosciences staff at Durham University. In particular, Miss Joanne Robson and Dr. Tim Hawkins in Bioimaging/Advanced Light Microscopy for their guidance in the use of equipment used to achieve the research goals of this project. Additionally, I would like to thank Dr. Sergej Šesták for the creation and providing of the plasmids used in this work.

Finally, I would like to thank my family and friends for their support and belief in completing this Masters projects and supporting me throughout my academic career.

5.0 **Statement of copyright**

The copyright of this thesis rests with the author. No quotation from it should be published without the author's prior written consent and information derived from it should be acknowledged.

6.0 **Introduction**

6.1 *The unfolded protein response*

Resident molecular chaperones and protein foldases in the endoplasmic reticulum (ER) prevent the aggregation and accumulation of unfolded and misfolded proteins (Gething and Sambrook, 1992; Stevens and Argon, 1999; Credle et al., 2005). Under normal cellular conditions the rate of protein folding and the levels of secretory protein synthesis is balanced (Joshi *et al.*, 2015). When ER stress is induced by the accumulation of unfolded or misfolded proteins there must be a response from the cell allowing for tolerance of this stress (Walter and Ron, 2011). This response must facilitate the appropriate processing of unfolded proteins to maintain cell survival (Cox et al., 1993). Accumulation of proteins can occur as a result of the inefficient or slow protein folding capacity of the ER (Smith et al., 2011) and the resulting ER stress is a critical aspect in a number of diseases including type II diabetes (Özcan et al., 2004) and neurodegenerative diseases (Nishitoh et al., 2002). The unfolded protein response (UPR) is an intracellular signalling pathway which allows tolerance and adaptation to the ER stress caused by unfolded protein accumulation in the ER (Tanaka et al., 2015). Any proteins that fail to fold, or are incorrectly folded and accumulate in the ER are targeted for degradation by endoplasmic reticulum associated degradation (ERAD) (Gardner *et al.*, 2013). This degradation is facilitated by poly-ubiquitylation of the protein in the cytosol, following the removal of the protein from the ER lumen by molecular chaperones (Smith *et al.*, 2011). In the event of ER stress, the UPR allows the cell to respond by inducing the expression of genes involved in transport of accumulated unfolded or misfolded proteins out of the ER for degradation permitting ER stress tolerance (Snapp, 2012). Specific gene expression is facilitated by the splicing of *HAC1* mRNA. The mature (spliced) mRNA is translated to produce the Hac1 protein (Hac1[i]) which acts a transcription factor (Travers et al., 2000) by binding to the unfolded protein response element (UPRE) within the promoter of UPR-associated genes allowing for specific induction of UPR genes (Mori et al., 1992).

The UPR in *S. cerevisiae* is initiated by Ire1 (Wiseman *et al.*, 2010). Ire1 is a type I transmembrane protein, possessing ER lumenal and cytosolic domains. Within the cytosolic domain there is a serine/threonine-specific protein kinase element (Shamu and Walter, 1996) and an endoribonuclease (RNase) element (Mori, 2000). These elements are critical in the activation of the UPR. Fig. 1 below shows the structure of Ire1 across the ER membrane and the elements of both the lumenal and the cytosolic domains.
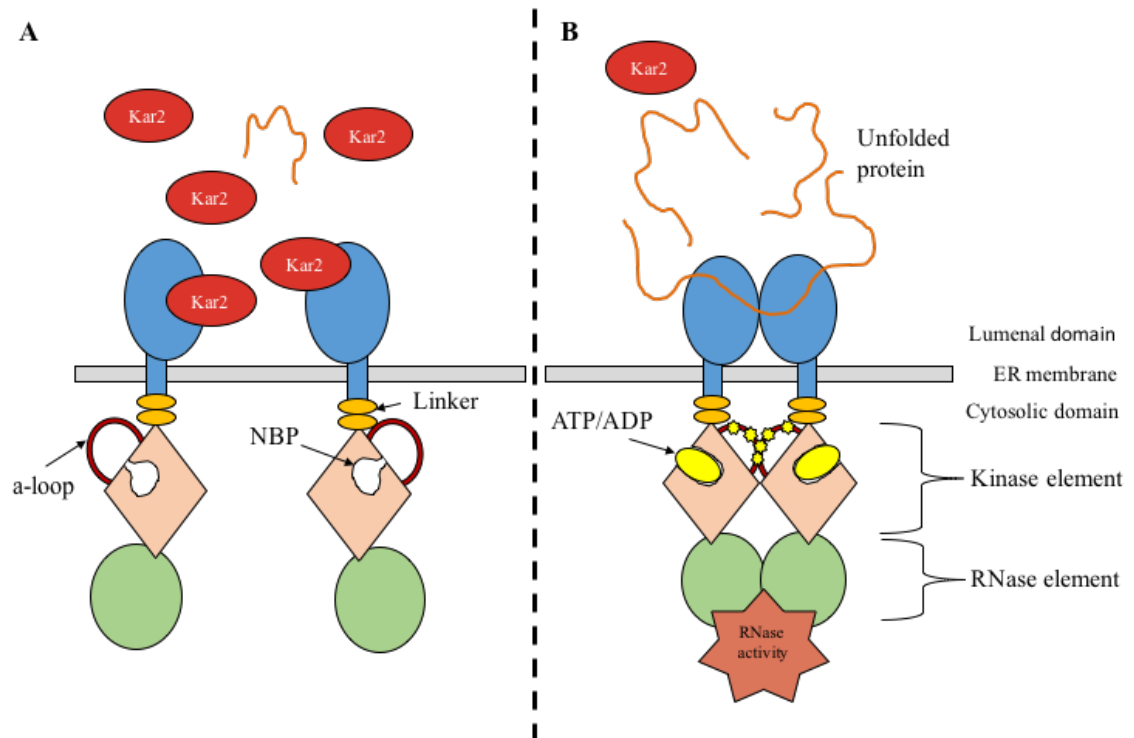
Fig 1. Schematic of Ire1 protein showing its lumenal and cytosolic domains. (A) shows the arrangement of Ire1 when under no ER stress and the inactive RNase domain. (B) Unfolded proteins initiate dimerisation or possibly oligomerisation of the Ire1 lumenal domain element. Following this, the kinase domain is activated by either phosphorylation of the a-loop (Lee et al., 2008; Nolen et al., 2004) or by oligomerisation which is stabilised by phosphorylation of the a-loop (Korennykh et al., 2009). Binding of ATP results in *trans*-autophosphorylation of the activation loop (a-loop) of neighboring Ire1 molecules (Gardner et al., 2013). The hydrolysis of the ATP by the kinase domain promotes the RNase active conformation (Lee et al., 2008). Once activated, the RNase element is involved in the splicing of *HAC1* mRNA to produce the induced protein Hac1[i] resulting in expression of UPR-associated genes including genes encoding for molecular chaperones or ERAD-associated protein machinery (Snapp, 2012).

It is the cytosolic elements that are of interest in the role of phosphorylation in activation and regulation of the UPR as they contain the protein kinase and RNase domains. Responsibility of nucleotide binding and phosphorylation falls to the kinase domain and the cleavage of *HAC1* mRNA is facilitated by the RNase domain when in its active

conformation. However, in the first instance it is the lumenal domain that detects unfolded protein accumulation.

6.2 *Activation of the lumenal domain*

In yeast, Ire1 is the only known sensor to respond to unfolded protein accumulation in the ER and transduces this information across the ER membrane (Anken et al., 2014). There are two theories regarding how the lumenal domain of Ire1 detects the accumulation of unfolded proteins within the ER. One theory is that the Ire1 lumenal domain senses unfolded proteins in the ER lumen and directly binds these proteins, allowing for the formation of higher order oligomers (Credle et al., 2005; Mathuranyanon et al., 2015; Pincus et al., 2010). Alternatively, it is proposed that proteins such as Kar2 (BiP) act as regulators by binding to the Ire1 lumenal domain receptor and do so in competition with unfolded proteins (Kimata et al., 2007; Shamu and Walter, 1996; Zhou et al., 2006); (Fig. 1). To take the example of molecular regulators, under ER stress conditions unfolded proteins are more numerous and compete for binding to Ire1 with molecular regulators. This reduces the occurrence of regulator binding to the Ire1 lumenal domain and increases the occurrence of the binding of unfolded proteins, allowing for dimerisation of the Ire1 lumenal domain and autophosphorylation of its neighbours (Liu, Schröder and Kaufman, 2000), which ultimately activates the UPR. Both theories agree that the dimerisation or oligomerisation of the lumenal domain of Ire1 is essential for signal propagation across the membrane. It may indeed be the case that both theories are correct and the lumenal domain of Ire1 can be activated by multiple methods (Snapp, 2012). The lumenal domain is not simply a detection domain for ER stress, it is a precursor for downstream signalling (Liu et al., 2000). Ire1 has been show to produce *foci* sites *in vivo* when ER stress is induced. Furthermore, these clusters of Ire1 were no longer visible when cells were washed and incubated in conditions that did not induce ER stress, suggesting that these clusters are not simply aggregates of Ire1 (Kimata et al., 2007) but directly linked to the UPR. Additionally, clustering was observed in a kinase inactive mutant as well as a *HAC1* knockout mutant (Kimata et al., 2007). This suggests that kinase activity and UPR-associated gene expression are not prerequisites for the formation of clusters of Ire1, but that the clustering of Ire1 is required for UPR activation. Should Ire1 not cluster upon the induction of ER stress then it is suggested that the UPR would not be induced, or induced at a reduced capacity due to the lack of Ire1 activation (Credle et al., 2005). This is supported by evidence that point mutations that prevent or deform interfaces between Ire1

molecules in the lumenal domain, involved in dimerisation or oligomerisation, reduce Ire1 activity suggesting that the formation of interfaces is critical both in the lumenal and cytosolic domains of Ire1 (Credle et al., 2005).

6.3 *The Kinase domain of Ire1 and its role in RNase domain activation*

Specific elements of the role of the kinase domain of Ire1 are still unknown, such as the specific role phosphorylation of the a-loop plays in how Ire1 regulates RNase activity. Regions, within the kinase domain such as the activation loop (a-loop), the magnesium binding loop, the β10 domain, and the P+1 region (collectively known as the activation segment, Fig. 2) are critical to the regulation of RNase activity of Ire1. This is because these conserved regions contain residues thought to be involved in phosphorylation (serines 837, 840, 841, and 850 and threonine 844 (Lee et al., 2008; Shamu and Walter, 1996)), and interactions involved in kinase activity (aspartic acid 828 (D828) (Papa et al., 2003)). The a-loop is thought to promote *trans*-autophosphorylation of positive regulatory sites within the protein kinase domain, namely serine 840 and 841 (S840 and S841) as a minimum (Shamu and Walter, 1996). *Trans*-autophosphorylation of Ire1 by neighbouring Ire1 molecules is thought to result in an active conformation of the cytosolic domain and subsequent activation of the RNase domain of Ire1 (Sidrauski and Walter, 1997; Welihinda and Kaufman, 1996). Autophosphorylation of S841 and threonine 844 (T844) was found to be a requirement of Ire1 kinase domain activation (Korennykh et al., 2009; Lee et al., 2008; Mannan et al., 2013). Furthermore, mass spectroscopy revealed phosphorylation on the previously reported serine residues (S840 and S841) (Shamu and Walter, 1996) as well as at T844 and serine 850 (S850) (Lee et al., 2008). However, subsequent investigation of S850 found that mutation at this residue did not result in impairment of Ire1. S837 was first suggested as possible phosphorylation sites in the 1990's (Shamu and Walter, 1996) however there is no primary data thus far to support this.
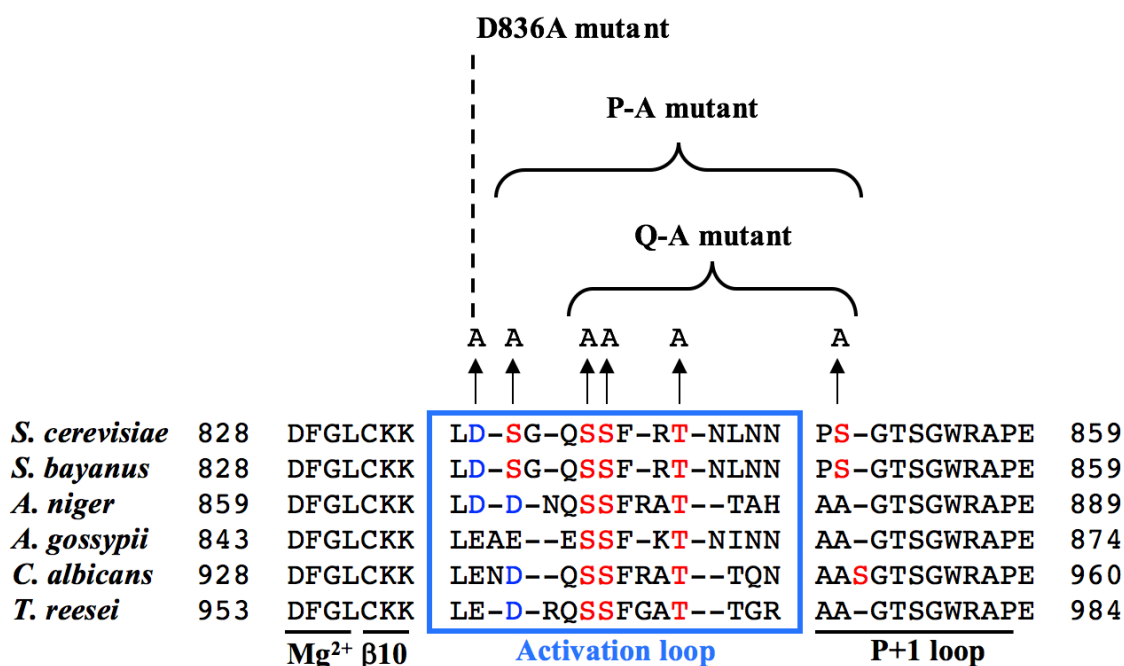
Fig. 2 The conservation of phosphorylation sites within the activation loop of *S. cerevisiae*. The S840 and S841 residues show a high level of conservation, within the a-loop, this is also true for T844. S837 and S850 however show lower levels of conservation. This inclusion of the S837A residue to the P-A mutant (S837A-S840A-S841A-T844A-S850A) and its exclusion from the Q-A mutant (S840A-S841A-T844A-S850A) allows its role in Ire1 activation to be characterised, as this information is presently not available in the literature. The aspartic acid at position 836 (D836) can also be studied by this design. With the inclusion and exclusion of an alanine mutation at D836 (D836A) the effect of the combination of D836A with phospho-mutants on UPR activation can be investigated. Through the construction of mutants containing different combinations of different mutation sites within the activation segment (Mg^{2+}, β10, the activation loop and P+1 domains) it is possible to investigate the possible role the mutated residues may have on Ire1 activation.

D828 is a critical residue in the catalytic loop of the kinase domain of Ire1 as it coordinates the β and γ phosphates of ATP with Mg^{2+} in the kinase pocket (Chawla et al., 2011; Korennykh et al., 2011). This residue is found in the region of the activation segment known as the magnesium binding loop (Fig. 2). Mutants possessing the D828A mutation have been described as "kinase dead" due to the lack of a protein kinase active site (Papa et al., 2003), although the concentration of the kinase inhibitor used (20 μM) should be taken

into consideration regarding disassociation rates whereby this may be insufficient to represent Ire1 function when binding nucleotide. Furthermore, D797 and K799 residues have been identified as catalytic sites with a predicted function of coordination of the γ phosphate of ATP bound to the kinase domain (Rubio et al., 2011). It has been shown that the binding of a kinase inhibitor can still result in RNase activity (Papa et al., 2003) suggesting the importance of nucleotide binding induced conformation changes in the kinase domain. Also, previous unpublished work in the Schröder Laboratory at Durham University found that with mutants lacking kinase activity (K799A, N802A, and D828A) show a retention of levels of RNase activity close to that found in the wild type (WT) (Chawla *et al.*, 2011; Rubio *et al.*, 2011). This suggests that kinase activity may be dispensable in terms of RNase activation.

In the examples above the RNase domain was still activated, suggesting that RNase activation could still be occurring due to the occupation of adenine and ribose subsites, thought to stablise the kinase active sites in the open conformation favouring Ire1 self-association (Korennykh *et al.*, 2009). An example of Ire1 self-association with the binding of ADP to the nucleotide binding pocket (NBP) can be seen in Fig. 3.
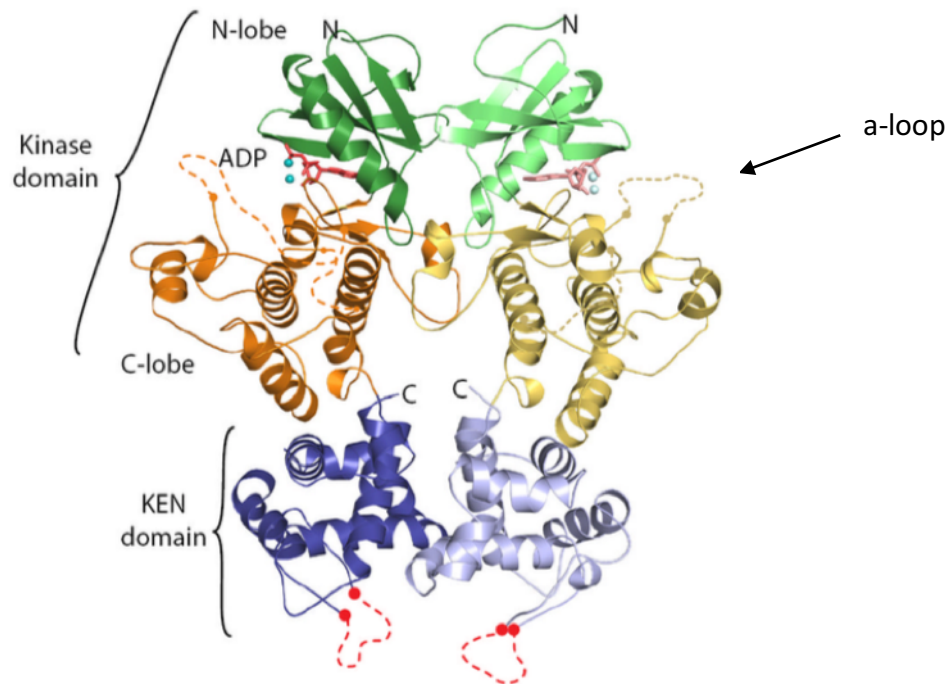
Fig. 3 The crystal structure of the cytosolic domain of a pair of Ire1 proteins (Lee et al., 2008). The figure highlights the binding of ADP to the NBP. The RNase domain, located within the kinase-extension nuclease (KEN) region on this figure (blue) facilitates *HAC1* mRNA splicing. The a-loop is indicated in the kinase domain. Dashed lines within this figure indicate these regions failed to be fully modeled due to disorder.

Despite numerous factors in kinase domain activation, the key to RNase activation seems to be the conformational change of the kinase domain resulting from kinase activation, either from a-loop interactions (Lee et al., 2008; Nolen et al., 2004) or oligomerisation (Korennykh et al., 2009). This is important as it is the RNase activation which facilitates *HAC1* mRNA splicing allowing for induction of UPR-associated genes.

6.4 *HAC1 mRNA splicing by the Ire1 RNase domain*

The Ire1 signaling cascade ultimately causes activation of the cytosolic RNase domain of Ire1 (Tanaka *et al.*, 2015). In order to produce functioning protein (Hac1[i]), *HAC1* mRNA must be spliced, removing a 252-nucleotide sequence, (Mori, 2000) (Fig. 4), removing the intron which contains a transcriptional attenuator (Rüegsegger et al., 2001). The remaining

two exons are ligated by tRNA ligase (Gardner *et al.*, 2013) and translated. Without the removal of the intron *HAC1* mRNA remains untranslated due to an interaction between the intron (still in the sequence) and the 5'-untranslated region (5' UTR) of *HAC1* (Rüegsegger et al., 2001; Sathe et al., 2015). The translated Hac1[i] contains a potent bZIP transcription factor (Gardner *et al.*, 2013). It is this transcription factor that is required for the expression of UPR genes including *KAR2, PDI1* and *LHS1*, which code for molecular chaperones (Schröder, Chang and Kaufman, 2000) and aid in the tolerance and recovery from ER stress.

Fig. 4 The intron of *HAC1* mRNA to be spliced; U indicating unspliced mRNA and S indicating spliced mRNA. *HAC1* being the yeast mRNA, *bZIP60* the mRNA of plants and *XBP1* the mRNA of metazoans (Zhang et al., 2016). The red aligned bases indicate conservation of the mRNA sequence.

In order to express UPR-associated genes, the bZIP transcription factor of Hac1[i] associates with a conserved promoter sequence known as the unfolded proteins response element (UPRE) (Mori et al., 1992; Kohno et al., 1993; Kimata et al., 2003; Montenegro-Montero et al., 2015). This UPRE is what gives the UPR it's specificity in gene expression response.

6.5   Activation loop phosphorylation and its role in RNase activation

There are currently two models that differ slightly in their thoughts regarding phosphorylation of the a-loop and RNase activation. The first model is based on phosphorylation of the a-loop resulting in conformational changes in the a-loop and kinase domain which facilitates nucleotide binding. These conformational changes promote kinase activity resulting in the hydrolysis of ATP to ADP. The resulting ADP bound state positions the Ire1 in a dimer and the RNase domain is activated, potentiated by ADP in the

NBP (Lee et al., 2008; Shamu and Walter, 1996). It has been suggested that the phosphorylated a-loop interacts with specific residues of the kinase domain to promote the conformational changes mentioned. When the active state of a cyclic adenosine monophosphate- (cAMP) dependent kinase structure was solved it showed the interaction between a phospho-residue within the a-loop and residues on the surface of the kinase domain due to their positive charge (Knighton et al., 1991). This interaction takes place at a conserved arginine preceding a conserved aspartic acid within the catalytic loop of the kinase, which allows for regulation of kinase activity (Johnson et al., 1996). The arginine and aspartic acid residues were named the "RD pocket" and kinases that possessed this pocket were termed RD kinases. In RD kinases, the electrostatic interaction between phospho-residues within the a-loop and the RD pocket is critical for driving the conformational change required for kinase activity (Nolen et al., 2004). Nolen et al., (2004) suggest that the arginine does not directly relay a signal of activation to the kinase catalytic loop, but that the change in the a-loop structure mediated by the RD pocket, facilitates the conformational change to the N and C-terminal anchors of the a-loop allowing for nucleotide binding, a step thought to be essential in Ire1 activation (Papa et al., 2003). Additionally, this model also supports the idea that phosphorylation can be bypassed in phosphorylation-independent protein kinases. In the case of phosphorylation-independent RD kinases, stabilising the active conformation of the a-loop can be achieved with the use of separate regulatory domains or changes within the amino acid sequence within the kinase domain (Nolen et al., 2004). The negative charge of a glutamate residue within the a-loop allows for pocket stabilisation in phosphorylase kinase (PhK) (Johnson et al., 1996) and the use of glutamates in the a-loop Ire1 also suggested this (Mannan et al., 2013). The stabilisation of the RD pocket by these methods may further promote nucleotide binding. This illustrates a possible mechanism of kinase activation independent of phosphorylation within the a-loop.

A variation on this model, presented by Korennykh et al., (2009), is that the cytosolic domain forms an oligomer via a two step process. Initially the cytosolic domain forms back-to-back dimers. To promote the self-association required for the initial dimer and subsequent oligomer formation, the adenosine and ribose subsites of Ire1 should be occupied (Korennykh et al., 2009), which is suggested to be completed by ADP binding to the unphosphorylated Ire1. This self-association is thought to promote a conformational change within Ire1 permitting kinase activity, *trans*-autophosphorylation and subsequent ATP binding. The binding of ATP to the now active kinase domain results in

phosphorylation of the a-loop and the locking of Ire1 into an oligomerisation compatible state. This oligomerisation-compatible state is facilitated by a phosphate-mediated salt bridge at IF3[c] resulting from ATP binding. The IF3[c] interface is believed to be essential for the formation of higher order oligomers (Korennykh et al., 2009). The growth of the oligomer relies on the formation and cooperation of three interfaces, (IF1[c], IF2[c] and IF3[c]). Interface 3 (IF3[c]) links the cytosolic domain monomers. Interfaces 1 (IF1[c]) and 2 (IF2[c]) link the kinase domains (Lee et al., 2008) and the RNase domains of the associated monomers respectively. This sequence of events results in a form of positive feedback, as the creation of salt bridges at IF3[c] facilitates the addition of more Ire1 molecules forming a higher-order oligomer. The dimers are added to the growing oligomer at a rate of one for every 51.4º of clockwise turn. This Ire1 oligomer and its associated interfaces are believed to control the RNase activity of Ire1 (Korennykh et al., 2009). It is suggested that IF1[c] and IF2[c] form a continuous linkage of the RNase domains within the oligomer and that IF2[c] stabilises the helix-loop element (HLE) of the RNase domain which is believed to control RNase activity (Korennykh et al., 2009). This model considers oligomerisation as the critical step in RNase activation, with a-loop phosphorylation playing more of a supportive role by stabilising oligomer-associated interface formation. *Trans*-autophosphorylation in the oligomer model could be the solution to the issue of how Ire1in a dimer would *trans*-autophosphorylate when the a-loops are positioned more than 40 Ångströms (Å) away from one another, an arrangement which would seem unproductive in terms of the *trans*-autophosphorylation observed *in vivo* (Shamu and Walter, 1996) (A-loop position in Fig. 3).

Although these two theories share some themes, they differ in that the first model is based on phosphorylation being the driving force in kinase activation and the resulting RNase activity whereas oligomerisation is the critical step in kinase activation and RNase activity in the alternative model. The models also share some flaws. In the first model, the interaction between the phosphorylated a-loop and the RD pocket is thought to facilitate a conformational change to facilitate nucleotide binding. As Ire1's phosphorylation is based on autophosphorylation this would suggest that there must already be kinase activity to phosphorylate the a-loop. This could be explained by two theories. The first is that the kinase domain always has levels of ATP binding due to the high concentration of ATP in the cell but that its kinase function is very low. When the a-loop becomes phosphorylated the conformation change in the kinase domain permits more efficient kinase function, dramatically increasing the rate of a-loop phosphorylation. As the Ire1 molecules are

brought together under ER stress this increases a-loop phosphorylation results in the increase of *trans*-autophosphorylation outlined in the model. Alternatively, the active and inactive status of the kinase domain may be in equilibrium. The activation and clustering of Ire1 through ER stress brings the Ire1 molecules together which tips this equilibrium to favour the active ATP-binding state. This balance tilt is because, as the *trans*-autophosphorylation between the ATP bound Ire1 occurs, this will promote conformational changes to the inactive Ire1 which in turn activates other inactive Ire1 kinase domains through *trans*-autophosphorylation.

With the RNase activation model based on oligomerisation, ADP binds to initiate the oligomer, which promotes the conformational change in the kinase domain. So how does nucleotide bind to inactive kinase? The answer to this may be that the kinase domain can bind nucleotides but has no kinase activity in this non-oligomer conformer. ADP simply allows for the formation of the initial dimer/oligomer, which results in a conformational change within the kinase domain. Under no ER stress this would not result in dimerisation as Ire1 would not be brought together by the lumenal domain. This puts the kinase domain in its active state allowing ATP binding and *trans*-autophosphorylation permitting the formation of oligomers.

In the models described above, phosphorylation is involved in either the activation of the kinase domain or formation of oligomers, both of which are claimed to result in the activation of the RNase domain. The activation of the RNase domain of Ire1 results in *HAC1* mRNA splicing which, when translated produce the Hac1[i] protein, acts a transcription factor for UPR-associated genes by interacting with the UPRE within the promoter of UPR-associated genes (Mori et al., 1992; Kohno et al., 1993; Kimata et al., 2003; Montenegro-Montero et al., 2015). From this, a complete loss of *HAC1* mRNA splicing *in vivo* would be expected in mutants possessing mutations in all of the a-loop phosphorylation sites of Ire1, as in the absence of phosphorylation it is expected that RNase activation would not occur (if indeed Ire1 is phosphorylation-dependent) (Shamu and Walter, 1996). In the case of S840A-S841A, Q-A and P-A mutants (Fig. 2) it has been found that this is not the case (unpublished work from the Schröder Laboratory, Durham University). Data showed that a reduced level of RNase activity was being retained, indicated by the presence of spliced *HAC1* mRNA on a northern blot (Fig.5).
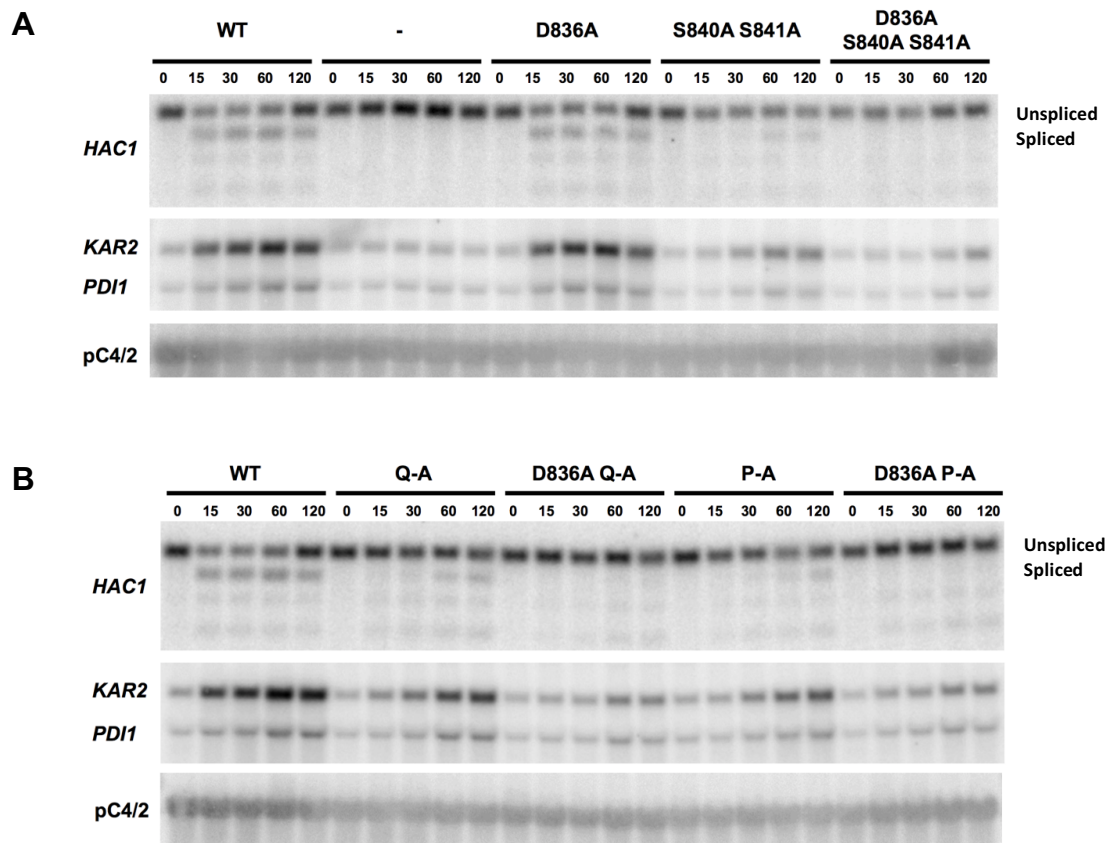
Fig 5. Northern blot data of a-loop phospho-mutants and D836A mutants, data gathered by Dr. Martin Schröder. The presence of the top row of bands of the *HAC1* section indicates the levels of unspliced *HAC1* mRNA, the second row of bands is the spliced *HAC1* mRNA coding for the active Hac1[i] protein. *KAR2* and *PDI1* are UPR-associated genes and the increasing intensity of bands over time is indicative of UPR gene activation, this is complemented by increasing intensity of spliced *HAC1* bands. pC4/2 is a loading control. The D836A mutant behaves much the same as seen in the WT, however, when combined with phospho-acceptor mutants P-A, Q-A and S840A-S841A the residual *HAC1* mRNA detection is further attenuated to almost undetectable levels.

The Schröder Laboratory at Durham University also found that with mutations of specific residues, K799A, N802A, and D828A no protein kinase activity was recorded but levels of RNase activity close to that found in the wild type (WT) were observed (Rubio *et al.*, 2011). These mutants were found to suffer no loss in ATP or ADP binding efficiency *in vitro*, and furthermore rescued the RNase activity of a kinase defective mutant, D797A. This lead to the proposition that the phosphorylation of the a-loop by the kinase activity of

20

Ire1 does not play an indispensable role in the binding of nucleotides, oligomerisation or RNase activity. This lead to the question, if there were small levels of RNase activity detected by the presence of spliced *HAC1* mRNA, by what mechanism was Ire1 being activated the was independent of phosphorylation? The addition of a mutation of the aspartic acid 836 (D836) to an alanine (D836A) to the same phospho-residue mutants (S840A-S841A, Q-A and P-A), resulted in spliced *HAC1* mRNA levels which appeared to be the same as those found in the negative control suggesting that D836 plays a role in RNase activation (Fig. 5). The conclusions were that the D836 residue may act as a substitute for phosphorylation within the a-loop and that the kinase domain is involved in control of the RNase activity only after nucleotide(s) binding to the NBP.

If the D836 residue facilitates the retention of attenuated levels of RNase activity, then this may allow for RNase domain activation (at a reduced level) and induction of the UPR without the requirement for phosphorylation within the a-loop. As mentioned earlier, the positive charges within the kinase domain catalytic site interact with the negative charges of the a-loop (in the RD model) are thought to interact, allowing for nucleotide binding. Aspartic acid is negatively charged hence the D836 residue may mimic this interaction and the substitution of aspartic acid for alanine prevents this imitation of phosphorylation interaction. The reasoning behind only a partial retention of RNase activity may be because of the theory that there is a preferential order to phosphorylation sites within the a-loop of protein kinases, with one site being known as the primary site (Nolen et al., 2004; Shamu and Walter, 1996). This would suggest that this primary site would have the largest impact on kinase activation, therefore a secondary site less so, and a compensatory system, such as proposed here with D836 may have even more limited kinase activation ability.

6.6   *Aims and objectives*

A hypothesis investigating if D836 can substitute for phosphorylation of phospho-acceptor sites in the a-loop of Ire1 in the event of loss of phospho-activity was tested. The goal of the hypothesis being to further characterise the role of phosphorylation in the a-loop of Ire1 and the role this plays on RNase activity. The aims were to; 1. Characterise the levels of Ire1 expression in the mutants used. 2. To investigate how phosphorylation mutations within the a-loop effect ER stress signal transduction by Ire1 and to what extent D836 played a role in retention of signal transduction if phospho-mutants. 3. The further review of the ER stress tolerance in phospho-acceptor mutants and if D836A-inclusive phospho-mutants were further affected by ER stress *in vivo*. 4. To review the clustering of Ire1 in

mutants in response to ER stress. These four goals were achieved using a range of mutants of *Saccharomyces cerevisia*e to monitor the unfolded protein response to ER stress, S840A-S841A, D836A-S840A-S841A, Q-A (S840A-S841A-T844A-S850A) and D836A-Q-A and P-A (S837A-S840A-S841A-T844A-S850A), D836A-P-A (Details in Fig. 2). By comparing the D836A-inclusive mutants to the non-D836A mutants, and any change in the unfolded protein response, the role D836 plays in the activation of the RNase activity in Ire1 could be further characterised. If the hypothesis regarding the ability of D836 to bypass phosphorylation is correct, a complete loss of UPR activation should occur with the inclusion of D836A to phospho-acceptor mutants. To test the UPR, the ER of cells will be stressed with 2 mM dithiothreitol (DTT) (or increasing concentrations of DTT and tunicamycin (Tn) in spotting assays) to induce ER stress by preventing di-sulphide bond formation and prevent glycosylation respectively. This should result in the introduction of ER stress. Sections 6.6.1 – 6.6.4 briefly explain these approaches.

6.6.1   Ire1 protein expression in mutants

Western blot analysis utilising the HA-tagged Ire1 allows for evaluation of the steady-state expression levels of Ire1 of the mutants. Should the mutants be lacking in Ire1 or show the phenotype of a dramatic reduction or induction of Ire1 then this would serve as an explanation as to any differences in ER stress response. The standardisation of Ire1 protein against an abundant non-UPR-associated protein (in this case *β*-actin) allows for comparison between mutants.

6.6.2   *β-galactosidase-reporter assay to determine activation of the UPR*

In unstressed cells, *HAC1* mRNA is not readily translated, however, when ER stress is introduced the resulting splicing and ligation of *HAC1* mRNA produces a translatable mRNA coding for Hac1[i] (Bertolotti and Ron, 2001). Translation of Hac1[i] will result in expression of UPR-associated genes through UPRE interaction (Mori et al., 1996), detectable with the reporter assay. The northern blot data gathered (Fig. 5) shows levels of mRNA (both spliced and unspliced) over the time course of ER stress. Fig. 5 also shows mRNA levels of *KAR2*. However, due to the unstable nature of RNA these data are not necessarily indicative of protein levels *in vivo* under ER stress, only of the splicing achieved by the RNase domain quantified by the detected levels or mRNA. Systems such as the UPR need to be evaluated not only by mRNA expression profiles but in terms of the activity of proteins. The common occurrence of post-transcriptional regulation and

modification of mRNA make mRNA expression profiles alone imperfect in understanding a process such as ER stress response (Ghaemmaghami et al., 2003). The use of the UPRE-associated-β-galactosidase-reporter assay will quantify the UPRE-associated reporter protein (β-galactosidase) in the lysate extract and this will allow for quantification of any subtle differences in the ER stress signal transduced by Ire1 in the mutants. The use of mutants constructed in the way used in this work (Fig. 2) will allow for an assessment of how much particular phosphorylation sites impact the UPRE-associated reporter activity.

6.6.3   Effect of ER stress tolerance in vivo

Spotting assays allow for the effect of a reduction in ER stress tolerance to be reviewed *in vivo*. Any deficiencies in ER stress tolerance, as a result of the mutations made to Ire1, will result in reduced survival of ER stress, indicated by a reduction in growth of colonies. By increasing the concentrations of ER stressors (DTT and Tn) over several agar plates the capability of the UPR to respond to ER stress can be viewed at different ER stressor concentrations. This is critical as the UPRE-associated reporter protein assays are *in vitro* and only show the response from the UPR at the time point at which samples were prepared. Spotting assays allow the impact of any mutations to Ire1 to be reviewed *in vivo* allow for study of the effect of the mutations on cell fate.

6.6.4   Visualisation of the clustering of Ire1 under ER stress

When the lumenal domain of Ire1 is activated it is known to form clusters *in vivo* (Aragón et al., 2009; Kimata et al., 2007). To view this fluorescence microscopy is to be used. Through the labelling of Ire1 using mCherry, clustering of Ire1 can be viewed in real time. Additionally, the labelling of the Sec63 protein with GFP allows for localization of the Ire1clusters to the ER membrane. The use of real time *in vivo* imaging of the clustering of Ire1 under ER stress allows for confirmation that the decreased *HAC1* mRNA splicing observed (Fig. 5) is not a result of a defect in Ire1 clustering.

7.0 **Materials and Methods**

7.1   Materials

7.1.1   Buffers and solutions

Tables 1 and 2 outline the composition of the buffers and solutions used in the work presented, where appropriate catalogue numbers and supplier information has been provided.

Table 1. Commonly used solutions and buffers and their composition.

Solution	Quantity	Recipe
EDTA, 0.5 M	500 ml	1. Dissolve 93.1 g $Na_2EDTA \cdot 2H_2O$ in ~350 ml H_2O. 2. Adjust pH to 8.0 with 10 M NaOH (~25 ml) 3. Add H_2O to 500 ml. 4. Autoclave.
$MgCl_2$, 1 M	100 ml	1. Dissolve 20.33 g $MgCl_2 \cdot 6\ H_2O$ in ~ 80 ml H_2O. 2. Add H_2O to 100 ml. 3. Autoclave.
Na_2CO_3, 1 M	500 ml	1. Dissolve 53.0 g Na_2CO_3 in ~ 400 ml H_2O. 2. Add H_2O to 500 ml.
NaH_2PO_4, 0.4 M	500 ml	1. Dissolve 24 g NaH_2PO_4 in ~400 ml H_2O. 2. Add H_2O to 500 ml. 3. Autoclave.
Na_2HPO_4, 0.4 M	500 ml	1. Dissolve 28.4 g Na_2HPO_4 in ~400 ml H_2O. 2. Add H_2O to 500 ml. 3. Autoclave.
10% (w/v) SDS	500 ml	1. Dissolve 50 g SDS in ~450 ml H_2O. 2. Add H_2O to 500 ml. 3. Do NOT autoclave.
Tris·HCl (pH 6.8), 1 M	1 l	1. Dissolve 121.14 g Tris in ~800 ml H_2O. 2. Adjust pH to 6.8 with conc. HCl (~ 42 ml).

Buffer	Composition	Quantity	Recipe
			3. Add H$_2$O to 1 l.
			4. Autoclave.
Tris·HCl (pH 8.0), 1 M	1 l		1. Dissolve 121.14 g Tris in ~800 ml H$_2$O.
			2. Adjust pH to 8.0 with conc. HCl (~ 42 ml).
			3. Add H$_2$O to 1 l.
			4. Autoclave.
10% (v/v) Tween 20	50 ml		1. Dissolve 5.55 g Tween 20 in ~ 40 ml autoclaved H$_2$O.
			2. Add H$_2$O to 50 ml.
			3. Filter sterilise.
Buffer	**Composition**	**Quantity**	**Recipe**
50 x TAE	2 M Tris·HOAc 0.1 M EDTA pH ~ 8.5	1 l	242 g Tris 57.1 ml HOAc 37.2 g Na$_2$EDTA·2H$_2$O Add H$_2$O to 1 l
1 x TAE	40 mM Tris·HOAc 2 mM M EDTA pH ~ 8.5	1 l	20 ml 50 x TAE Add H$_2$O to 1 l
10 x TE (pH 8.0)	100 mM Tris·HCl (pH 8.0) 10 mM EDTA	4 l	400 ml 1 M Tris·HCl (pH 8.0) 80 ml 0.5 M EDTA Add H$_2$O to 4 l Autoclave

Table 2. Specialist solutions and their composition.

Solution	Composition	Quantity	Recipe
30% (w/v) acrylamide, 0.8% (w/v) methylene bisacrylamide	30% (w/v) acrylamide 0.8% (w/v) methylene bisacrylamide	100 ml	30 g acrylamide 0.8 g methylene bisacrylamide Dissolve in ~90 ml H_2O, add H_2O to 100 ml. Add 5 g Dowex MR-3 mixed bed ion exchanger, and stir for 1 h at RT. Filter over a 0.22 μm filter and store at 4ºC in the dark.
50 mg/ml ampicillin	50 mg/ml ampicillin	50 ml	2.5 g ampicillin, sodium salt Dissolve in ~40 ml H_2O, add H_2O to 50 ml, and filter sterilise. Store in 1.0 ml aliquots at -20°C.
2 x assay buffer	200 mM $Na_xH_{3-x}PO_4$ (pH 7.3) 2 mM $MgCl_2$ 100 mM β-mercaptoethanol 1.33 mg/ml 2-nitrophenyl-β-D-galactopyranoside	400 ml	177 ml 0.4 M Na_2HPO_4 23 ml 0.4 M NaH_2PO_4 0.8 ml 1 M $MgCl_2$ 2.8 ml β-mercaptoethanol 532 mg 2-nitrophenyl-β-D-galactopyranoside Add H_2O to 400 ml and mix. Store in 50 ml aliquots at -20°C.
1 M dithiothreitol	1 M dithiothreitol (DTT)	10 ml	1.54 g dithiothreitol Dissolve in ~ 9 ml H_2O. Add H_2O to 10 ml. Filter sterilise. Store at -20°C. Use at 2 mM to inhibit protein folding in the yeast ER.
10 x DNA gel electrophoresis sample loading buffer	20% (w/v) Ficoll 400 0.1 M EDTA 1% (w/v) SDS 2.5 g/l bromophenol blue	50 ml	10 g Ficoll 400 125 mg bromophenol blue 10 ml 0.5 M EDTA (pH 8.0) Add H_2O to ~ 35 ml. Dissolve. Add H_2O to 45 ml.

			Autoclave. Add 5 ml 10% (w/v) SDS.
5.0 mg/ml ethidium bromide	5.0 mg/ml ethidium bromide	50 ml	250 mg ethidium bromide Dissolve in ~ 40 ml sterile H_2O. Add sterile H_2O to 50 ml. Store at 4°C protected from light.
30% (v/v) glycerol	30% (v/v) glycerol	500 ml	189 g glycerol Add H_2O to ~400 ml, mix well by stirring. Add H_2O to 500 ml and autoclave.
1 M KH_2PO_4	1 M KH_2PO_4	500 ml	68.05 g KH_2PO_4 Add H_2O to ~450 ml and dissolve. Add H_2O to 500 ml and filter sterilise.
1 M K_2HPO_4	1 M K_2HPO_4	500 ml	87.09 g K_2HPO_4 Add H_2O to ~450 ml and dissolve. Add H_2O to 500 ml and autoclave.
1 M LiOAc	1 M LiOAc	250 ml	25.50 g LiOAc·$2H_2O$ Dissolve in ~200 ml H_2O. Add H_2O to 250 ml. Filter sterilise.
Lysis buffer I	50 mM $Na_xH_{3-x}PO_4$ (pH 7.3) 150 mM NaCl 10% (v/v) glycerol 1 mM EDTA	500 ml	14.4 ml 0.4 M NaH_2PO_4 48.1 ml 0.4 M Na_2HPO_4 4.38 g NaCl 63 g glycerol 1 mM 0.5 M EDTA (pH 8.0) Add H_2O to ~ 400 ml, and dissolve. Add H_2O to 500 ml. Store at 4°C.
1% (w/v) NaCl	1% (w/v) NaCl	100 ml	Dissolve 1 g NaCl in ~90 ml H_2O. Add H_2O to 100 ml and autoclave.
50% (w/v) PEG 4000	50% (w/v/) PEG 4000	500 ml	250 g PEG 4000 Add ~200 ml H_2O Stir for a few minutes, add H_2O to ~ 450 ml, stir until PEG4000 is nearly

			completely dissolved, add H₂O to 500 ml and mix. Filter sterilise.
10 x SDS-PAGE buffer	1.92 M glycine 0.248 M Tris 10 g/l SDS	1 l	144.13 g glycine 30.03 g Tris 10.00 g SDS Add H₂O to ~ 900 ml, stir until completely dissolved, then add H₂O to 1 l.
6 x SDS-PAGE sample buffer	350 mM Tris·HCl, pH 6.8 30% (v/v) glycerol 10% (w/v) SDS 0.5 g/l bromophenol blue 2% (v/v) β-mercaptoethanol	10 ml	3.50 ml 1 M Tris·HCl, pH 6.8 3.78 g glycerol 1.00 g SDS 1.25 ml 4.0 g/l bromophenol blue 200 µl β-mercaptoethanol Add H₂O to ~ 9 ml, dissolve overnight if necessary. Add H₂O to 10 ml.
Semidry transfer buffer	0.1 M Tris 0.192 M glycine 5% (v/v) methanol	1 l	12.11 g Tris 14.41 g glycine 50 ml methanol Add H₂O to ~900 ml, stir until completely dissolved, then add H₂O to 1 l.
Stripping solution	2% (w/v) SDS 100 mM β-mercaptoethanol	50 ml	1 g SDS 350 µl β-mercaptoethanol Dissolve in H₂O, then make up to 50 ml with H₂O.

Bicinchoninic acid protein assay working solution.	Reagent A: 10 g/l bicinchoninic acid disodium salt, 20 g/l $Na_2CO_3 \cdot H_2O$, 1.6 g/l disodium tartrate, 4.0 g/l NaOH, 9.5 g/l $NaHCO_3$. Adjusted to pH 11.25 with 10 M NaOH. Reagent B: 40 g/l $CuSO_4 \cdot 5H_2O$	15 ml	Mix 50 parts of reagent A with 1 part of reagent B. Note: when mixing reagents A and B a white precipitate may form $[Cu(OH)_2]$ this will dissolve upon further mixing of the reagents.
10 x TBST	200 mM Tris·HCl, pH 7.6 1.37 M NaCl 1% (v/v) Tween 20	1 l	Dissolve 24.2 g Tris, 80 g NaCl, and 10.6 g Tween 20 in ~900 ml H_2O. Adjust pH 7.6 to 7.6 with conc. HCl, and add H2O to 1 l. Note: this was diluted with deionised H_2O to 1 x for use in washing of PVDF membranes.
10 mg/ml tunicamycin	10 mg/ml tunicamycin in DMSO	1 ml	Add 1 ml DMSO to 10 mg tunicamycin (content of one bottle). Mix to dissolve. Store in 50 or 100 µl aliquots at -20°C. Use at 0.1 – 2.0 µg/ml to inhibit protein folding in the yeast ER.

7.1.2 Media composition for culturing of cells

Yeast were grown in YPD (2% (w/v) dextrose, 2% (w/v) peptone, 1% (w/v) yeast extract) or synthetic medium to maintain plasmids. Synthetic media were prepared using 2% (w/v) glucose (Fluka #49138), 0.67% (w/v) yeast nitrogen base without amino acids (ForMedium #CYN0405) and 2% agar (ForMedium #AGA03). For plates, agar was added to a final concentration of 2% (w/v) before autoclaving the medium. Amino acids were added as outlined in Table 3. For β-galactosidase assay experiments an amino acid dropout was used to ensure a standard medium throughout the repeats, (complete media supplement – uracil dropout, ForMedium #DCS0161), of which 0.77 g were added per litre of required broth, total required volume was made up with deionised filtered water. Both broth and solid media were autoclaved before use. In microscopy experiments, a medium was made using individual amino acids as this protocol requires differing concentrations of tryptophan and adenine sulphate (both 100 mg l^{-1}). Amino acid information can be found in Table 3.

Table 3. The concentrations of components used in the composition of synthetic media broths lacking uracil (- U) or lacking Uracil and Leucine (- U - L) for cell culture. For solid medium, 2% (w/v) agar was added. L-Asp and L-Thr were added after autoclaving. The increased concentrations of tryptophan and adenine in the SD-U-L medium are to attempt to reduce or eliminate the auto-fluorescence in cells associated with the biosynthetic pathways of these amino acids.

Component	Supplier	Cat. No.	Conc. [mg/l]		
			SD-U	SD-U-L	SD-U-L (Microscopy)
L-Tyr	ForMedium Norfolk, UK	DOC0192	30.00	30.00	30.00
Uracil	ForMedium, UK	DOC0213	-	-	-
L - Arg·HCl	Sigma-Aldrich, Cramlington, UK	W38 191 - 8	20.10	20.10	20.10
L - His·HCl	ForMedium, UK	DOC0144	20.10	20.10	20.10
L - Met	ForMedium, UK	DOC0168	20.10	20.10	20.10
L - Trp	ForMedium, UK	DOC0188	20.10	20.10	99.90
L - Ile	ForMedium, UK	DOC0152	30.15	30.15	30.15
L - Lys·HCl	ForMedium, UK	DOC0161	30.15	30.15	30.15
L - Val	ForMedium, UK	DOC0197	150.75	150.75	150.75
L - Ser	ForMedium, UK	DOC0181	376.88	376.88	376.88
Adenine SO_4	ForMedium, UK	DOC0229	19.95	19.95	99.90
L - Phe	ForMedium, UK	DOC0173	49.88	49.88	49.88
L - Glu	Calbiochem, Watford, UK	3510	99.75	99.75	99.75
L - Leu	ForMedium, UK	DOC0157	100.35	-	-
L - Asp	ForMedium, UK	DOC0121	100.00	100.00	100.00
L - Thr	ForMedium, UK	DOC0185	201.00	201.00	201.00

7.1.3 Commercially available kits

In some cases, commercial kits were used, for example, for plasmid extraction or β - galactosidase assays. Such kits are outlines below in Table 4.

Table 4. The commercial kits used, showing supplier, catalogue number and kit used.

Name of kit	Supplier	Use	Catalogue no.
E.Z.N.A Plasmid Midi Kit	Omega Biotek	Plasmid extraction	D6904-03
Perfectprep kit midi	Eppendorf	Plasmid Extraction	Discontinued
β-Galactosidase Enzyme Assay System with Reporter Lysis Buffer	Promega	β-Galactosidase assays	E2000
Pierce ™ ECL Western Blot Substrate	Thermofisher Scientific	Chemiluminescent detection	32106
Pierce ™ ECL Plus Western Blot Substrate	Thermofisher Scientific	Chemiluminescent detection	32132

Saccharomyces cerevisiae was used in the work. Specific strains were used with different genotypes which are outline in Table 5.

Table 5. *S. cerevisiae* strain information. PWY 260 was the strain used for western blot and for β-galactosidase experiments, MSY14-02 was used in microscopy work due to its more stable expression of the plasmids used in the microscopy work and Y01907 was used in spotting assays of the single mutants of the Q-A multipoint mutant providing a repeat in another *S. cerevisiae* strain.

Strain	Genotype	Source
PWY 260	W303 *MATa ire1Δ::TRP1 ade2-1 can1-100 his3-11,-15::HIS3*^{+}UPRE-*lacZ leu2-3,-112::LEU2*+UPRE-*lacZ trp1-1 ura3-1*	Papa, 2003
MSY14-02	CRY1 Δ*ire1::kan*MX2	M. Schröder
Y01907	BY4741 *ire1Δ::kan*MX4	EUROSCARF (Winzeler et al., 1998)

Plasmids were created and transformed into of *E. coli* (the XL10-GOLD strain) by Dr. Sergej Šesták (Slovak Academy of Sciences, Bratislava, Slovakia) and sent to myself to be extracted and used in this work. Plasmid maps (Fig. 6) show the use of amino acid synthesis markers for the YCplac33 (uracil), pEvA97 (leucine) and pJK59 (uracil) plasmids.
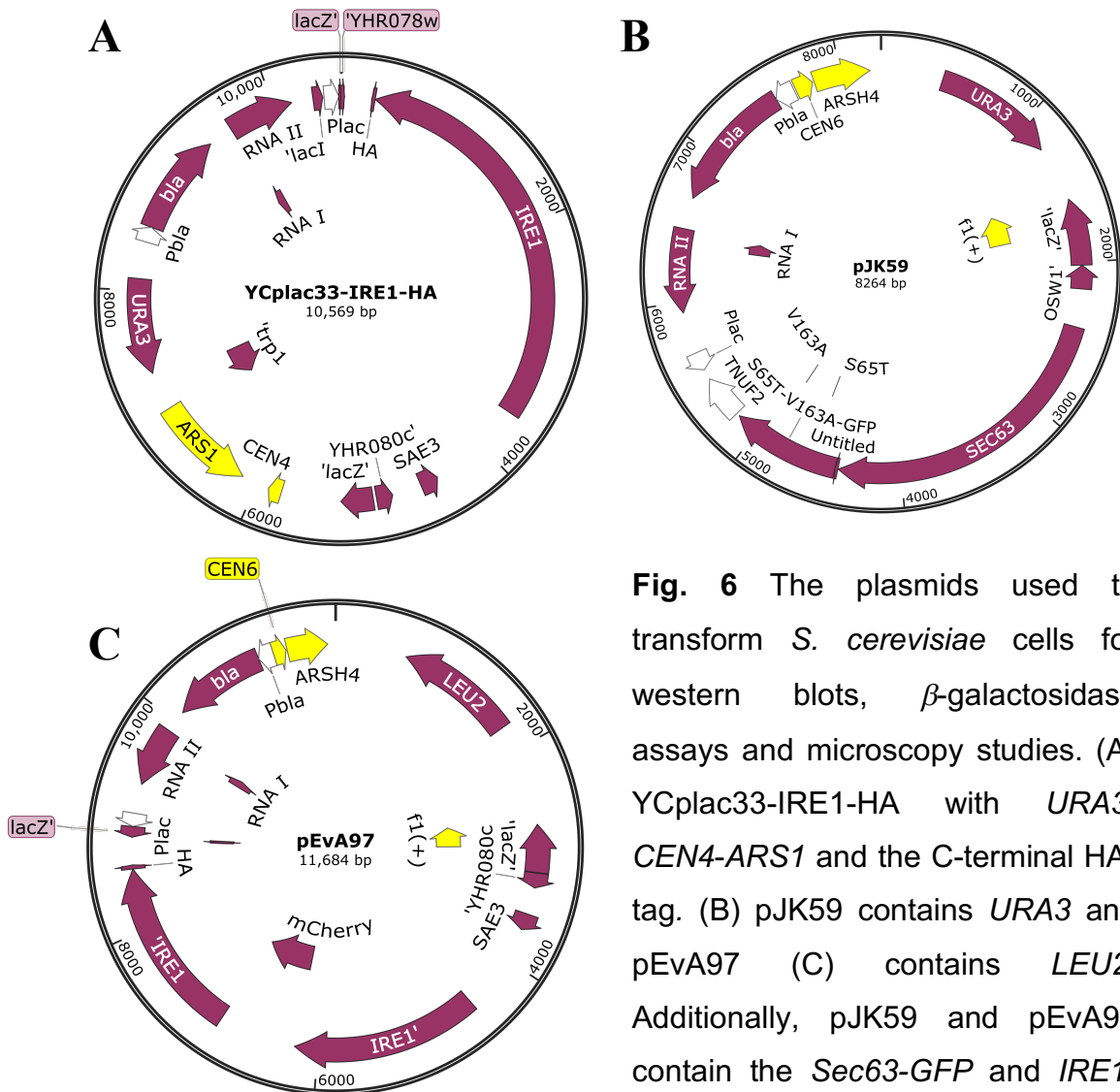
Fig. 6 The plasmids used to transform *S. cerevisiae* cells for western blots, *β*-galactosidase assays and microscopy studies. (A) YCplac33-IRE1-HA with *URA3*, *CEN4-ARS1* and the C-terminal HA-tag. (B) pJK59 contains *URA3* and pEvA97 (C) contains *LEU2*. Additionally, pJK59 and pEvA97 contain the *Sec63-GFP* and *IRE1-mCherry* for microscopy analysis, respectively. All plasmids were single copy.

7.1.6 Antibodies

The antibodies used to detect the Ire1 tagged with the HA epitope and the actin loading control are outlined in Table 6.

Table 6. Antibodies used in the western blot and chemiluminescent detection protocol.

Antibody	Species	Clonality	Supplier	Cat. no.	Batch/lot no.	Dilution factor
anti-HA	Rabbit	Polyclonal	Sigma-Aldrich	H6908	015M4868V	1000
anti-rabbit IgG (H+L)-peroxidase HRP linked	Goat	Polyclonal	Cell Signalling	7074S	24	2000
anti-β-actin	Mouse	Monoclonal [8F10G10]	Abcam	ab170325	GR184354-8	20,000
anti-mouse IgG (H+L)-peroxidase	Goat	Polyclonal	Pierce	31432	OE17149612	30,000

7.2 Methods

7.2.1 Plasmid extraction from E. coli

Plasmid extractions from *E. coli* were completed using two different commercially available kits (Table 4.). Methodologies for each of these kits are outline below.

7.2.1.1 E.Z.N.A kit

Following growth of *E. coli* precultures overnight at 37 °C at ~ 230 rpm to saturation in 2 ml of LB broth containing 50 μg ml^{-1} of ampicillin, flasks of 200 ml of LB broth again containing 50 μg ml^{-1} of ampicillin were inoculated and grown to an OD_{600} of 1.5 − 2.0 at 37 °C at ~ 230 rpm. Cultures were centrifuged at 10,000 × *g* for 5 min at room temperature to obtain a pellet, and the supernatant was discarded. Pellets were resuspended in 5 ml of solution 1 / RNase A. Once fully resuspended the culture was transferred to a screwcap centrifuge tube. 5 ml of Solution 2 were added and this was mixed by inverting tubes 10

times to obtain a clear lysate after which tubes were left at room temperature for 1 – 2 min. 7 ml of solution 3 were added and mixed by immediately and thoroughly inverting the tube until a white precipitate formed. Tubes were centrifuged at $23,500 \times g$ for 30 min at 4 ˚C. 4 ml of supernatant were transferred to a HiBind DNA Midi column in a 15 ml collection tube. The column and collection tube were centrifuged at $3900 \times g$ for 5 min at room temperature and the flow through was discarded, remaining lysate was added (4 ml at a time) and the column centrifugation process repeated until all lysate had been passed through the column (again with the flow through being discarded). 3 ml of Buffer HB were added to the column and centrifuged at $3900 \times g$ for 5 min at 4 ˚C, after which the flow through discarded. 4 ml of DNA wash buffer (diluted with ethanol as per the kit's guidelines) were added to the column and centrifuged at $3900 \times g$ for 5 min at 4 ˚C, this was then repeated and the flow through was discarded. The column was centrifuged a final time at $3900 \times g$ for 10 min at 4 ˚C to ensure the column was empty and any traces of ethanol were removed. The dry column was then transferred to a sterile 15 ml centrifuge tube and 2 ml of elution buffer were added to the column matrix and this was left at room temperature for 1 – 2 min. Tubes were centrifuged at $3900 \times g$ for 5 min at 4 ˚C and the purified plasmid was transferred to two sterile 2 ml tubes. 0.1 volume of 3 M NaOAc was added followed by 0.7 volume of isopropanol. Tubes were inverted to ensure mixing and centrifuged at $23,000 \times g$ for 10 min at 4 ˚C. Following centrifugation, the supernatant was discarded and the pellets left to air dry for 10 min. One pellet was resuspended in 20 μl of sterile TE buffer and this was then used to resuspend the partner tube. Plasmid DNA extracts were stored at – 20 ˚C.

7.2.1.2 *Eppendorf Perfectprep kit*

E. coli pre-cultures were grown to saturation overnight in 2 ml of LB broth containing 50 μg ml^{-1} of ampicillin at 37 ˚C, ~ 230 rpm. From these pre-cultures 200 ml of LB broth again with 50 μg ml^{-1} of ampicillin were inoculated and grown to an OD_{600} of 1.5 – 2.0 at which point cells were spun at $10,000 \times g$ for 5 min at room temperature. 4 ml of ice cold solution 1 were used to re-suspend the pellet, the suspension was incubated at room temperature for 10 min followed by 5 min on ice. 4 ml of solution 2 were added to the suspension and gently mixed by inverting, and place back on ice for 5 min. 4 ml of ice cold solution 3 were added to the suspension and mixed again by inverting and placed back on ice for a further 10 min. The suspension was centrifuged at $23,000 \times g$ for 30 min at 4 ˚C after which the supernatant was transferred to a 50 ml falcon tube. 10 ml of ice cold, well-

mixed, DNA binding matrix were added and mixed by repeated vigorous shaking and inverting. A spin column was added to another 50 ml falcon tube and the matrix bound sample was poured into the column (the previous tube was not discarded). The column and its retaining 50 ml falcon tube were centrifuged at 2000 × g for 5 min and room temperature and the filtrate was discarded. 10 ml of purification solution (diluted with ethanol as per guidelines in the kit) were added to the used 50 ml falcon tube, which had been kept, and this was then added to the "cake" in the column. The column and its retaining tube were centrifuged again at 2000 × g for 5 min at room temperature and again the filtrate was discarded. The column was centrifuged a final time at 2000 × g to ensure it was dry and all suspension had passed through. The column was then transferred to a fresh 50 ml falcon tube and 3 ml of elution buffer were added directly to the "cake" retained in the column. This was then spun at 3900 × g for 10 min at room temperature and the eluted plasmid that was collected in the falcon tube was transferred to a 12 ml centrifuge tube suitable for high g forces. 70 µl of 5 M NaCl and 60 µl of mussel glycogen were added to the elute and mixed. 6 ml of 100% EtOH were added and mixed well. This mix was then centrifuged at 23,000 × g for 30 min at 4 ˚C and the supernatant was discarded. A wash using 2 ml of 70% EtOH was repeated twice, both times at 23,000 × g for 15 min at 4 ˚C, the supernatant was discarded between washes. Any remaining EtOH was removed and pellets left to air dry for ~ 15 min. Once dry the pellet was resuspended in 25 µl of sterile TE buffer and stored at − 20 ˚C.

7.2.2   Plasmid quantification

To quantify the concentration of plasmid DNA from the extraction, plasmid DNA was diluted 1:10 using sterile TE buffer to a total volume of 50 µl loaded onto a Greiner 96 well UV transparent plate (Sigma-Aldrich, # M3812) and read on the Molecular Devices SpectraMAX 190 plate reader (Molecular Devices, Sunnyvale, USA, model no. 190) at 260, 280 and 320 nm.

7.2.3 Enzymatic digest

A master mix was prepared (Table 7) of H_2O, 10 X buffer, *Kpn*I enzyme (10,000 units/ml) and BSA (20 mg/ml) (enzyme and buffer were from New England Biolabs #R0142S). 3 µl of plasmid extract (diluted to a concertation of 100 ng $µl^{-1}$) were added to two tubes per sample, one to be digested and one to remain uncut to be used as a control. Once the contents of the tubes were mixed, tubes were placed in a water bath heated to 37 ˚C for 1 h after which samples were loaded onto an agarose gel. see section 7.2.4 for details.

Table 7. The master mix preparation for enzymatic digests of extracted plasmids.

Reagent	Volume (µl) (1 prep)	Volume (µl) (20 preps)
H_2O	14.30	286.00
10 X Buffer	2.00	40.00
*Kpn*I Enzyme	0.50	10.00
BSA	0.20	4.00
Total volume (µl)	17.00	340.00

7.2.4 Agarose gels

A 1% (w/v) agarose gel was cast by dissolving agarose powder in 1 X TAE buffer using a microwave. Once this had cooled to ~ 55 ˚C, 0.5 µg per ml of ethidium bromide was added to stain the gel. Samples were prepared using 1 µl of plasmid or plasmid digest product, 9 µl of H_2O and 2 µl of 6 X loading buffer. The gel was placed in a tank filled with 1 X TAE buffer. Samples were loaded into the lanes along with a lane containing 5 µl of Gene Ruler DNA ladder 1 kb (Fermentas, Lithuania, cat. No. #SM0331) in order to size the bands that were detected.

7.2.5 Sequencing and sequence alignment

5 µl of plasmid at a concentration of 100 ng $µl^{-1}$ were mixed with the 2721K primer (1 µl). The 2721K primer sequences were `GAAAACCTGAAATTACAG` with a melting temperature (Tm) of 44.1 ºC. Plasmids were then sequenced by DBS Genomics (Durham University, Durham, UK). Sequences were then aligned using BioEdit (Ibis Biosciences, Carlsbad, California) (Fig. 9).

7.2.6   Strain transformation (Gietz and Schiestl, 2007)

A preculture of cells was grown in 2 ml of SD-U media for 48 h. An OD_{600} reading was taken and 5 ml of SD-U media per desired transformation were inoculated and grown to a final OD_{600} of ~ 1.0 (e.g. for 5 transformations 55 ml of media would be inoculated). Cultures were transferred to a sterile 50 ml tube and spun at 3750 × g for 2 min at 4 ˚C after which the supernatant was discarded and the cell pellet placed on ice. The pellet was resuspended in 9 ml of 1-step buffer, (1 part 0.2 M LiOAc and 4 parts 40% (w/v) PEG 4000 (Sigma, #1546569-1G)). The cell suspension was centrifuged again at 3750 × g for 2 min at 4 ˚C, after which again the supernatant was discarded and the pellet placed back on ice and left for 1 – 2 min to allow for the remaining 1-step buffer to collect at the bottom of the tube and be removed. 88 µl of 1-step buffer were added for each transformation required and an additional 88 µl to ensure sufficient cell suspension was available. The pellet was resuspended ensuring no clumps remained. 88 µl of suspension were added to a sterile 1.5 ml tube containing 12 µl of sheered salmon sperm DNA (Invitrogen #15-632-011) (pre-boiled for 5 min in a heat block) and 1 µl of the desired plasmid and the tubes vortexed at maximum speed for 15 s. The plasmids were created by Dr. Sergej Šesták (Slovak Academy of Sciences, Bratislava, Slovakia) and sent to myself to be extracted and used in this work, (Fig. 6) Tubes were incubated at 42 ˚C in a water bath for 30 min before being briefly spun at max speed (~ 13,000 × g for 10 s at room temperature) to collect the pellet and the supernatant was removed. The cell pellet was resuspended in 200 µl of sterile H_2O and the full suspension was spread on a SD agar plate with an appropriate amino acid dropout (dictated by amino acid synthesis gens used in the plasmid). Plates were incubated at 30 ˚C for ~ 5 days to allow for single colonies to grow.

7.2.7   Replica plating and acetate testing

To ensure that the cells grown on plates were not cells containing a mutation preventing growth on media containing only non-fermentable carbon source, known as petite cells, replica plating from the SD-dropout plates to yeast peptone acetate plates (YPAc) was utilised. This was achieved by placing the SD-dropout plate onto a sterile piece of velvet and applying gentle pressure. A YPAc plate was then placed onto the velvet and again gentle pressure applied allowing for the transferring of colonies. YPAc plates were then incubated at 30 ˚C for ~ 48 h to allow for single colonies to grow. These colonies were then matched to the SD-dropout plates to confirm which cells were not petites. It was these

non-petite cells that were streaked onto a fresh SD-L-U plate and incubated again at 30 ˚C for ~ 48 h to allow for single colonies to grow for use in future experiments.

7.2.8   Cell culturing and DTT stressing for S. cerevisiae

A sterile wooden toothpick was used to select cells from a plate containing cells of the appropriate strain and mutation. This toothpick was then placed into 2 ml of media (either YPD or SD depending on the experiment) and cultured for 48 h prior at 30 ˚C, ~ 200 rpm (pre-culture). For the inoculation of larger volumes, 100 μl of pre-culture were added to 900 μl of fresh media and an optical density reading was taken at 600 nm (OD_{600}) using a colour density meter (WPA, Cambridge, UK. model no. CO8000). This allowed for initial OD_{600} readings to be calculated for inoculations of larger volumes of medium. For all *S. cerevisiae* experiments cells were cultured using the same parameters. Incubation was in a rotary incubator with a temperature of 30 ˚C and a shaking speed of ~ 220 rpm. DTT stressing was achieved by the treatment of cell cultures with 2 mM of DTT dispensed from a 1 M stock solution (stored at − 20 ˚C when not in use).

7.2.9   Protein extraction for western blotting analyses (Papa et al., 2003)

PWY260 containing the required mutation carried on the YCplac33 plasmid was grown over 48 h in 2 ml of SD-U media (pre-culture). 105 ml of fresh SD-U media were inoculated and grown in a 250 ml flask to an OD_{600} reading of 0.3 − 0.8 (mid-log phase). Once the culture had grown to within the desired OD_{600} range 50 ml were transferred to a 125 ml flask and treated with 2 mM of DTT. Flasks both with and without DTT were incubated for 2 h at 30 °C and 220 rpm. After 2 h, 50 ml of culture from DTT treated and untreated cells were transferred into separate, sterile 50 ml falcon tubes. Cultures were spun at 3750 × *g* for 2 min at 4 °C to separate the cells from the medium, the supernatant was discarded. Cells were washed with 5 ml of ice cold H_2O by spinning at 3750 × *g* for 2 min at 4 °C. The supernatant was discarded and the cells were washed again with 1 ml of ice-cold H_2O. The cells were resuspended in 1 ml of ice-cold H_2O and transferred into a 2 ml screw cap tube suitable for homogenisation. Cells were spun at 12000 × *g* for 1 minute at 4 °C and the supernatant was discarded. 200 μl of lysis buffer (8 M urea, 2.5% (w/v) SDS, 50 mM Tris·HCl pH 7.5 at 4 °C, 6 mM EDTA, 5 mM β-mercaptoethanol, 2 mM PMSF and 6 mM AEBSF) were added to the cells and around 0.5 volume of glass beads (Thistle Scientific, Glasgow, UK, cat. no. #11079105) were added. The cells were homogenised in a Precellys 24 instrument (Bertin Instruments, Montigny-le-Bretonneux,

France) at 6500 rpm for 3 cycles of 15 s at 4 °C. The cells were placed on ice for 5 min between cycles. The cells were then centrifuged at 12000 × *g* for 10 min at 4 °C, the supernatant was transferred to a fresh, sterile 1.5 ml screw cap tube and flash frozen in liquid nitrogen and stored at − 80 ˚C until required.

7.2.10 *Bicinchonic Acid (BCA) protein assay (Smith et al., 1985)*

To quantify how much protein was extracted a bicinichonic acid (BCA) assay was used. Protein lysates, BSA standards (0, 62.5, 125, 250, 500, 1000 and 2000 μg ml^{-1}) and blanks were diluted 1:10 with 0.1 M 2-iodacetamide in 0.1 M Tris-HCl (pH 8.0) and incubated in a 37 °C water bath for 20 min, this is to destroy the *β*-mercaptoethanol present in the lysate. 10 μl of sample were added to the bottom of a U-bottom 96 well plate. 200 μl of working solution (Table 2.) were added to each well, the plate covered and incubated at 60 °C for 30 min. Absorbance could then be read at 562 nm using the Molecular Devices SpectraMAX 190 (Molecular Devices LLC, Sunnyvale, California). These values allowed for the required dilutions for equal loading on the SDS-PAGE gel to be calculated.

7.2.11 *SDS-PAGE (Laemmli, 1970)*

Protein lysates were run on a 8% SDS-PAGE gel with a 1 mm spacing between the glass plates. The gel was made of a stacking gel and a separating gel. The composition of the stacking gel was 30% (w/v) acrylamide, 0.8% (w/v) bisacrylamide (2 ml), 1M Tris·HCl, pH 8.9 (1.875 ml), H$_2$O (3.603 ml), 10% SDS (50 μl), 10% ammonium persulphate (APS) (45 μl) and Tetramethylethylenediamine (TEMED) (10 μl). The separating gel composition was 30% (w/v) acrylamide, 0.8% (w/v) bisacrylamide (340 μl), 1M Tris·HCl, pH 6.8 (625 μl), H$_2$O (1.549 ml), 10% SDS (6.25 μl), 10% ammonium persulphate (APS) (22.5 μl) and Tetramethylethylenediamine (TEMED) (7.5 μl). These volumes were to cast one gel. After the addition of H$_2$O, the solution was degassed for 5 minutes.

Once polymerised, samples were diluted using H$_2$O to a concentration of 100 μg ml^{-1}. Prior to loading, 20 μl of protein at 100 μg ml^{-1} was mixed with 4 μl of 6 x SDS-PAGE loading buffer. This was then heated at 70 °C for 10 min, left to cool to room temperature and 20 μl were loaded into the wells. A molecular weight marker (Thermo Fisher Scientific, Cramlington cat. no. 26616) loaded into the first lane of the gel. The gel was run for 2 h at 100 V in a Fisherbrand TV100 gel system.

7.2.12 Western blotting and chemiluminescent detection (Towbin et al., 1979)

The gel was removed from the electrophoresis unit and the stacking gel removed. The separating gel was placed in semi-dry electrotransfer buffer for 30 min at 50 rpm at room temperature. A PVDF membrane (GE healthcare, Little Chalfont, Buckinghamshire, UK cat. no. 10600021) was cut to the size of the gel with an additional ~ 10% in both dimensions and soaked in 100% methanol for 10 min followed by 30 min in semi-dry electrotransfer buffer. 8 pieces of Whatmann 3 MM paper were cut to the size of the gel, with an additional ~ 10% in both dimensions, and soaked for 10 min in semi-dry electrotransfer buffer. Once all the components were prepared they were stacked onto the semi-dry horizon blot system (Atto, East Sussex, UK, Model #AE-6675L). The stacking of the components first involved the wetting of the anode and cathode plates of the blot transfer system with semi-dry electrotransfer buffer. 4 pieces of Whatmann paper were stacked onto the cathode with air bubbles removed from between each piece by rolling a glass tube over the stack with gentle pressure. The PVDF membrane was then placed over the Whatmann paper followed by the SDS-PAGE gel. Again, any air bubbles were removed as above. The final 4 pieces of Whatmann paper were stacked on top of the gel and again air bubbles were removed. The blot system was then closed to allow for transfer. The transfer was performed with a constant current of 2 mA/cm^2 of membrane for 1 h and 15 min. Once transferred, the membrane was stored in 5% milk-TBST at 4 °C on a shaker at 35 rpm for a minimum of 1 hour, ideally overnight.

The proteins were detected using specific antibodies. The appropriate antibodies were selected depending on the protein of interest. Antibody information can be found in Table 6. The membrane was incubated on a roller mixer at room temperature in 3 ml of 5% milk-TBST containing the appropriate primary antibody at an appropriate dilution (Table 6.) for 1 h. After incubation, the membrane was washed 4 times in 50 ml TBST at 50 rpm for 5 min each wash. The membrane was incubated as before with the appropriate secondary antibody with appropriate dilution (Table 6.), again the membrane was washed in TBST as above.

To detect the tagged proteins on the membrane a choice between two detection reagents was made, for lower amounts of loaded protein (< 10 µg) ECL2 (Pierce Thermo Fisher Scientific, UK, cat. no. 32132) was used. For higher amounts of loaded protein (> 10 µg) a detection reagent of 5 ml Tris·HCl pH 8.5 + 0.1% (v/v) Tween 20, 25 µl 250 mM luminol (Schneppenheim et al., 1991), 11.1 µl 90 mM *p*-coumaric acid and 1.45 µl 30% H_2O_2 was

used, or ECL (Pierce Thermo Fisher Scientific, Cramlington, UK, cat. no. 32106). 1 ml of the selected detection reagent was applied and allowed to develop at room temperature for 5 min.

Films were exposed to Thermo-Scientific CL – X-Posure X-ray film (Thermo Fisher Scientific, Cramlington, UK, cat. No. 34091.) for varying exposure times, from 30 s to 5 min, this was completed in a dark room. Films were developed using the Xograph Compact X4 (Xograph imaging systems, Stonehouse, UK).

7.2.13 Stripping of western blots

The PVDF membrane was washed in 50 ml 100 mM Tris·HCl + 0.1% (v/v) Tween 20 pH 8.5 for 5 min. The membrane was then incubated in 50 ml 100 mM Tris·HCl + 200 mM β-mercaptoethanol + 0.1% Tween 20 pH 8.5 for 15 min, this incubation was repeated with 50 ml of fresh 100 mM Tris·HCl + 200 mM β-mercaptoethanol + 0.1% Tween 20 pH 8.5 wash buffer, again for 15 min. The membrane was then washed twice in 50 ml of TBST at room temperature for 5 min. The membrane was then incubated twice at 37 ˚C for 15 min for each incubation in 100 mM glycine·HCl + 0.1% Tween 20, pH 2.5. Following this, the membrane was washed twice in 50 ml of TBST at room temperature for 5 min for each wash. Following this final wash, the membrane was placed in 5% milk + TBST and stored at 4 ˚C. Following stripping, the membrane could be re-probed with new antibodies if required.

7.2.14 Densitometric analysis

Densitometric analysis of the western blots exposed to X-ray film was completed using the ImageJ software (Public software developed at the National Institutes of Health, USA). Each band was selected in the software and its densitometry calculated by the software. Each of the Ire1 bands were standardised against the actin loading control bands for that lane on the gel.

7.2.15 Protein extraction for β-galactosidase assays

PWY260 containing the required mutation carried on the YCplac33 plasmid was grown over 48 h in 2 ml of SD-U medium (pre-culture). 55 ml of SD-U media were inoculated using the pre-culture and cells were grown to an OD_{600} of $0.3 - 0.8$ (mid-log phase). Once within this range a 15 ml sample from each culture were taken, spun at $3750 \times g$ for 2 min at 4 °C, the supernatant was discarded and the pellet flash frozen in liquid nitrogen and

stored at − 20 °C. The remaining culture was treated with 2 mM of DTT from a 1 M stock, and further 15 ml samples taken at 1 h and 2 h time points, pellets were collected and frozen as before. Once pellets for all time points were collected the frozen cell pellets were thawed and placed on ice. 1 ml of sterile H_2O was added to each tube and the pellet re-suspended. All of the cell suspension was transferred to a 2 ml flat-bottom screw cap tube. Tubes were centrifuged at 12000 × g for 1 min at room temperature and the supernatant was removed. The tubes were centrifuged again at 12000 × g for 1 min at room temperature and any remaining supernatant was removed. 100 µl of ice-cold Reporter Lysis Buffer (RLB) were added to each sample and pellets re-suspended by vortexing. ~ 150 mg of glass beads (Thistle Scientific, #11079105) were added to each tube and the tubes homogenised in the Precellys 24 instrument at 6500 rpm for 3 cycles of 10 s, a 5 min break was taken between each cycle during which time the samples were placed on ice. Following homogenisation 100 µl of ice cold RLB buffer were added to each sample and each tube was briefly vortexed. Samples were centrifuged at 12000 × g for 2 min at 4 °C to separate the supernatant which contained the protein. This supernatant was removed and placed in a screwcap tube suitable for cryo-storage. Protein lysate samples were flash frozen in liquid nitrogen and stored at − 80 °C.

7.2.16   DC protein assay

To quantify the total amount of protein in the lysate a DC assay (Bio-Rad, Hemel Hempstead, UK, cat. no. #500-0113 and #500-0114) was run. A BSA protein standard was prepared in H_2O with concentrations of 62.5, 125, 250, 500, 1000 and 2000 µg ml^{-1}, and 5 µl was added to a U-bottomed well (one well per standard). A 1:10 dilution (diluted in H_2O) of lysate was prepared of which 5 µl was added per well. 25 µl of DC assay reagent A (Bio-Rad #500-0113) were added to wells containing either the standard or the lysate followed by 200 µl of DC assay reagent B (Bio-Rad #500-0114). The plates were left at room temperature for 15 min after which the absorbance was read at 750 nm using the Spectramax 190 plate reader.

7.2.17 β-galactosidase assay (Miller, 1972; Schenborn and Goiffon, 1993)

To test the levels of β-galactosidase activity and therefore the expression of UPRE-associated genes the β-galactosidase reporter assay kit (Promega, Table 4.) was used. 1 µl of 1 U µl^{-1} of β-galactosidase was added to 99 µl of ice cold reporter lysis buffer (RLB),

mixed and placed on ice to create the 1:100 dilution. 10 µl of this 1:100 dilution were added to 900 µl of ice-cold reporter lysis buffer (RLB) to make a 1:10,000 dilution. A standard range was created of 0, 0.5, 1.0, 1.5, 2.0, 2.5, 3.0, 3.5, 4.0, 4.5 and 5.0 mU of β-galactosidase. Standards were diluted where appropriate in RLB. The appropriate volume of RLB was added to each well, followed by the required volume of sample to a total volume of 50 µl. 50 µl of 2X assay buffer (200 mM $Na_xH_{3-x}PO_4$ (pH 7.3), 2 mM $MgCl_2$, 100 mM β-mercaptoethanol, 1.33 mg ml^{-1} 2-nitrophenyl-β-D-galactopyranoside) were added to each well and the plate covered with parafilm and incubated at 37 °C for 30 min. Following incubation, 150 µl of Na_2CO_3 were added to each well to stop the reaction. The plate was then read on the Spectramax 190 plate reader at 419 nm.

7.2.18 Spotting assays

SD-U plates were used to spot WT, empty vector and mutants of the PWY260 and Y01907 strains. A pre-culture was grown in 4 ml of SD-U media at 30 °C at 220 rpm for 48 h and an OD_{600} reading was taken. Cells were diluted using fresh SD-U medium to the lowest recorded OD_{600} reading to ensure that equal numbers of cells were loaded to each plate for each mutant. DTT or tunicamycin (Tn) were used as ER stressors in increasing concentrations of 0, 1.5, 2.0, 3.0 and 4.0 mM DTT and 0, 0.2, 0.5, 1.0 and 2.0 µg/ml of tunicamycin.Samples were serially diluted from an undiluted culture down to a factor of $\times 10^{-5}$ of cells present in the undiluted culture. 3 µl of each dilution were spotted onto plates. Plates were incubated at 30 °C for 72 h before being photographed using the Enduro GDS Touch image capture system by Labnet (Windsor, UK, model GDS-1302) with an exposure time of 10 ms.

7.2.19 Cell culture for fluorescence microscopy

Cells were grown in 2 ml preculture in SD-L-U, containing increased concentrations of tryptophan and adenine sulphate (100 mg/l). 15 ml of the same media were inoculated with an initial OD_{600} of 0.05 and grown overnight at 30 °C at 220 rpm. Cells were harvested after overnight growth by centrifugation at 3750 × g for 2 min at room temperature. Cell pellets were then re-suspended in 1 ml of SD-L-U medium (as described above) and transferred to a 1.5 ml Eppendorf tube and centrifuged at 13,000 × g for 15 s at room temperature. The supernatant was removed and the pellet re-suspended in 250 µl SD-L-U media. In the case of stressed cells, DTT was added (2 mM concentration) to the re-suspended pellet at this point. 5 µl of cell suspension were placed on a glass slide and the

cover slip attached and sealed using nail polish. Slides were imaged using the Zeiss LSM 880 with Airyscan confocal inverted light microscope (Zeiss Ltd, Cambridge, UK). Details of system parameters can be found in Fig. 7.

7.2.20 Microscopy analysis

The microscope was set up using a two-channel approach to detect the GFP signal and the mCherry signal. For *Sec63*-GFP signal the Ch1-T1 (photomultiplier tube) channel was used with an excitation wavelength of 488 nm, an emission wavelength of 531 nm and a detection wavelength of 498 – 564 nm. For the *IRE1*-mCherry signal the Ch2 GaAsP-T2 (gallium arsenide phosphide detector) channel was used with an excitation wavelength of 594 nm, an emissions wavelength of 611 nm and a detection wavelength of 694 – 754 nm. The GaAsP channel was used as it has the increased sensitivity required for the signal detection of *IRE1*-mCherry. The objective lens used was the Plan-Apochromat 63x/1.4 Oil DIC M27 using the MDS 488/594 beam splitter. The 488 nm laser was used at a power of 5 – 8% and the 594 nm laser at a power of 28 – 40% to optimise image quality. Gain settings of 650 – 900 were used, again to maximise image quality and to reduce any background noise. Microscope settings are presented in Fig. 7 and were reused for each image capture.

	Channel 1	Channel 2
Contrast Method	Fluorescence	Fluorescence
Channel Name	Ch1-T1	Ch2 GaAsP-T2
Channel Description		
Channel Color	🟩	🟥
Excitation Wavelength	488	594
Emission Wavelength	531	611
Detection Wavelength	498-564	604-754
Depth of Focus		0.95 µm
Binning Mode	1x1	1x1
Detector	PMT	PMT
Detector Gain	750.0	750.0
Detector Offset	0	0
Detector Digital Gain	1.0	1.0
Airyscan Mode	Off	Off

Fig. 7 Settings of the Zeiss LSM 880 with Airyscan microscope. For each mutant, these settings were reused.

7.2.21 Zen Blue lite image presentation

Images captured using the Zeiss 880 Airyscan confocal laser scanning microscope were edited for presentation and file format conversion using the Zen blue lite 2.1 software (Zeiss Ltd, Cambridge, UK). The pseudo-colour for each channel was set to the best linear fit recommended by the software and scale bars added to each channel. This scale bar was used in figure preparation to ensue all images were scaled to the same size using the 5 µm scale bar as a reference. The images were saved and exported as JPEG files of the individual channels and the original data were kept.

7.2.22 Statistical analysis

Data from repeats of experiments (western blots, protein assays and β-galactosidase assays) were compiled and averages were calculated in Prism 7 software by GraphPad Software, Inc. (La Jolla, California). It was from these averages (mean) that the standard error of the mean (SEM) values were calculated, again in Prism 7. For all data where statistical analysis has been completed, the error bars are representative of SEM. To determine statistical difference ($p < 0.05$) between means of data sets a 2-way ANOVA test was used. The parameters of the test included the use of a Tukey test to correct for multiple comparisons using statistical hypothesis testing. A multiplicity adjusted p value was reported for each comparison, the adjustment was to account for multiple comparisons. A confidence level of 0.05 was used. As the ANOVA test assumes equal variance. β-galactosidase reporter data was logged using a natural base (ln). This was because the values gathered across the three repeats of β-galactosidase assays had unequal variances, tested using the Brown-Forsythe test in Microsoft Excel.

8.0 **Results**

8.1 Characterising the effects of ER stress on expression levels of IRE1

8.1.1 Rationale

To determine how *IRE1* expression in mutants was influenced by ER stress a biochemical approach was used. This is of interest as Ire1 is a ER stress response protein and the induction of ER stress in the differing a-loop mutants may affect *IRE1* expression differently. Additionally, it is important to confirm that the mutants are able to express *IRE1* from the plasmid, as a lack of expression would be detrimental to UPR activation and tolerance of ER stress (Cox et al., 1993; Morl et al., 1993). The plasmid contains an *IRE1-HA* gene which is critical to this experiment. The production of HA-tagged proteins by the cells allows for protein specific targeting utilising anti-HA antibodies (see materials and methods, Table 6). This means that by using the appropriate antibodies Ire1 protein can be detected through western blots. To quantify the relative levels of Ire1 a loading control was used. *β*-actin was chosen as it does not change expression with ER stress and should be uniform across mutants. Again, this can be detected using appropriate antibodies (Table 6) and using densitometric analysis the levels of Ire1 could be standardised against the levels of *β*-actin detected. Any increase in *β*-actin would indicate uneven loading of the gel. Prior to western blotting, the YCplac33 plasmid required transforming in PWY260 strain *S. cerevisiae*. YCplac33 was extracted from *E. coli*, enzymatically digested and the plasmid sequenced to ensure the correct mutations were present on the plasmid. Once confirmed the cells could be transformed with YCplac33 and the investigation into Ire1 levels completed.

8.1.2 Enzymatic digest results

Plasmids containing the a-loop mutations within the *IRE1* gene were extracted from the *E. coli* in which they were expressed (see materials and methods). These plasmids were digested using the *Kpn*I restriction enzyme (see materials and methods). This digest would confirm the plasmid by the production of three fragments of predicted sizes using the plasmid sequence information. Once digested, plasmids were run on a 1% agarose gel alongside uncut plasmid extract to view the fragments (Fig. 9). This was completed for the YCplac33 plasmid for use in *β*-galactosidase assays due to the incorporation of the UPRE-associated *LacZ* reporter and pEvA97 plasmid for use in fluorescent microscopy due to the incorporation of *IRE1*-mCherry.
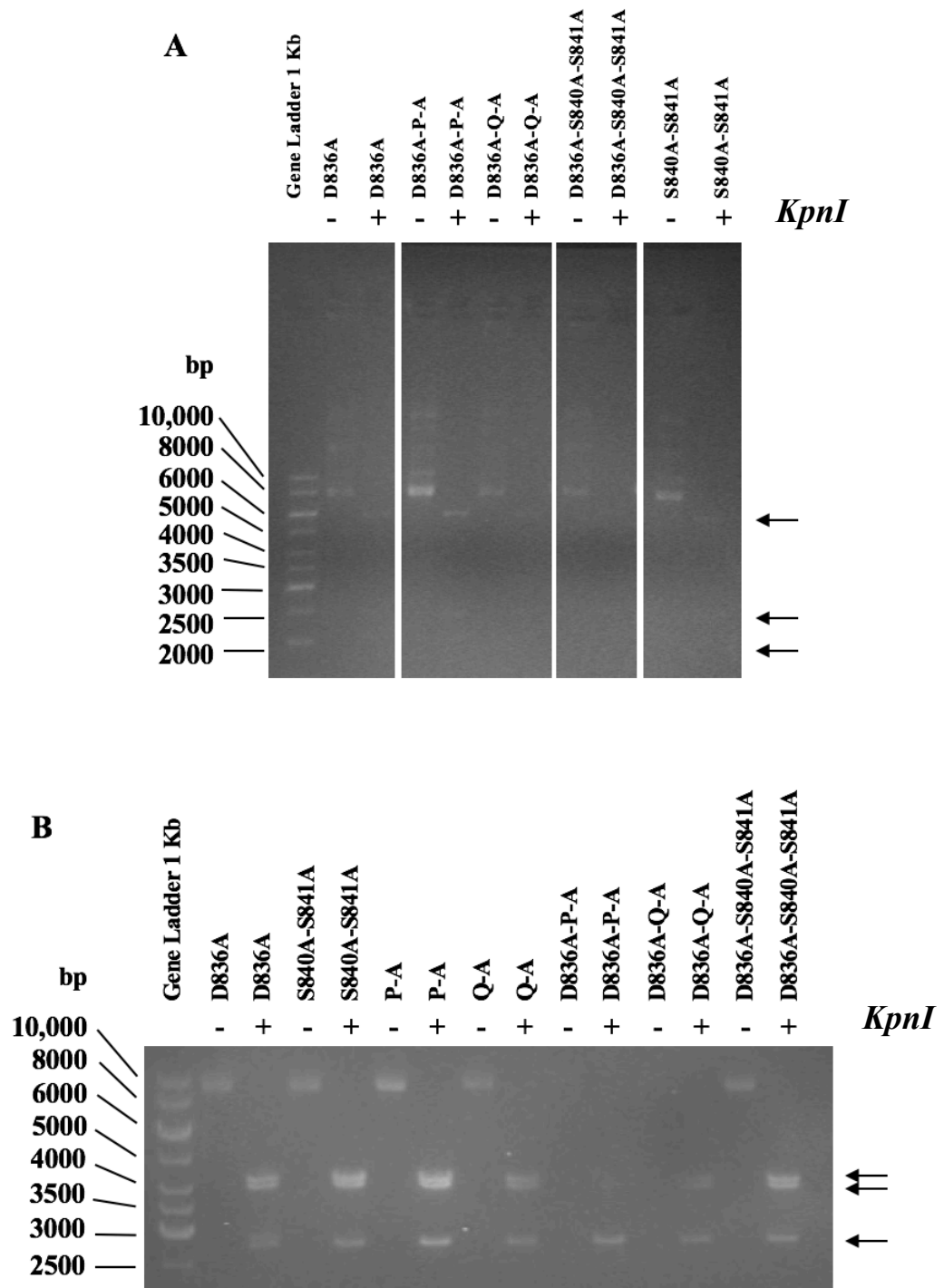
Fig. 8 Agarose gels of the plasmid extract and digested plasmid product of the YCplac33 plasmid (A) and the pEvA97 plasmid (B). In both cases the digested plasmid was cut into three fragments (this is less obvious on gel A however the additional two fragments can be seen towards the bottom of the gel). Digested products in both cases were produced through incubation with the *Kpn*I enzyme, presence of the enzyme is indicated by the - / + above each lane.

The fragments allowed for the sizing of the plasmid. YCplac33 is 10,569 bp in length, Fig. 8 A shows a band in the lane containing the digested product at around 6000 bps, a second band at around 2500 bp and a third at around 1500 bp, totalling around 10,000 bp. pEvA97 (Fig. 8 B) is 11,684 bp in length and shows bands of sizes around, 4300 bp, 4200 bp and 2800 bp, totalling around 11300 bp. In both cases, digestion of plasmid produced bands of lengths expected by the use of this plasmid and restriction enzyme. Due to the supercoiled nature of the undigested plasmids they do not migrate at the correct positions on the agarose gel as the coiled plasmid travels further down the gel.

8.1.3   Plasmid sequencing results

Following the digest of the plasmids and confirmation on the agarose gel, the plasmids were sent for sequencing using the 2721K primer. After confirming the plasmid was successfully extracted it is important to validate that the correct mutations were present in the nucleotide sequence, resulting in the change of the native amino acid to an alanine. Following sequencing (see materials and methods), the newly acquired nucleotide sequences were added to the BioEdit software and sequence alignment was completed (Fig. 9). At the sites where the sequence did not match the WT, the change was investigated. This was to confirm that the native amino acid residue seen in the WT was being changed to an alanine in the correct position in the *IRE1* gene on the plasmid and not another mutation. To give an example from Fig. 9 and Table 8 below, the WT at positions 7725 – 7727 in the sequence has a codon of GAC which codes for aspartic acid (the D836 residue to be exact). The sequence below the WT is of D836A which at the same position has a codon of GCT which codes for alanine (D836A). This confirmation was carried out for each plasmid that was sequenced. In the case of D836A-P-A a different codon is used from the single D836A mutant. This was not considered an issue providing the correct amino acid was coded for. In this case, GCC also codes alanine. Changes to the nucleotides at all the residues used in this work are in Table 8. The relative positions of these mutations can be seen in Fig. 2.
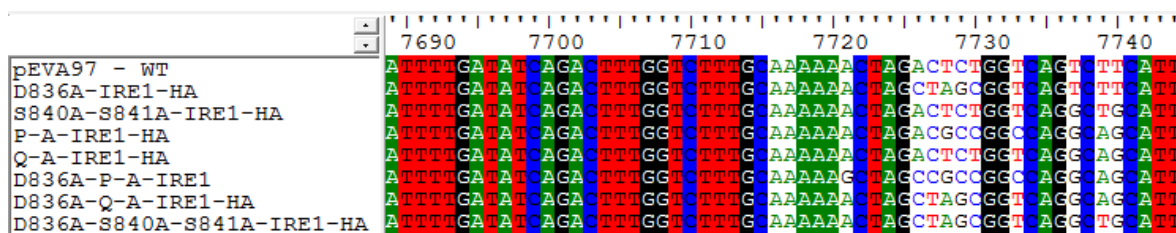
Fig. 9 An example of the sequence alignment used, in this case showing the pEvA97 plasmids using the BioEdit software. The coding sequence was compared to that of the WT to ensure the expected mutations were present and that the change to the coding sequence was correct.

Table 8. pEvA97 plasmid mutants. This table shows the reading frame of the sequences and the changes made to the nucleotide sequence create the desired mutant. The analysis of the changes to the sequence shown here illustrate how the differences in sequence alignment in the BioEdit software were validated (Fig. 9). Fig. 2 highlights the mutations included in Q-A and P-A mutants.

Mutant	Position (836)	Position (837)	Position (840)	Position (841)	Position (844)	Position (850)
WT	GAC → Asp	TCT → Ser	TCT → Ser	TCA → Ser	ACA → Thr	TCT → Ser
D836A	GCT → Ala	AGC → Ser	TCT → Ser	TCA → Ser	ACA → Thr	TCT → Ser
S840A-S841A	GAC → Asp	TCT → Ser	GCT → Ala	GCA → Ala	ACA → Thr	TCT → Ser
P-A	GAC → Asp	GCC → Ala	GCA → Ala	GCA → Ala	GCA → Ala	GCA → Ala
Q-A	GAC → Asp	TCT → Ser	GCA → Ala	GCA → Ala	GCA → Ala	GCA → Ala
D836A-P-A	GCC → Ala	GCC → Ala	GCA → Ala	GCA → Ala	GCA → Ala	GCA → Ala
D836A-Q-A	GCT → Ala	AGC → Ser	GCA → Ala	GCA → Ala	GCA → Ala	GCA → Ala
D836A-S840A-S841A	GCT → Ala	AGC → Ser	GCT → Ala	GCA → Ala	ACA → Thr	TCT → Ser

Once the plasmids had been aligned and mutations confirmed PWY260 and MSY14-02 cells were transformed with the plasmids, (see materials and methods and Fig. 6).

8.1.4 Western blot results

The mutants created through the transformation of PWY260 cells with YCplac33 required testing to ensure expression of the Ire1 present on the YCplac33 plasmid. This utilised the HA tag present on plasmid encoded *IRE1*. It was of interest to know if cells would attempt to compensate for a lack of Ire1 capable of accepting phosphates to the a-loop by producing more Ire1 to attempt to rectify inefficient UPR activation of Ire1 phospho-mutants and elevate the ER stress. Additionally, it is important to ensure that mutants behave as close to the WT in terms of levels of Ire1 protein production as possible. This will ensure that any reduction in UPR activation in these mutants is not simply an artefact of reduced Ire1 protein levels in cells whilst under ER stress, when compared to the WT. Proteins were extracted from cells during their mid-log phase. After 100 µg of the proteins were separated on an 8% SDS-PAGE gel, they were transferred onto PVDF membranes and blotted for Ire1-HA and the actin loading control (Fig. 10 A) as described in materials and methods. Following blotting and exposure to X-ray film the bands were subjected to densitometric analysis using ImageJ software. (Fig. 10 B).
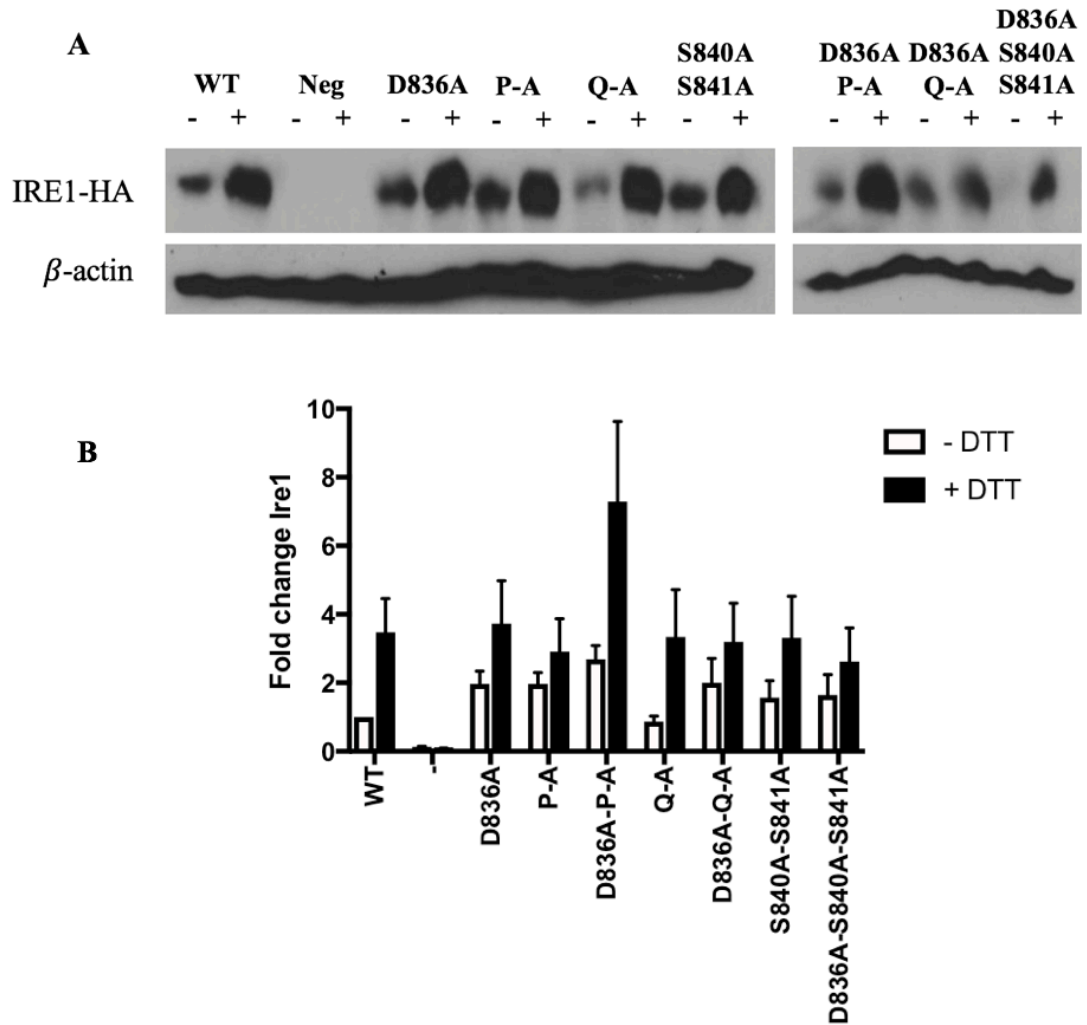
Fig. 10 Representative blot data for a-loop mutants. (A) Western blot for Ire1-HA (~ 127 kDa) and β-actin as a loading control (MW ~ 35 kDa). This blot used 100 µg of protein lysate and ECL as the detection reagent. (B) Densitometric analysis of blots was completed using ImageJ. Induction of Ire1 with ER stress can be seen with a minimum of ~ 2-fold change in all mutants when compared to the unstressed wild type, (ER stress induced using 2 mM DTT). Between the mutants and WT under the same ER stress conditions, no statistical difference was calculated. Relative Ire1 was measured against β-actin as a loading control and fold change was calculated by standardising against WT under no DTT stress. The error indicated is the standard error of the mean across three repeats.

Fig. 10 (A) shows that with 2 mM DTT treatment an increase Ire1 expression was observed in all mutants and the WT. Fig. 11(B) shows that in all cases the increase in Ire1 expression is ~ 2.0 - 4-fold, when compared to WT under no ER stress. D836A-P-A shows ~ 6.5-fold increase in detected Ire1 when compared to the untreated WT, however, it can be seen that the standard error of the mean (indicated by the error bars) is the largest for this sample. It was found that there is no statistical difference using a 2-way ANOVA test between different mutants under the same stress conditions when compared to the WT. This is important as it suggests that in all mutants, there is no difference in relative Ire1 expression levels with the introduction of ER stress when compared to the WT. In terms of the UPR, this suggests all mutants are equally capable of Ire1 protein expression and they all induce this expression at levels seen in the WT. In an experiment designed to investigate the role phosphorylation plays in relation to RNase activity of Ire it is important to ensure that all the mutants express Ire1 protein effectively and that this expression is comparable to the WT under stress conditions. Here, the data suggest that the induction of *IRE1* and the levels of Ire1 protein from the WT and mutants under both stressed and non-stressed conditions is comparable. This means that the increase or decrease or decrease in *HAC1* mRNA splicing seen in Fig. 5 is not resulting from varying Ire1 levels across the mutants.

8.2   *Characterising the effects of mutations within the a-loop on the induction of an UPRE-β-galactosidase reporter*

8.2.1   *Rationale*

The retention of some level of RNase activity by mutants that lack phospho-acceptor residues within the a-loop of Ire1 (Fig. 5) presented the question of, is there a compensatory system in place for the activation of the RNase domain of Ire1 in the event of a loss of phospho-acceptor? A likely candidate was deemed to be the D836 residue within the a-loop based on its negative charge and a possible ability to mimic the interactions of the phosphorylated a-loop. Additionally, should the D836 residue provide a basic level of RNase activation, then would the mutation of this residue to D836A result in a phenotype when compared to the WT? Furthermore, if the hypothesis that D836 can compensate for loss of phosphorylation of the a-loop is true, does this compensation affect different phospho-mutants to the same extent? To characterise the role of D836 and the effect of phospho-acceptor site mutations within the a-loop and how these affect the activation of the UPR, activation was measured using a UPRE-associated-β-galactosidase

reporter assay. Should the D836 residue allow for a bypass of the phospho-acceptor residues within the a-loop then UPR-activation should not be exhibited in phospho-mutants containing a D836A mutation.

β-galactosidase is an enzyme that catalyses the hydrolysis of β-galactosides such as the ortho-nitrophenyl-β-galactoside (ONPG) contained within the 2X assay buffer used in this assay. The reporter is constructed so that the *E. coli* gene *lacZ* (which encodes β-galactosidase) uses the promoter of the UPR-induced gene *KAR2* which displays increased expression under ER stress (Kohno et al., 1993). As ER stress induces the UPR, *KAR2* is expressed, due to the UPRE within its promoter, and consequently *lacZ* is also expressed. The β-galactosidase produced cleaves ONPG producing galactose (colourless) and *o*-nitrophenol (yellow) allowing for a measure of colour change (measured at 419 nm) indicative of reporter activity, see materials and methods. The UPR-associated gene *KAR2* requires mature *HAC1* mRNA to be translated to activate expression (Mori et al., 1992; Kohno et al., 1993; Kimata et al., 2003; Montenegro-Montero et al., 2015), therefore the RNase domain must be activated to splice *HAC1* mRNA to produce this mature product. To combine all of this, a stronger colour change suggests a stronger induction of UPRE-associated genes, suggesting stronger RNase activation and UPR-activation. The detection of both spliced and unspliced *HAC1* mRNA in northern blots (Fig. 5) is sufficient to indicate the presence of mRNA in the sample however to elevate ER stress, the UPR utilises proteins. It has been shown in a global analysis of protein expression in yeast that the concentrations of many proteins within a cell are not predictable by mRNA levels (Ghaemmaghami et al., 2003). The use of a UPRE-associated reporter assay allowed for investigation of the UPR protein expression activity induced by Ire1 ER stress signalling through the activity of an associated reporter. To quantify this response, the quantity of β-galactosidase was standardised against total protein content calculated from DC assays. This gave mU of β-galactosidase per mg of total protein. The WT and empty vector (negative) cells served as baselines to which the activation of the UPR in all mutants could be compared. Additionally, the mutants containing a D836A mutation were compared to phosphorylation mutants which contained the native D836. If indeed D836 is playing a compensatory role, then the residual UPR activation should be completely halted with the inclusion of the D836A mutation to phospho-acceptor site mutants. As the concentration of β-galactosidase reduces dramatically in the event of a-loop phospho-acceptor site mutation, to analyse the β-galactosidase data values were logged using the natural log base

(ln) allowing for 2-way ANOVA analysis to be completed. The data are logged for ANOVA because the data are heteroscedastic, which violates the ANOVA assumption of homoscedastic data, this was confirmed with the use of a Brown-Forsythe test.

8.2.2 *β-galactosidase reporter assay results*

To assess reporter activity 15 ml samples were taken at the 0 h time point and compared with 15 ml samples after 2 h of exposure to 2mM DTT. It was found that the extent of the reduction in phospho-acceptor residues affected levels of attenuation in UPR activation observed in the assay. The S840A-S841A mutant seemed to suffer the least attenuation, with P-A having the highest and Q-A the middle level (Fig. 11). This suggests that with an increase in the number of mutations to phosphorylation sites within the a-loop comes an increased attenuation in the UPR indicated by reporter activity. The S837 residue and its role in ER stress response has not previously been documented experimentally. The data presented here show that a mutation at this site negatively impacts on the reporter activity suggesting a reduction in the effectiveness of the UPR. The Q-A mutant and the P-A mutant are identical apart from P-A includes S837A. The data show that the P-A mutant, which includes S837A, shows less reporter activity than that shown by the Q-A mutant (Fig 11 and Table 9), suggesting that the S837 residue is involved in the activation of Ire1. When the reporter activity of the S840A-S841A, Q-A and P-A mutants was compared to the empty vector negative control it was found that in all cases there was a statistical difference (2-way ANOVA). This implies that a level of ER stress response is retained, as the empty vector should serve as a baseline for no Ire1 activity.
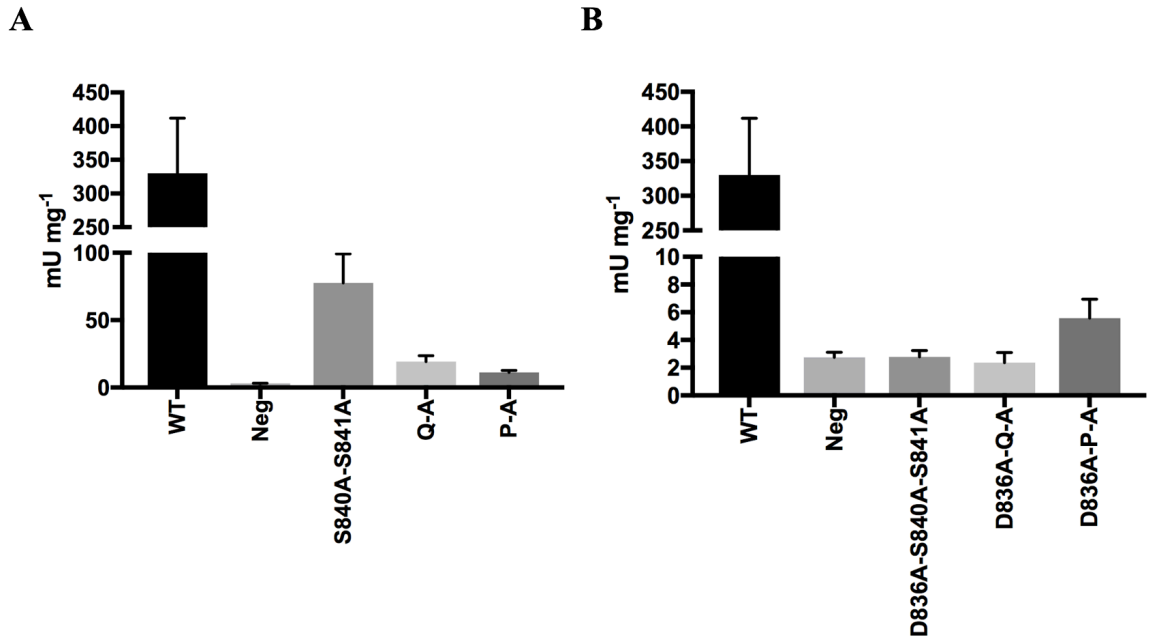
Fig. 11. Compiled data from three repeats of the *β*-galactosidase reporter assays show that the more extensive phospho-acceptor mutants have a more diminished ER stress response (A). The S840A-S841A mutant retains the highest level of UPRE-associated reporter expression, indicated by reporter activity. The Q-A mutant, with the S837 residue remaining shows the next highest levels of reporter activity when compared to the WT. The inclusion of the S837A mutation in the P-A mutant reduces activity the most when compared to the WT. The inclusion of the D836A mutation to the phospho-mutants reduces ER stress response to levels seen in the empty vector (Neg), confirmed with 2-way ANOVA statistical analysis.

Next the D836 residue was investigated to determine if it is providing a level of compensatory Ire1 activation in the event of a loss of phosphorylation capability within the a-loop. To investigate this, first the WT was compared with an empty vector negative control and the D836A mutant (Fig. 12 panel A). The data show that the mutation of the D836 residue within the a-loop alone, as this mutant still possesses a-loop phosphorylation capacity, does not attenuate expression of the *lacZ* reporter and by extension *KAR2* which implies RNase activation and UPR activation. When compared statistically using a 2-way ANOVA, no difference was observed between the WT and D836A mutant in data gathered from three repeats (Table 9) indicating that the D836 residue does not play a primary or indispensable role in RNase activation on its own. Next the effect of combining the D836A mutation with the phosphorylation site mutations was investigated (Fig 12 panels B, C and

D). This is presented alongside the data for phosphorylation residue mutants without the D836A mutation. The data show that in all cases there is significant reduction in the activation of the reporter and when compared to the WT, (analysed using 2-way ANOVA, information in Table 9.) The inclusion of the D836A mutation to the S840A-S841A, Q-A and P-A phospho-mutants eliminates the residual activity detected in phospho-mutants (Fig. 11). To analyse the level of this further attenuation, a two-level statistical analysis approach was taken. Firstly, it was assessed if the inclusion of D836A produced a significantly different ($p < 0.05$) result from the phospho-acceptor mutants lacking D836A. This was shown to be true for S840A-S841A and Q-A mutants (Fig. 12). When D836A was included in these two mutants there was statistical difference calculated (Table 10) using a 2-way ANOVA. The same statistical difference was not seen in the P-A vs. D836A-P-A test (Fig. 12 D). This may be due to the highest reduction in β-galactosidase reporter activity being in the P-A mutant when compared to the WT (Fig. 11). Since the P-A mutant had the lowest recorded reporter activity this could explain why the difference between the P-A and D836A-P-A mutant may not be significant, as the P-A mutant is already at such a low level the ANOVA test may be unable to determine a statistical difference between the means of the data sets and would require a higher number of repeats than the three used here.

The next statistical comparison made was between the D836A-phospho-acceptor mutants and the empty vector. This allowed for it to be determined if the inclusion of D836A eliminated the residual ER stress response or if it simply attenuated the response further. It was found that there was no statistical difference (2-way ANOVA) between the D836A-S840A-S840A, D836A-Q-A and D836A-P-A mutants when compared to the empty vector (Neg) (Table 9) suggesting that the reduction in ER stress response was absolute.
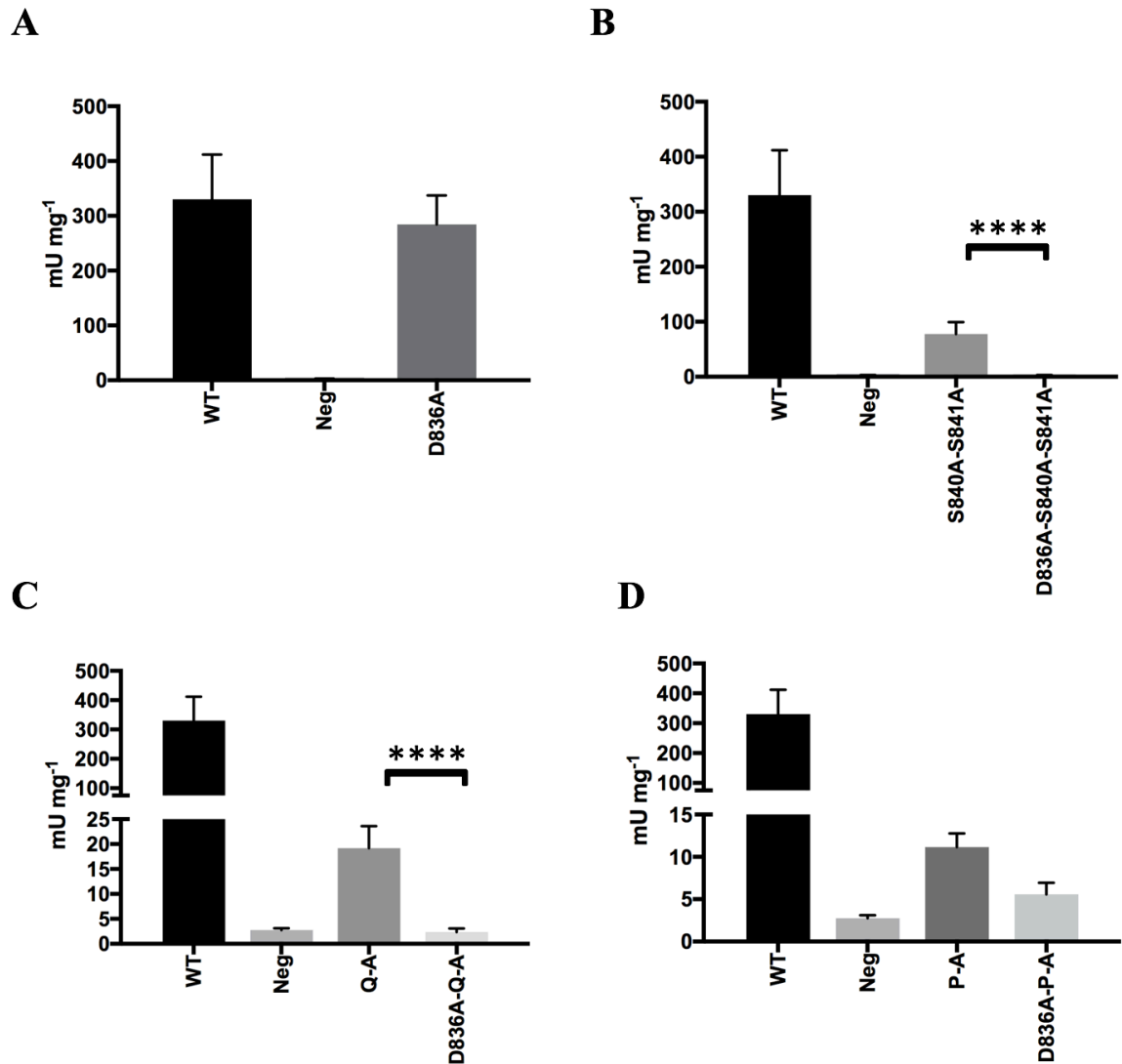
Fig. 12 Complied data from three repeats of the β-galactosidase assays. These data were subject to a 2-way ANOVA test to determine statistical difference ($p < 0.05$) using all data. This analysis showed that there were statistical differences when the means were compared between S840A-S841A and D836A-S840A-S841A mutants as well as between Q-A and D836A-Q-A mutants. WT and empty vector (Neg) data is repeated data in each panel however is compiled from three repeats.

Table 9. The p values calculated from the 2-way ANOVA between WT and the mutants and the empty vector (Neg) and the mutants. It was found that when compared to the WT all the phospho-acceptor mutants were statistically different. This was also the case with phospho-acceptor mutants containing D836A mutations. Importantly there was no statistical difference between WT and the D836A mutant. When compared to the negative control, the phospho-acceptor mutant differences were all statistically significant, however, with the inclusion of the D836A in these mutants showed no significant difference when compared to the negative control.

Tukey's multiple comparisons test	Significant	Adjusted P Value
WT vs. Neg	Yes	< 0.0001
WT vs. D836A	No	> 0.9999
WT vs. S840A-S841A	Yes	0.01
WT vs. D836A-S840A-S841A	Yes	< 0.0001
WT vs. Q-A	Yes	< 0.0001
WT vs. D836A-Q-A	Yes	< 0.0001
WT vs. P-A	Yes	< 0.0001
WT vs. D836A-P-A	Yes	< 0.0001
Neg vs. D836A	Yes	< 0.0001
Neg vs. S840A-S841A	Yes	< 0.0001
Neg vs. D836A-S840A-S841A	No	> 0.9999
Neg vs. Q-A	Yes	0.0005
Neg vs. D836A-Q-A	No	0.9974
Neg vs. P-A	Yes	0.0238
Neg vs. D836A-P-A	No	0.8544

Table 10. Statistical comparison using 2-way ANOVA between the a-loop phospho-acceptor mutants and a-loop phospho-acceptor mutants containing D836A.

Tukey's multiple comparisons test	Significant?	Adjusted P Value
S840A-S841A vs. D836A-S840A-S841A	Yes	< 0.0001
Q-A vs. D836A-Q-A	Yes	< 0.0001
P-A vs. D836A-P-A	No	0.7118

8.2.3   D836 plays a role in Ire1 stress signal transduction

In all β-galactosidase assay experiments, the D836A mutant exhibited the same levels of UPR activation as the WT with no statistical difference in any of the repeats (Fig 12 A and Table 9). However, with all mutants containing a-loop phospho-acceptor mutations there is an attenuation of reporter activity in the assay suggesting that UPR activation is reduced (Fig. 11 A). This lack of ER stress response may be because of reduced RNase activation in phospho-acceptor site mutants. This is because it is thought that phosphorylation of the a-loop plays a role in RNase activation through the stabilisation of an oligomer-compatible conformation (Korennykh et al., 2009), or through activation of the kinase domain (Lee et al., 2008) possibly by interacting with catalytic sites within the kinase domain (Johnson et al., 1996; Knighton et al., 1991; Nolen et al., 2004). The increase in the number of phosphorylation site mutations in S840A-S841A, Q-A and P-A mutants corresponds to a reduction in the levels of β-galactosidase reporter activity (Fig. 11 A). Maximum retention of reporter activity was observed in the S840A-S841A mutant, which still possesses phosphoserine at positions 837 and 850 and phosphothreonine at 844. Whereas the minimum reporter activity was measured in the P-A mutant which possesses no phospho-acceptor sites within the a-loop. In the cases of the D836A-S840A-S841A, D836A-Q-A, and D836A-P-A mutants, no statistical difference was observed between the D836A-phospho-mutants and the empty vector (Table 9). These data suggest that D836 plays a role in the ER stress response. Furthermore, that the level of the UPR activation, when reliant on D836, is influenced by phosphorylation of the S837, T844 and S850 residues. This also suggests that the S837, T844 and S850 resides are not capable of producing an ER stress response signal without the D836 residue. If these residues could produce an ER stress response the D836A-S840A-S841A mutant would have retained levels of reporter activity facilitated by the phosphorylation of S837, T844 and S850 and induction of the

UPR. This was not the case (Fig. 11 B), it was observed that in the D836A-S840A-S841A mutant β-galactosidase reporter activity was reduced to level of the empty vector (Fig. 12 B). Furthermore, this supports the notion that the S840 and S841 residues may play the role of primary phosphorylation sites within the a-loop (Nolen et al., 2004), and the S840 and S841 residues, perhaps working in tandem, are the primary phosphorylation residues (Shamu and Walter, 1996) as the D836A single mutant was unaffected in terms apparent of Ire1 activation. The shows that S840 and S841 does not require D836 to activate Ire1 through phosphorylation, contrary to the S837, T844 and S850 mutants.

To summarise, when phosphorylation within the a-loop is not possible D836 seems to be able to facilitate a reduced level of Ire1 activation. This compensatory system seems to allow for partial or complete loss of phosphorylation activity within the a-loop while still allowing for reduced levels of ER stress signal transduction. Should the phosphorylation of S837, T844 or S850 be possible, then the ability of D836 to mount this induction is maximised. The observation of different levels of reporter activity in the different phospho-mutants and the elimination of residual reporter activity in D836A-inclusive phospho-mutants prompted the investigation of ER stress tolerance of the mutants *in vivo* using spotting assays.

8.3 *Evaluating the effect of a-loop mutations on ER stress tolerance and survival*

8.3.1 *Rationale*

The UPR is known to be involved in ER stress tolerance, which promotes survivability of ER stress (Jäger et al., 2012). A reduced UPR activation should therefore result in reduced ER stress tolerance. To assess if the reduction in the ER stress response observed in the β-galactosidase assays translated into reduced survivability of ER stress *in vivo*, spotting assays were used. Spotting assays allow the survivability of ER of the mutants to be tested when grown on medium containing an ER stressor, in this case increasing concentrations of DTT and tunicamycin (Tn). Cells were serially diluted and spotted onto the DTT and Tn plates (see materials and methods). Stressing cells with mutations at a-loop phosphorylation sites thought to be crucial to UPR activation should highlight any deficiencies in ER stress survivability. It is of interest as to whether the more extensive mutants (Q-A and P-A) suffer with more reduced ER stress tolerance when compared to the less extensively mutated S840A-S841A and D836A mutants. Again, the inclusion of D836A to the phospho-acceptor mutants will allow for the role D836 plays in ER stress response to be characterised. When compared to the WT it was expected that the S840A-

S841A, Q-A and P-A mutants should show a reduction in ER stress tolerance manifested by a reduction in growth under ER stress. The D836A-S840A-S841A, D836A-Q-A and D836A-P-A mutants were expected to suffer an even larger reduction in ER stress tolerance that that seen in the other phospho-mutants. This was expected following the observations made in the β-galactosidase reporter assays. Mutants with and without the D836A mutations were spotted next to each other to visualise the impact of D836 on ER stress tolerance and survivability of ER stress. The spot on the far left of each row at each concentration, is the undiluted cells (all standardised to the lowest recorded OD_{600} value, see materials and methods). Each spot to the right reduces in the number of cells initially spotted by 10-fold to a final dilution of 10^{-5} of the original cell number.

8.3.2   Results

Spotting assays of Ire1 mutants show that D836 allows for better ER stress tolerance in phospho-mutants when compared to D836A-phospho-mutants. Fig. 13 shows that under DTT induced ER stress, the D836A mutant shows the same level of growth across the increasing concentrations of DTT as seen in the WT. Reviewing the phospho-acceptor mutants, S840A-S841A shows the next highest levels of tolerance, achieving growth at 4 mM of DTT in cells spotted with a dilution factor of 10^{-2}. There are also very low levels of growth of cells with a dilution factor of 10^{-3}. The Q-A was the next most tolerant of ER stress, again showing growth of cells at 4 mM DTT although not as strong growth as that seen in S840A-S841A, with cells growing only to the spot where the dilution factor was 10^{-1}. Finally, the P-A mutant showed the lowest tolerance of ER stress with growth at 3 mM and very limited growth at 4 mM in the undiluted cell spot (much lower growth than S840A-S841A and Q-A). Reviewing the addition of the D836A mutation to the phospho-acceptor mutants, D836A-S840A-S841A and D836A-Q-A both show around the same level of reduction in stress tolerance with growth stopping at around 2 mM of DTT, D836A-Q-A tolerating ER stress perhaps slightly better at this concentration (up to a dilution factor of 10^{-3}). The D836A-P-A mutant survives marginally worse with growth again until 2 mM DTT, but in this case, only at the undiluted cell spot with very marginal growth beyond that.
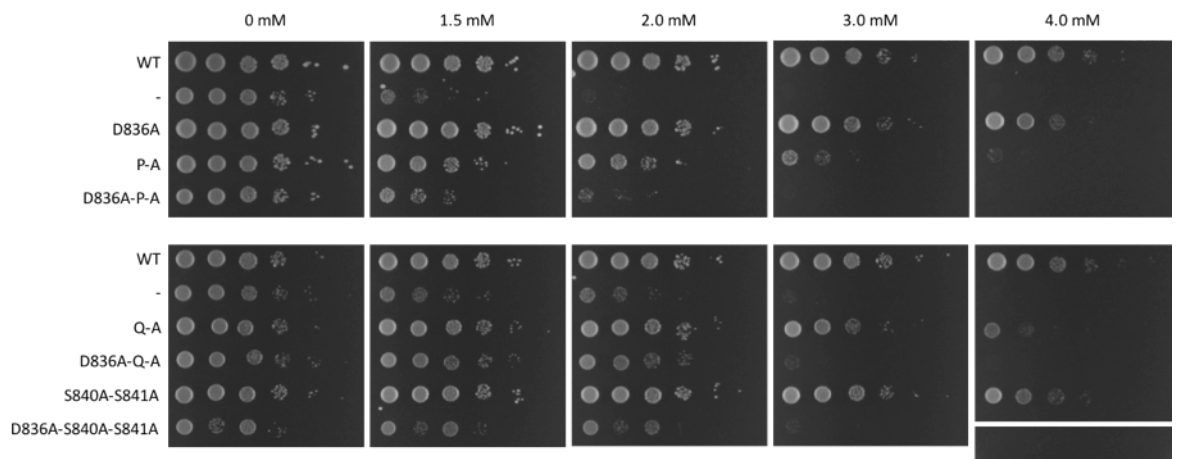
Fig. 13 Spotting assays of PWY260+YCplac33-IRE1-HA cells on plates with increasing DTT concentrations. The results show that the inclusion of the D836A mutation to the a-loop phospho-mutants decreases survivability of ER stress in cells at lower concentrations of DTT. These assays were repeated three times with reproducible results.

The same cell cultures of WT and the negative empty vector were spotted in Fig. 13. It can be seen that in the 2 mM plates, the empty vector shows growth on the bottom row, and no growth on the plate on the top row of the same concentration. As shown in the *β*-galactosidase reporter assay data, the D836A-inclusive-phospho-mutants show levels of UPR activation seen in the empty vector (Fig. 11), as well as the empty vector itself showing no reporter activity. These data would suggest that at the same concentration used in the *β*-galactosidase, there would be an inability to tolerate ER stress as the UPR would not be activated. So how is there some growth of the empty vector with 2 mM of DTT. This may be a result of DTT exposure in different culturing methods. In liquid culture the DTT exposure, and therefore ER stress induction, is uniform. This is due to the constant agitation of the culture during incubation ensuring all cells are equally exposed to DTT. This may not be the case in spotting assays. A concentration gradient may develop over time on the plates used in the spotting assay as a result of metabolism or oxidation of the DTT. This could result in some cells being exposed to differing levels concentrations of DTT than others.

The PWY260 cells were also spotted onto plates containing Tn (Fig. 14), in this case results were different. Cells showed little to no growth with the introduction of Tn induced ER stress. The D836A mutant however showed increased tolerance of ER stress when compared to the WT, with colonies visible up to Tn concentrations of 1.0 μg ml^{-1}. No other mutants showed growth, even at the lowest Tn concentration of 0.2 μg ml^{-1}.
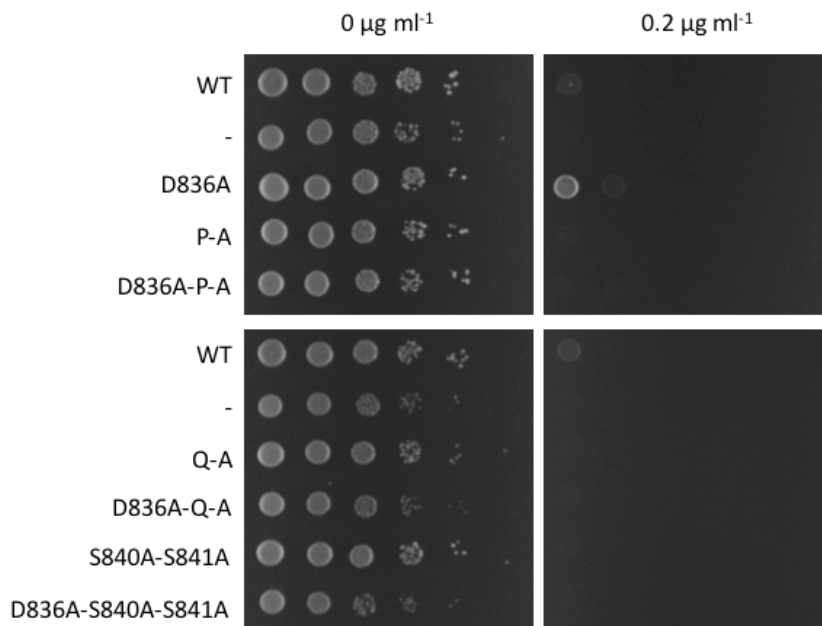
Fig. 14 Spotting assays of PWY260+YCplac33-IRE1-HA cells on plates increasing in Tn concentration. The results show the inclusion of all mutations within the a-loop decreases survivability of cells to the extent that growth is not recorded, exceptions being in WT and D836A at lower Tn concentrations. Interestingly the D836A mutant showed increased ER stress tolerance than that observed in the WT with stronger growth of cells at a dilution factor of 10^{-1} at a Tn concentration of 0.2 μg ml^{-1}. This phenotype was seen on all three repeats of these spotting assays.

In addition to the Q-A mutant, constituent mutants of Q-A (S840A, S841A, T844A and S850A) were spotted on plates of increasing DTT and Tn (Fig 15). These mutations were also on the YCplac33 plasmid, transformed into the Y01907 strain. Phosphorylation of the a-loop is documented, often by reviewing complex double, triple or even more extensive mutants. Using a single residue mutation approach, it is possible to characterise the level of

participation of individual phosphorylation sites within the a-loop in relation to ER stress tolerance.

In the case of DTT stress (Fig. 15 A), the S840A mutant possesses the highest tolerance of ER stress of the mutants when compared to the WT, achieving growth at 4 mM of DTT (growth achieved at the 10^{-2} dilution factor spot). The S841A and T844A mutants seem to suffer in stress tolerance to comparable levels to one another when compared to the WT, both achieving growth to 4 mM DTT (10^{-1} dilution factor spot). The S850A mutant, however, seems to show an increased tolerance to DTT-induced ER stress when compared to the WT showing growth up to the spot of cells diluted to a factor of 10^{-4}. The pattern of these findings was replicated with Tn-induced ER stress (Fig.15 B).
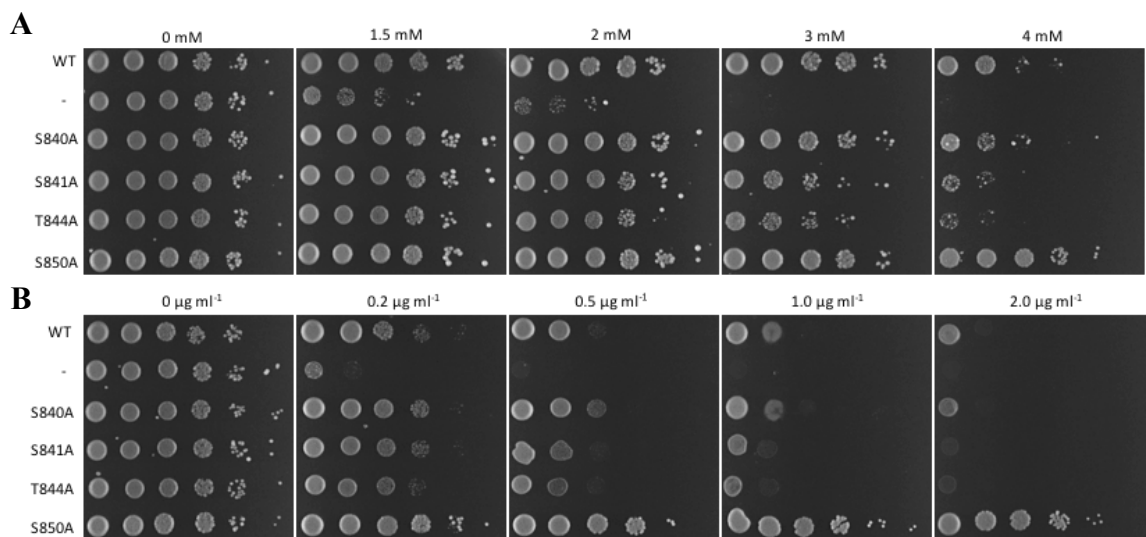
Fig. 15 Spotting assays of Y01907+YCplac33-IRE1-HA cells possessing the single point constituent mutants of Q-A within the a-loop on plates increasing in DTT (A) and Tn (B) concentration. Results show that in the case of both DTT and Tn, the mutation at phospho-acceptor sites reduces survivability with the exception of S850A, which appears to have improved survivability when compared to the WT. This phenotype was seen across the two repeats carried out.

8.3.3 D836A mutation results in the reduction of ER stress tolerance in phospho-mutants

Data presented suggests that the mutation of multiple phosphorylation residues has a cumulative effect on ER stress tolerance. The more extensive P-A mutant show the largest reduction in survival of ER stress whereas the S840A-S841A mutant showed the smallest reduction (Fig. 13). The D836 residue in all phospho-mutants further reduced the survivability of ER stress, to levels seen in the empty vector negative.

An interesting result was the improvement of ER stress survival of the S850A mutant when compared to the WT (Fig. 15). With the UPR promoting tolerance to ER stress (Jäger et al., 2012; Lin et al., 2007), the data from spotting assay experiments suggest that the S850 residue of the a-loop may provide a level of control to ER stress signalling when the other a-loop phospho-acceptor sites are phosphorylated. With the S850A mutation this control may be removed, allowing for unrestricted UPR activation resulting in improved survivability of ER stress compared to the WT.

The D836A mutant increasing survivability under Tn stress conditions in PWY260 is more obscure (Fig. 14). As seen in the *β*-galactosidase assay results, D836A mutants did not elicit higher levels of reporter activity suggesting that UPR activation was not elevated. This raises the question as to why the D836A mutant would achieve growth at higher Tn concentrations than achieved by the WT? It may be a possibility that the Tn may have a differing effect on Ire1 in PWY260 as this phenotype was not observed in cells grown under ER stress induced by DTT. However, in the literature it has been shown that WT *S. cerevisiae* cells should be able to tolerate concentrations of Tn used in this work (Lee et al., 2008; Schröder et al., 2003). This could mean that either the PWY260 cells are much more sensitive to Tn stress than Y01907. Alternatively, there may have been an error regarding the concentrations of Tn used. To establish either of these theories, the spotting assay would require repetition on plates with lower concentrations of Tn, using both PWY260 and Y01907 strains.

The role D836 plays in the ER stress response seems to impact on the ability for cells to tolerate ER stress. With DTT stress, the S840A-S841A and Q-A mutants showed reduced survivability when compared to the WT. The more extensive P-A mutant appeared to be more susceptible to ER stress (Fig. 13). This reduction in survival of ER stress was not absolute. With the inclusion of D836A to the phospho-acceptor mutants, all cells show a further reduction in ER stress tolerance induced by DTT, to that seen in the empty vector. The UPR in yeast is involved in promotion of cell tolerance, and survival of ER stress

(Chen and Brandizzi, 2013; Jäger et al., 2012; Lin et al., 2007) the results presented here indicate that the failure to alleviate ER stress results in reduced growth and maybe the cause of decreased survivability of ER stress. More extensive mutations to the a-loop phosphorylation sites of Ire1 appear to reduce the concentration of ER stressor required for reduced growth indicative of reduced ER stress tolerance. These data link the *in vitro* reporter assay activity results and the effect on ER stress tolerance *in vivo*. It should be taken into consideration that the single mutant constituents of Q-A utilised Y01907 strain of *S. cerevisiae* as opposed to PWY260 in the multi-point mutants. Although the plasmids are identical and show similar growth and expression data. For clarification, these mutants would need repeating in PWY260.

8.4   Characterising the clustering of Ire1 in a-loop mutants under ER stress

8.4.1   Rationale

When Ire1 detects unfolded proteins in the ER lumen, it forms dimers and possibly promotes oligomerisation. Although as mentioned previously, the exact mechanics of this process are debated (Credle et al., 2005; Kimata et al., 2007; Mathuranyanon et al., 2015; Pincus et al., 2010; Shamu and Walter, 1996; Zhou et al., 2006), it is agreed that the Ire1 molecules themselves "cluster" in the event of ER stress. With the use of the mutants in this work it is important to show that this clustering is being achieved in all mutants. This is because the clustering of Ire1 is indicative of an initiation of the ER stress response (Aragón et al., 2009; Kimata et al., 2007) and would ensure that the results seen in the *β*-galactosidase reporter assays and spotting assays were not simply a result of defects in Ire1 clustering resulting in a reduction in UPR activation. To investigate the Ire1 protein clustering following activation through unfolded protein accumulation, MSY14-02 strain *S. cerevisiae* cells were transformed with two plasmids, pJK59 and pEvA97. pJK59 was already transformed into the MSY14-02 strain and through the inclusion of the GFP-tagged *Sec63* allowed for visualisation of the membrane of the perinuclear and cortical ER and the determination of localisation of Ire along the ER membrane when using a fluorescently tagged Ire1, hence the use of this strain. Furthermore, in previous studies completed by the Schröder laboratory at Durham University, the MSY14-02 strain was found to express the pEvA97 plasmid with the best results. The pEvA97 plasmid, contained the mCherry-tagged *IRE1* (details in Fig.6) which allowed for the visualisation of Ire1 localisation. With the use of the Zeiss LSM 880 with Airyscan microscope, images were captured over a 1 h time course showing how cells responded to ER stress induced by 2 mM of DTT. Should

the activation of Ire1 not be initiated by ER stress then then Ire1 would not be expected to form *foci* (Aragón et al., 2009; Kimata et al., 2007). If Ire1 is behaving as would be expected in the WT, then after around 15 min, clustering of the mCherry signal should be apparent.

8.4.2 Results

To ensure cells expressing both Ire1 and Sec63 could be visualised, a 2-channel approach was used. Additionally, cells were only imaged if signals from both Ire1-mCherry and Sec63-GFP were detected. In cells under no ER stress, the Ire1 signal should be arranged in such a way as that there are no specific *foci* sites as the UPR is not being activated (Kimata et al., 2007). The Ire1 should be evenly spread along the cortical and perinuclear ER membrane (Fig. 16). Sec63 is an ER membrane protein and a commonly used ER marker in the field, (Prinz et al., 2000; Schuck et al., 2009; Voeltz et al., 2006) and should remain unchanged by the introduction of ER stress from DTT, this will serve as a control ensuring that a phenotype has not arisen in the arrangement of the ER from the introduction of the a-loop mutations as well as indicating that the Ire1-mCherry is local to the ER membrane.
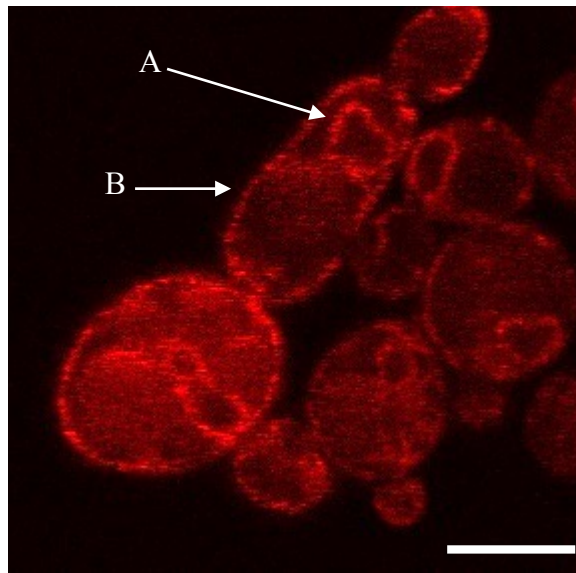
Fig. 16 MSY14-02 expressing Ire1 tagged with the mCherry fluorophore. The localisation of Ire1 protein to the perinuclear ER (A) and the cortical ER (B) under no ER stress. Scale bar 5 µm.

Under ER stress conditions Ire1 begins to form clusters, this can be seen from the 15 min time point in Figs. 17 – 24 below. This is as the Ire1 proteins cluster together along the ER and produce a stronger mCherry signal. To show the lack of any phenotype, all mutants, at all time points, should exhibit the same characteristics as those seen in the WT. All images presented below are representative of the mutants. Around 30 - 50 images were taken per mutant on the microscope, with each image containing an average of 2 – 5 cells. Ideally one cell at a time would be viewed over the time course but this is not possible because of photo-bleaching with prolonged laser exposure. However, the approach implemented here should accurately represent clustering of Ire1 in the mutants induced by ER stress using 2 mM of DTT.
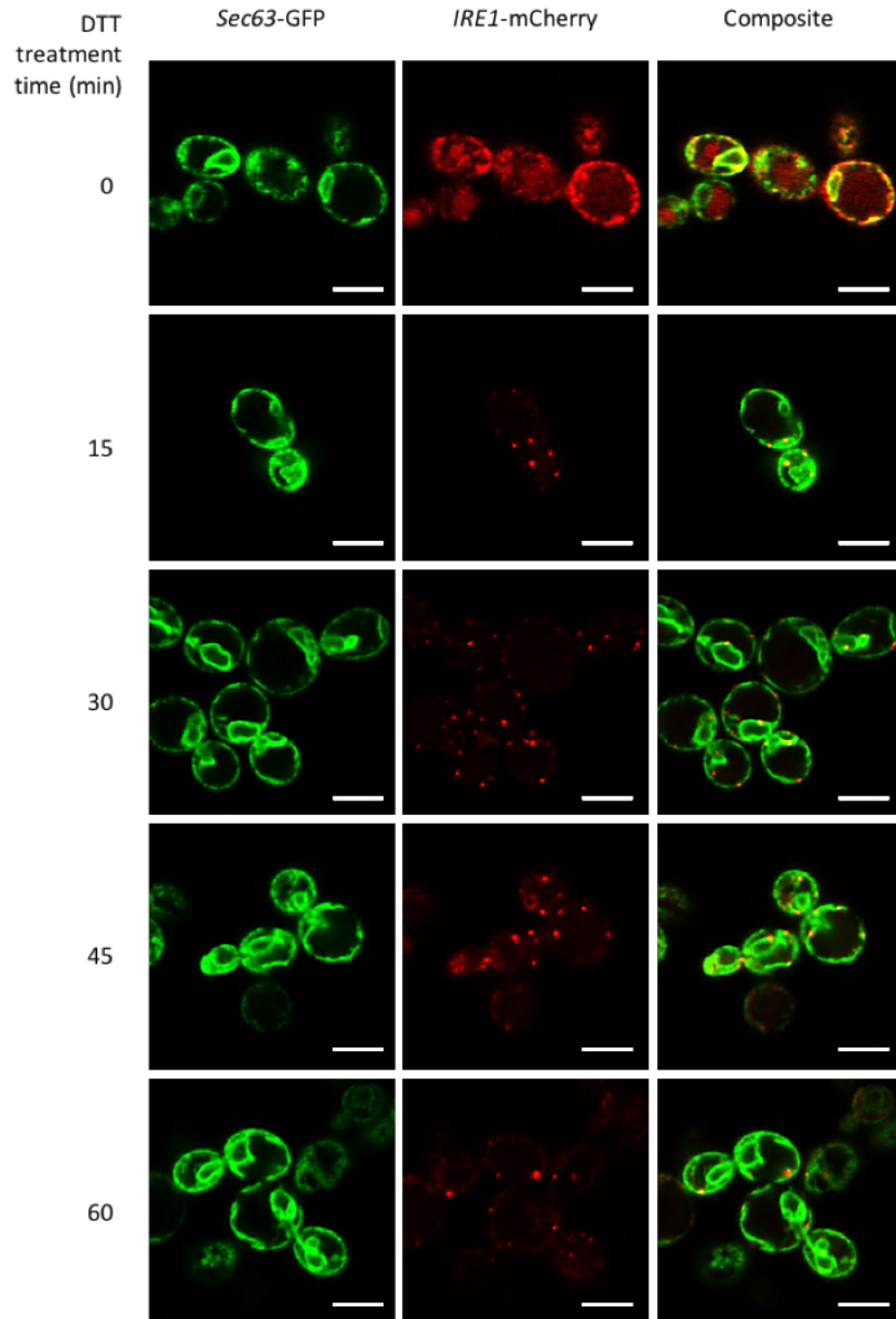
Fig. 17 Time course of the MSY14-02+pJK59 (WT) mutant. The 0 min time point shows the localisation of the Ire1 protein along the membrane of the cortical and the perinuclear ER. As DTT exposure time increased the Ire1 signal begins to cluster into *foci* sites. This is seen from the 15 min time point, some signal evenly spread along the cortical ER remains however this is reduced as the treatment time progresses. Upon 60 min of DTT exposure the Ire1 signal appears to be exclusively confined to the *foci* sites. Scale bar 5 μm.

Fig. 18 MSY14-02+pJK59+pEvA97-D836A time course. The D836A mutant elicits no phenotype regarding the clustering of Ire1 into *foci* sites. The Ire1 *foci* sites form again after 15 min. Upon 60 min of DTT exposure the Ire1 signal appears to be exclusively confined to the *foci* sites. Scale bar 5 μm.

Fig. 19 MSY14-02+pJK59+pEvA97-S840A-S841A time course. S840A-S841A shows the localisation of Ire1 signal to *foci* sites from the 15 min DTT treatment time point, as seen in the other mutants and the WT. Upon 60 min of DTT exposure the Ire1 signal appears to be exclusively confined to the *foci* sites. Scale bar 5 μm
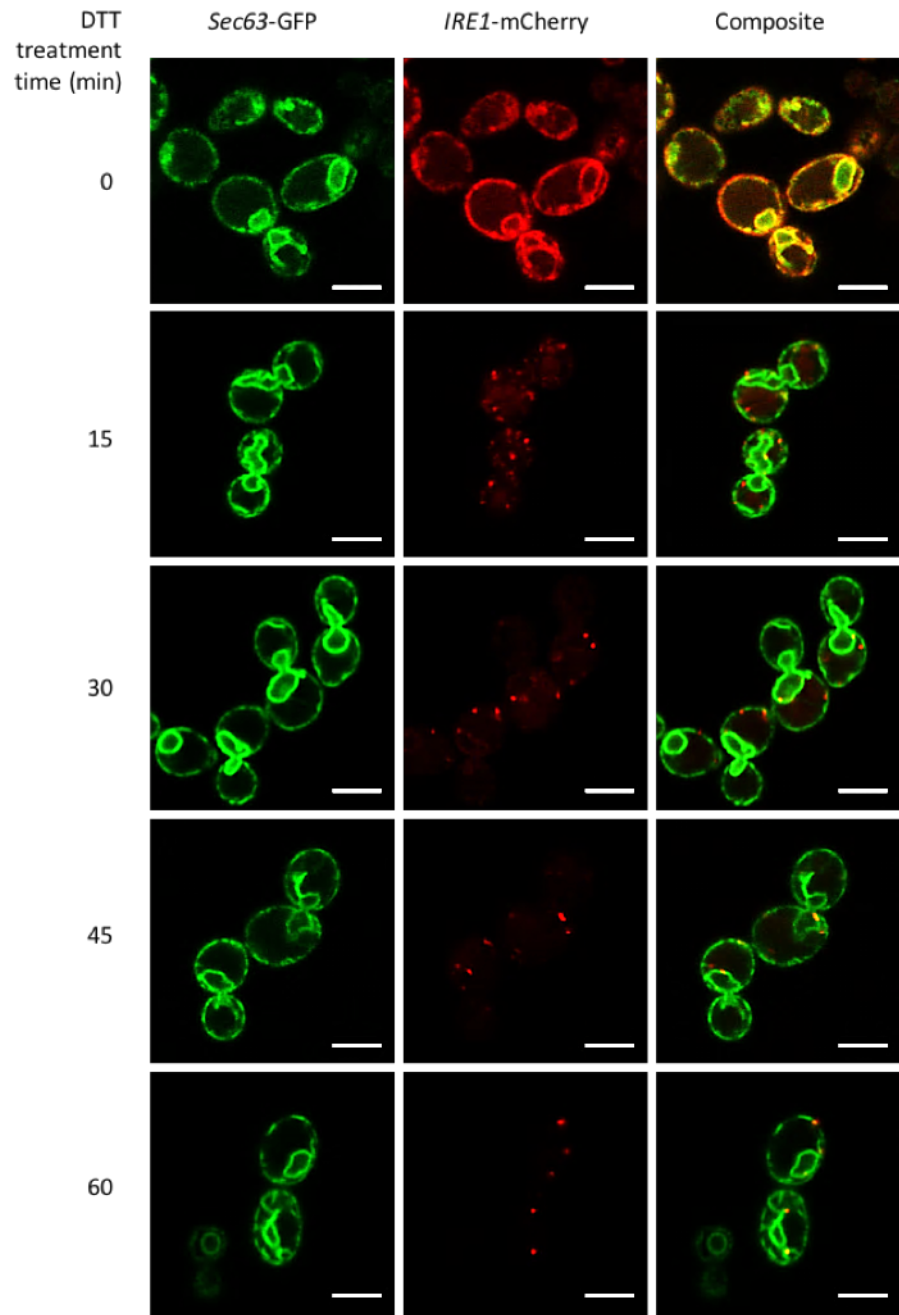
Fig. 20 MSY14-02+pJK59+pEvA97-D836A-S840A-S841A time course. D836A-S840A-S841A mutant arranges its Ire1 as seen in the other mutants and the WT. The Ire1 *foci* sites form, as before, following 15 min of DTT treatment. Upon 60 min of DTT exposure the Ire1 signal appears to be exclusively confined to the *foci* sites. The inclusion of the D836A mutation to the S840A-S841A mutant resulted in the same DTT stress *foci* site arrangement as seen in other mutants. Scale bar 5 µm.
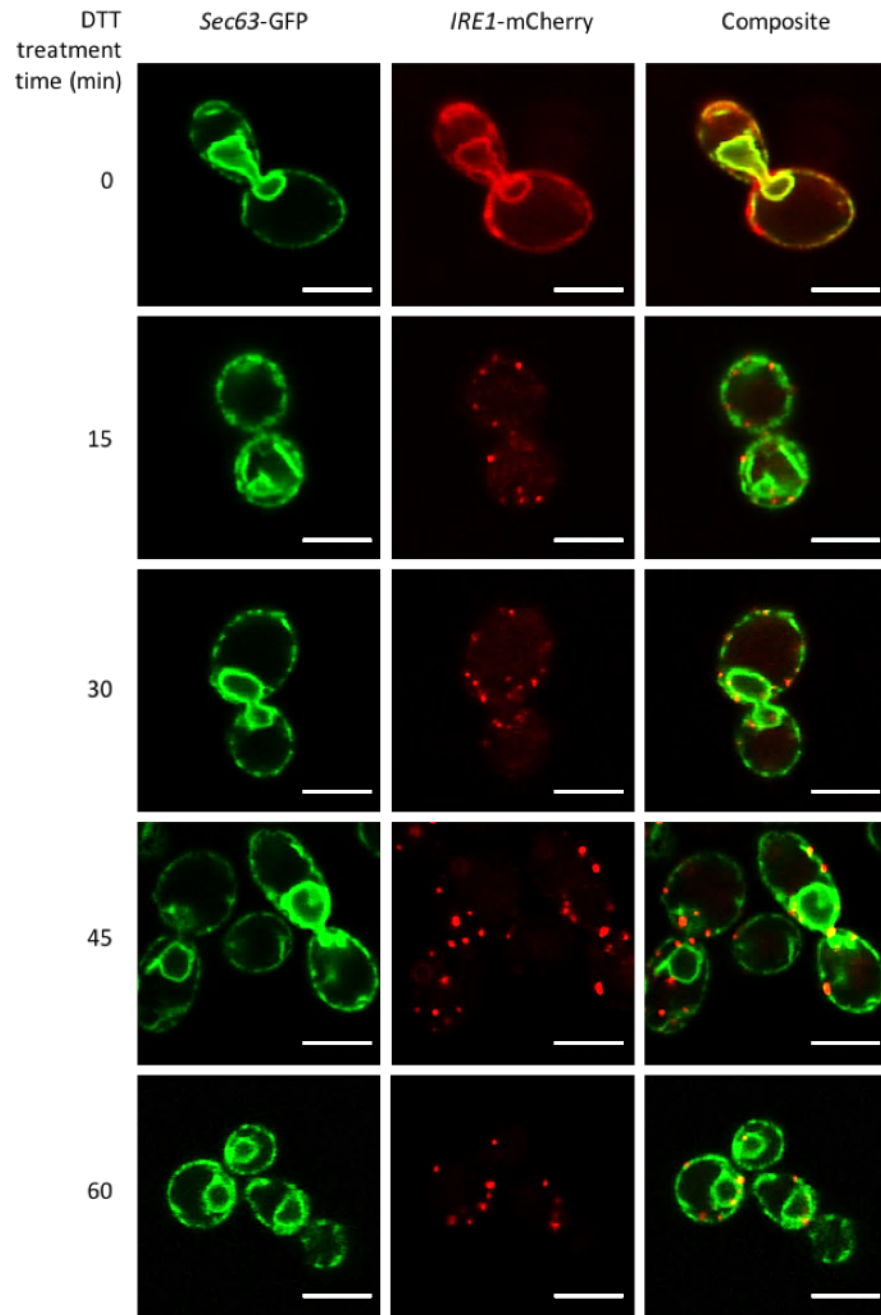
Fig. 21 MSY14-02+pJK59+pEvA97-Q-A time course. The Q-A mutant, as with the other mutants shows no phenotype regarding the clustering of Ire1 into *foci* sites. The Ire1 *foci* sites form, as before, after 15 min of DTT treatment. Upon 60 min of DTT exposure the Ire1 signal appears to be exclusively confined to the *foci* sites. Scale bar 5 μm.
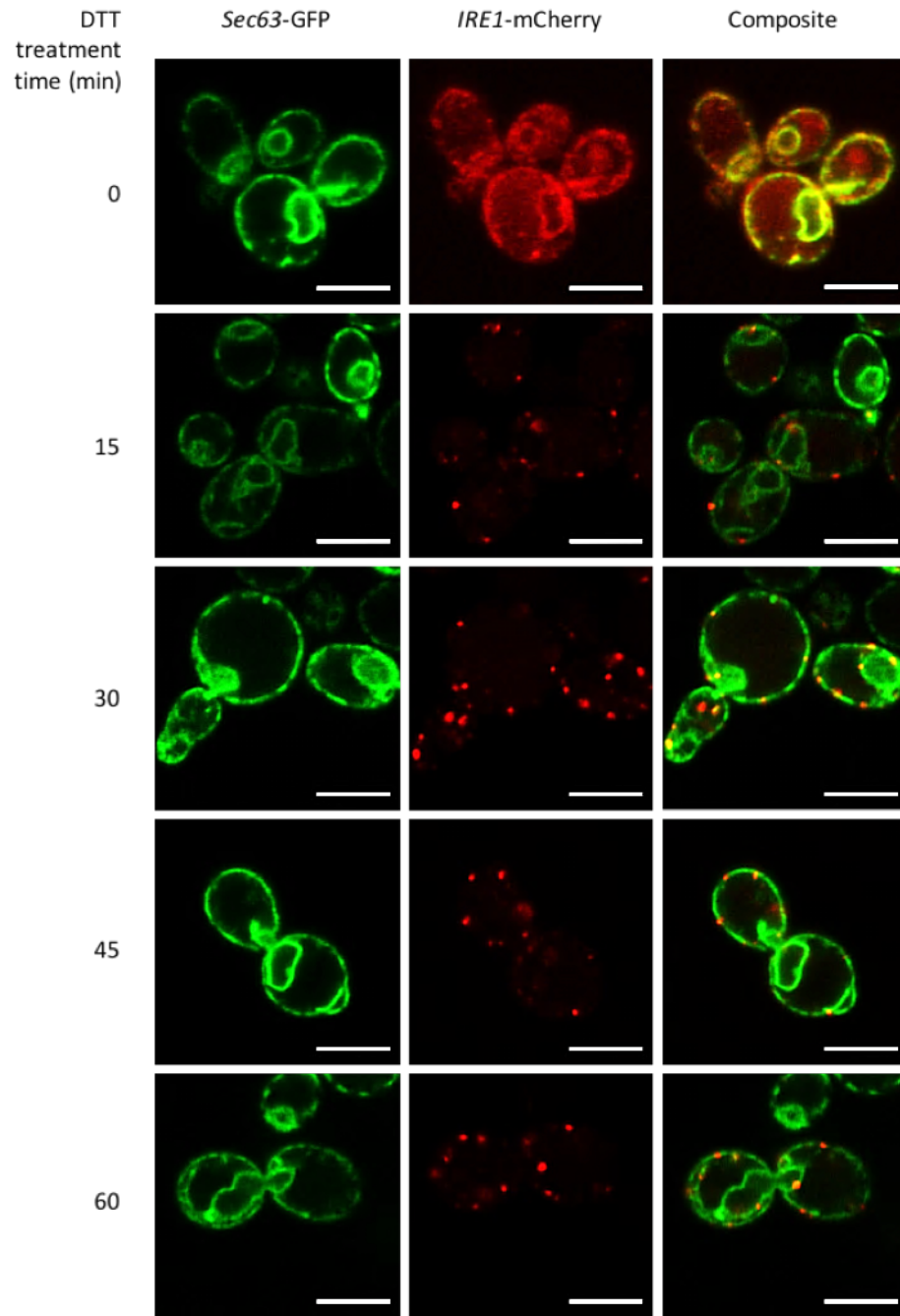
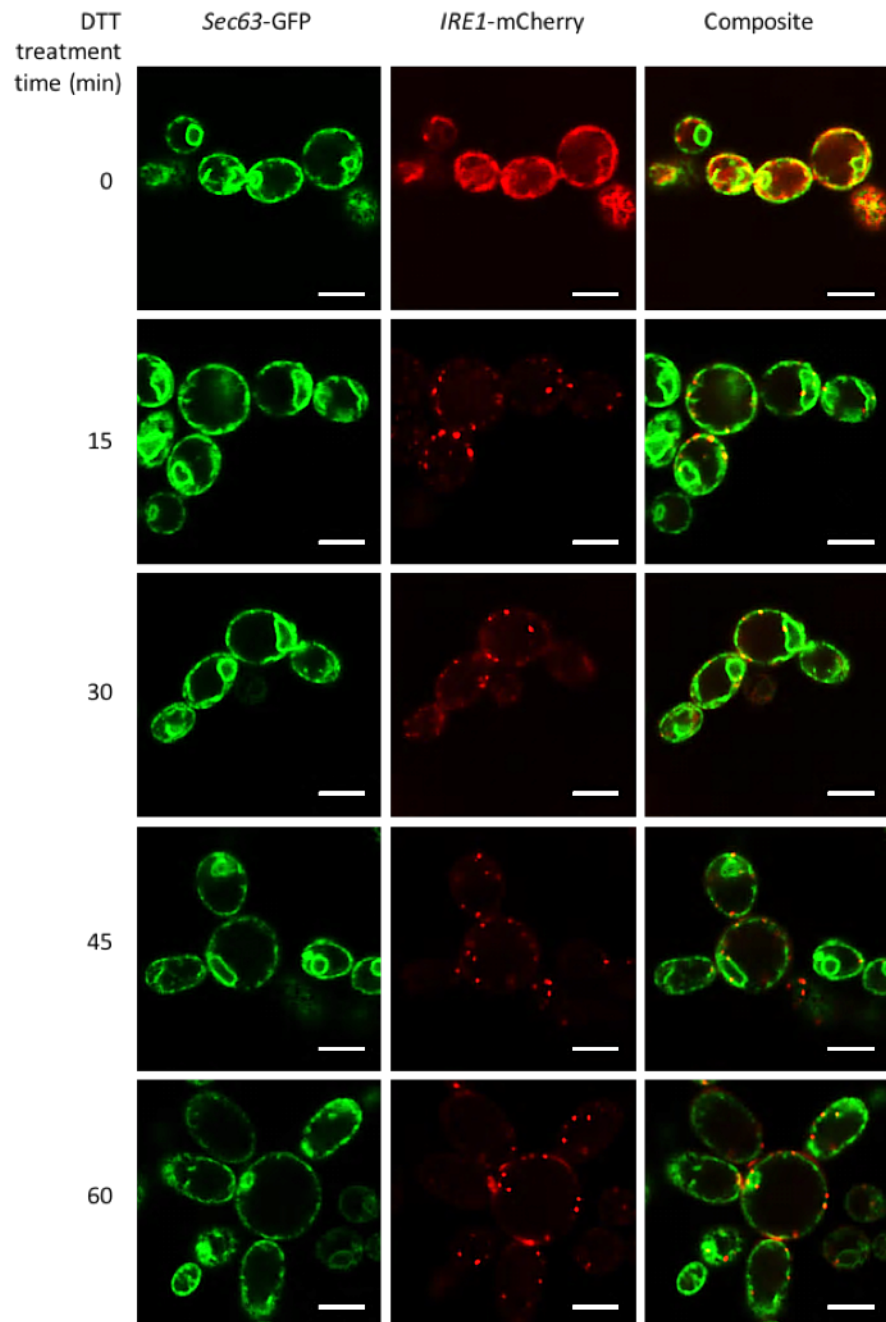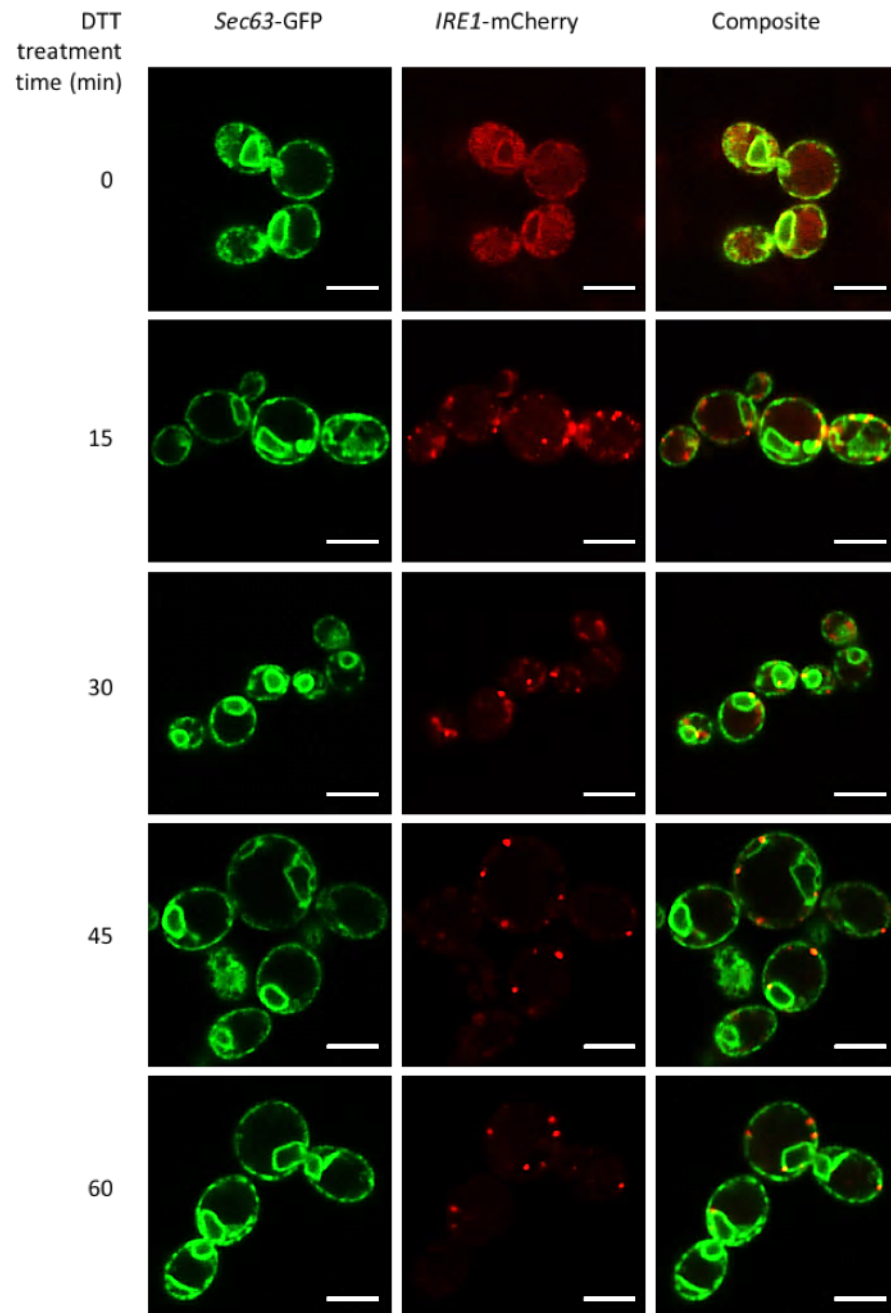**Fig. 22** MSY14-02+pJK59+pEvA97-D836A-Q-A time course. As with all previous mutants, the D836A-Q-A mutant results in no clustering phenotype. The Ire1 *foci* sites form, as before, after 15 min of DTT treatment. Upon 60 min of DTT exposure the Ire1 signal appears to be exclusively confined to the *foci* sites. These images show that the addition of the D836A mutation to the Q-A mutant resulted in the same DTT stress *foci* site arrangement as seen in the WT and mutants. Scale bar 5 μm.
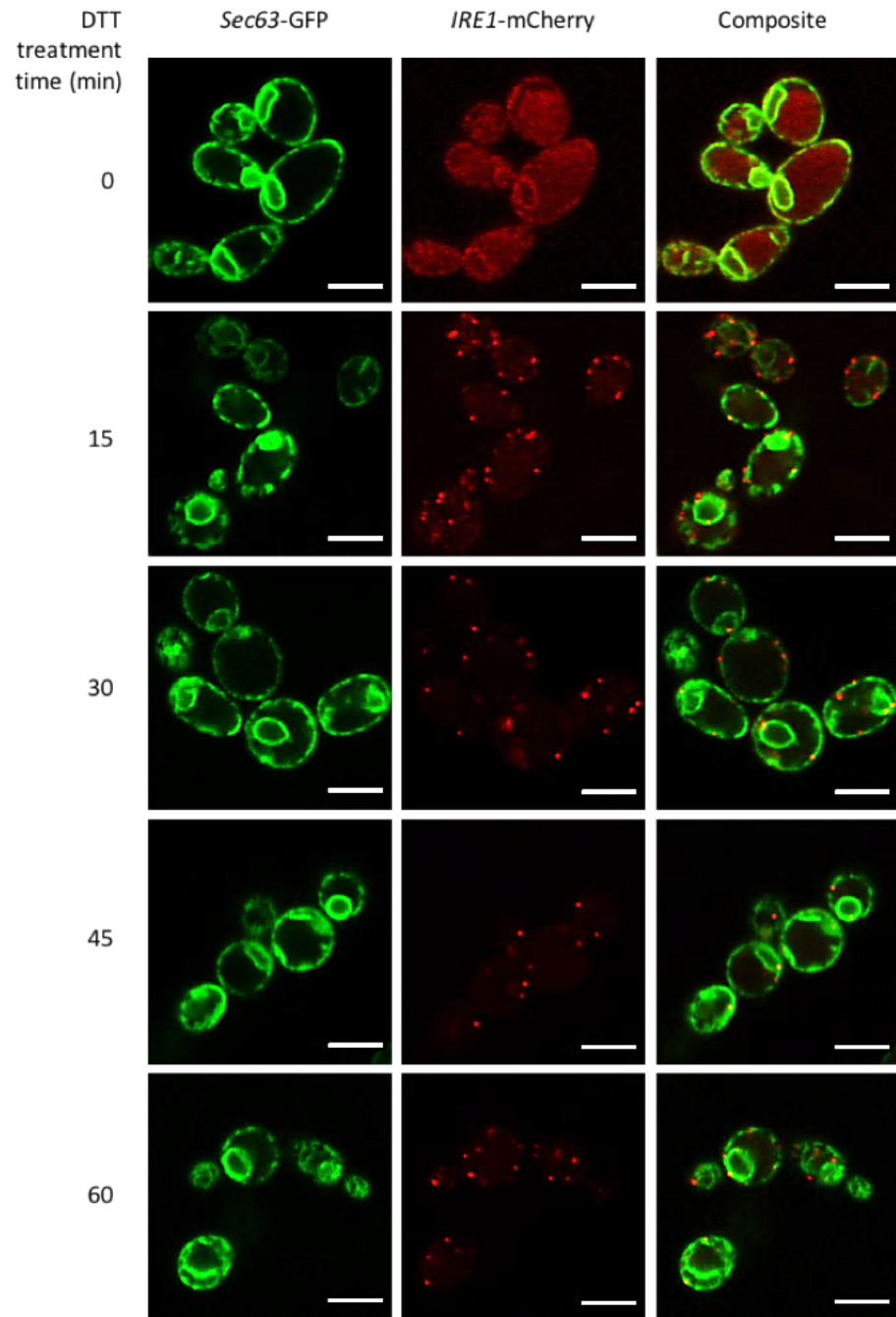
Fig. 23 MSY14-02+pJK59+pEvA97-P-A time course. The P-A mutant elicits no clustering phenotype. The Ire1 *foci* sites form after 15 min and continue to show this arrangement of *foci* site specific signal over the 60 min treatment. Scale bar 5 µm.
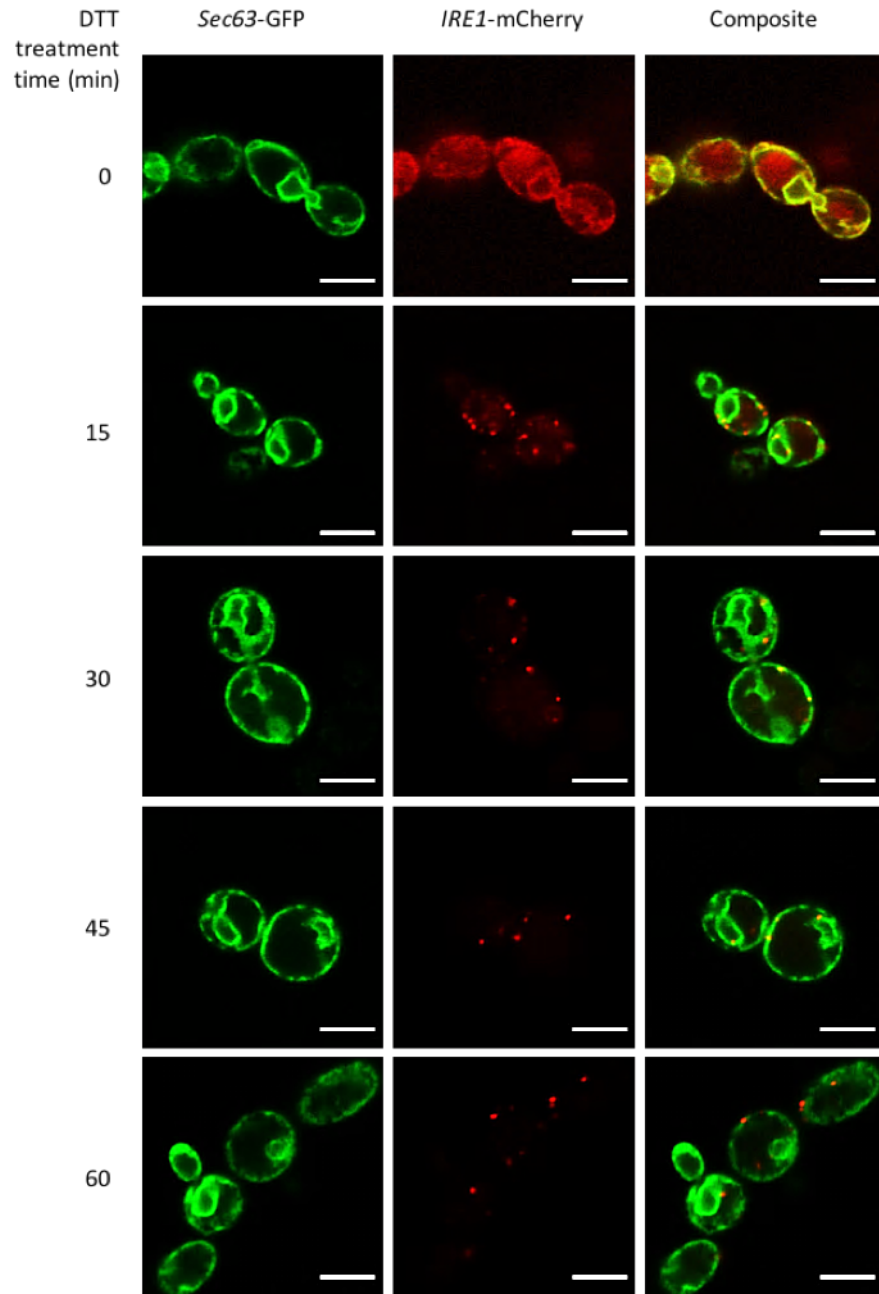
Fig. 24 MSY14-02+pJK59+pEvA97-D836A-P-A time course. The addition of the D836A mutation to the P-A mutant results in no phenotype regarding the clustering of Ire1 into *foci* sites. The Ire1 *foci* sites form after 15 min of DTT treatment. Upon 60 min of DTT exposure the Ire1 signal appears to be exclusively confined to the *foci* sites. It was important that the addition of the D836A mutation along with the a-loop phospho-site mutations did not produce phenotype which would explain the further attenuation of UPR shown by phospho-mutants containing a D836A. These images show that this is not the case and therefore any reduction in UPR is not resulting from a non-clustering phenotype. Scale bar 5 μm.

8.4.3 Mutants produce no clustering phenotype under ER stress

The images gathered from fluorescence microscopy highlight the clustering of the Ire1 protein along the ER membrane. The visualisation of the *foci* sites however does not confirm RNase activity, simply that the Ire1 has formed *foci* sites in response to unfolded protein accumulation in the ER lumen. To ensure that the apparent reduction of ER stress response in the phospho-mutants is not a result of an Ire1 clustering phenotype it would be expected that all mutants would behave as the WT. Figs. 17 – 24 show that the mutants follow the same clustering as the WT, whereby at the 15 min time point, the clustering is apparent and after 60 min of DTT exposure the Ire1 signal appears to be exclusively confined to the *foci* sites along the ER membrane. This shows that Ire1 still clusters in response to ER stress even with a D836A mutation or phosphorylation site mutations, or a combination of both, showing the mutations do not result in a lack of Ire1 clustering.

The role phosphorylation may be playing in the formation of clusters of Ire1 may not be indispensable. As discussed in section 6.5, phosphorylation of the a-loop was thought to facilitate nucleotide binding by activating the kinase domain (Lee et al., 2008) resulting in a dimer configuration and RNase activation. Alternatively, due to conformational changes following phosphorylation of the a-loop, phosphorylation was thought to promote autophosphorylation *in trans* promoting the formation of oligomers and that this oligomerisation was critical to RNase activity (Korennykh et al., 2009). The data presented in Figs. 17 – 24 show that there is no Ire1 clustering phenotype produced in WT cells or in phospho-acceptor site mutants, both including and excluding the D836A mutation. However, the observation of *foci* sites of Ire1 only illustrates clustering and does not confirm the formation of dimers or oligomers. To investigate the formation and structure of oligomers then the crystal structure of Ire1 exposed to ER stress would have to solved. The only conclusion that can be drawn from the visualisation of clusters of Ire1 is that, the reduction in ER stress signalling by Ire1 is not a result of a lack of clustering negatively impacting on the UPR activation (Aragón et al., 2009; Kimata et al., 2007).

9.0 **Discussion**

The data gathered above indicate that the D836 residue plays a role in the regulation of RNase activity, suggesting that phosphorylation alone is not the exclusive activator of RNase activity or that phosphorylation does not act alone in RNase activation. *β*-galactosidase reporter assay data shows that the phospho-acceptor mutants (S840A-S841A, Q-A and P-A) show an attenuation of the activation of UPR. Furthermore, this attenuation is increased relative to an increase in the number of phospho-acceptor-site mutations. The inclusion of the D836A to mutation to these mutants reduced UPR activation to levels seen in the empty vector negative control.

Linking UPR to cell survivability of ER stress, the results from spotting assays mimic those seen in *β*-galactosidase reporter assays, whereby S840A-S841A, Q-A and P-A mutants have a reduced survivability of ER stress conditions, again with P-A exhibiting the largest reduction in ER stress tolerance compared to the WT. Once again the inclusion of the D836A mutation to these mutants decreases tolerance of ER stress further, to levels seen in the empty vector control. Finally, the fluorescence microscopy highlights no Ire1 clustering phonotype or the ER arrangement in general when compared to the WT. This confirmed that all previous observations of the impact of mutants were not a result of reduced or eliminated clustering of Ire1 *in vivo* under ER stress.

9.1 Inclusion of D836A eliminates residual UPR activation in a-loop phospho-mutants

Phosphorylation within the a-loop was thought to activate the kinase domain by causing conformational changes to the a-loop and opening the nucleotide pocket to allow the binding of ATP, the hydrolysis of which resulted in the formation of a dimer which promotes RNase activity, dependent on the occupation of the NBP (Lee et al., 2008; Papa et al., 2003). The alternative model was that ADP binding would then induce Ire1 the dimerisation promoting kinase activity and facilitate the formation of oligomers. This oligomerisation compatible conformation was "locked in" by phosphorylation of the a-loop promoting the formation of an oligomer and activating the RNase domain (Korennykh et al., 2009; Shamu and Walter, 1996; Welihinda and Kaufman, 1996). The activation of the RNase domain initiates *HAC1* mRNA splicing and ultimately leads to the expression of UPR associated genes (Tanaka et al., 2015). Two observations in previous work go against parts of these models. Firstly, the D828A mutant described as kinase dead due to its lack of Mg^{2+} coordination (Chawla et al., 2011) and D797A-K799A mutant which no longer possess a catalytic aspartate (Rubio et al., 2011) still show RNase activity.

This suggests that the kinase activity is not indispensable for RNase activity. Secondly, in mutants that still possess kinase activity but lack some, or all, of their phospho-acceptor sites within the a-loop (S840A-S841A, Q-A and P-A) there was a retention of levels of RNase activity (Schröder et al., unpublished work) (Fig. 5). This suggests that phosphorylation also is not indispensable in RNase activation. All of these mutants possess an aspartic acid at residue 836 in the a-loop sequence. In the RD kinase model, phosphorylation within the a-loop promotes a-loop interaction with the RD pocket to promote nucleotide binding (Johnson et al., 1996; Knighton et al., 1991; Nolen et al., 2004). In the absence of phosphorylation, RD kinases have been shown to utilise a glutamate residue to mimic this interaction due to the negative charge of this amino acid (Johnson et al., 1996). It was proposed in this work that the phosphorylation could be bypassed by the mimicry of the active conformation of the a-loop by the negative charge of the D836 residue. To investigate the role of D836 in Ire1 the work presented here used a range of mutants with reduced or eliminated phospho-acceptor capability within the a-loop that had been used in previous studies by the Schröder laboratory, however, this time also used these same mutants with the addition of D836A (D836A, S840A-S841A, D836A-S840A-S841A, Q-A, D836A-Q-A, P-A and D836A-P-A) (Fig. 2). The findings show that in non-D836A mutants residual Ire1 activity was detected were seen again in this work, this time using an UPRE-associated β-galactosidase reporter assay (Figs. 11 and 12). The inclusion of D836A to the phosphorylation site mutants resulted in complete elimination of reporter activity (Fig. 12 B, C and D). The single mutant D836A, however, shows no reduction in reporter activity (Fig. 12 A). These data suggest that D836 is facilitating a basal level of Ire1 activity in the event of loss of phosphorylation. This compensatory effect seems to reduce with the more extensive mutants (Fig. 11 A). In the S840A-S841A mutant, D836 appears to be able to allow retention of most of the Ire1 activity. Q-A suffers higher attenuation of it's Ire1 activity than S840A-S841A, with P-A being the most reduced. All of these mutants possess a D836 residue, however S840A-S841A also retains the native S837, T844 and S850 sites, suspected phosphorylation sites (Lee et al., 2008; Shamu and Walter, 1996). The Q-A mutant has its T844 and S850 residues changed to alanine (S840A-S841A-T844A-S850A) but still possesses S837. The P-A mutant also has its S837 mutated to alanine (S837A-S840A-S841A-T844A-S850A). The increase in the number of a-loop phosphorylation sites correlates with a decrease in the compensatory effect of D836, suggesting that this effect is optimised by phosphorylation on the S837,

T844 and S850 residues, with less phosphorylation resulting in a reduced ability of D836 to activate RNase activity (Fig 11 A). The introduction of the S837A mutation in the P-A mutant compared to the Q-A mutant reduces the effect of D836, showing experimental evidence that S837 is involved in Ire1 activity, probably through phosphorylation. Direct observation of phosphorylation on this residue would be required to solidify this theory.

The theory that the compensatory effect of D836 is dependent on phosphorylation on the S837, T844 and S850 residues is validated by the result that in D836A-S840A-S841A mutants, reporter assay activity is at levels seen in the empty vector control. This means that despite the phosphorylation sites of S837, T844 and S850 being available, these are not sufficient to result in Ire1 RNase activity without D836. If D836 is providing a form of rescue from a defect in a-loop phosphorylation there are several questions to be reviewed. How does phosphorylation of the a-loop lead to Ire1 RNase activation and is this dispensable? How does D836 achieve its compensatory effect? Finally, what are the roles of the phospho-acceptor residues within the a-loop?

In response to the question of how phosphorylation activates Ire1 RNase activity and the dispensability of this system, it has been shown that phosphorylation of the a-loop of Ire1 is required for efficient *HAC1* mRNA splicing (Prischi et al., 2014) and that Ire1 molecules rely on *trans*-autophosphorylation (Korennykh et al., 2009; Lee et al., 2008; Pike et al., 2008; Pirruccello et al., 2006; Shamu and Walter, 1996) which promotes a conformation of the cytosolic domain compatible with RNase activation (the exact confirmation is debated see section 6.5 and above). It should be noted that the work completed by Prischi et al., (2014) utilised human Ire1α, which may behave differently to the Ire1 of *S. cerevisiae*. Based on the models above where phosphorylation ultimately facilitates the RNase compatible conformation of the RNase domain, in the event where all phosphorylation sites are mutated, such as in P-A, induction of the *β*-galactosidase reporter seen in Fig. 12 D must be achieved through a mechanism independent of phosphorylation. This conclusion can be drawn because if a mechanism relies on phosphorylation of the a-loop to phosphorylate its neighbours *in trans* then loss of phosphorylation at these sites must prevent this event. As shown however, Ire1 with no phospho-acceptor sites within the a-loop still shows reporter activity (Fig. 11 and Fig. 12 D) and *HAC1* splicing (Fig. 5) hence a-loop phosphorylation appears to be dispensable in Ire1 activity, however, RNase activity will be reduced.

The answer to the second question of if phosphorylation is dispensable then how does Ire1 regulate its RNase domain may lie in the RD kinase family. Ire1 possesses an "RD pocket" comprised of a conserved arginine at residue 796 (R796) followed by a conserved catalytic aspartic acid (D797) (Johnson et al., 1996; Nolen et al., 2004). The evidence that efficient *HAC1* mRNA splicing requires phosphorylation of the a-loop of Ire1α (Prischi et al., 2014) suggests that Ire1 is a phosphorylation-dependent RD kinase. However, as previously mentioned, Ire1α may not behave the same as yeast Ire1, but other studies have shown that UPR is at its most efficient with phosphorylation on primary residues within the a-loop (Shamu and Walter, 1996). It has been described that in RD kinases the phospho-acceptor residues within the a-loop are involved in an electrostatic interaction between with the RD pocket which is critical for driving the conformation change required for kinase activity (Nolen et al., 2004). Furthermore, Nolen et al., (2004) suggest that the arginine (R797 in *S. cerevisiae*) is not the source of a direct signal of activation to the kinase catalytic loop. It is suggested that the interaction between the a-loop and the RD pocket facilitates a conformational change to the N and C-terminal anchors of the a-loop. This change allows for nucleotide binding, thought to be important in RNase activation (Mannan et al., 2013; Papa et al., 2003). The role of phosphorylation may be providing a level of stability in the resulting conformational changes of the a-loop allowing for an open and extended conformation permitting this nucleotide binding (Huse and Kuriyan, 2002).

The theory that phosphorylation provides stability may be supported by data presented here. In the S840A-S841A mutant there was the highest recorded residual reporter assay activity, however, the D836A-S840A-S841A mutant showed no activity despite it possessing three functioning phosphorylation sites (Fig. 12 B). As already discussed this would suggest that D836 is reliant on the phosphorylation of S837, T844 or S850. The fact that the maximum effect of D836 on reporter activity is seen in mutants still capable of phosphorylation within the a-loop provides evidence that phosphorylation does indeed provide stability to the a-loop conformational changes suggested (Huse and Kuriyan, 2002) allowing for efficient nucleotide binding and RNase activation. To expand, when less phosphorylation sites are available (Q-A and P-A) the compensatory effect of D836 is reduced (Fig. 11 A), possibly because D836-induced a-loop conformational changes lack the stability provided by phosphorylation. The S841 site is positioned within the a-loop in such a way that it is thought to interact with the RD pocket and provide stability to the oligomer (Korennykh et al., 2009). This would suggest that S841 is a primary

phosphorylation site, as it is common for the primary phosphorylation site of phosphorylation-dependent RD kinases to interact with the RD pocket (Nolen et al., 2004). As it was suggested that S840 and S841 may work in tandem (Shamu and Walter, 1996), this may explain why in the mutants Q-A and P-A there is the largest attenuation of ER stress signal transduction.

If the favourable mechanism of phosphorylation of Ire1 in the a-loop relies on primary phosphorylation sites within the a-loop interacting with the RD pocket, D836 may mimic this conformational change to facilitate nucleotide binding. This conformational mimicry may be a result of the position of D836 within the a-loop and its negative charge. The stabilisation provided by phosphorylation of S837 in Q-A provides a more stable conformer allowing for more efficient nucleotide binding, hence the improved compensatory effect of D836. The S840A-S841A mutant with its highest level of residual ER stress response has the benefit of additional conformation stability provided by phosphorylation of one, two or all three of the S837, T844 or S850 residues. The idea of primary sites of phosphorylation also explains the loss of residual activity of D836A-S840A-S841A. There would be little evolutionary advantage to have a system whereby compensation for loss of phosphorylation is maximised by phosphorylation at the primary sites (especially if these sites are working in tandem as suggested (Shamu and Walter, 1996)). Should the primary sites lose phospho-acceptor capability, a compensatory system based on this method would be redundant. The use of secondary phosphorylation sites such as S837, T844 and S850 would allow for an alternative pathway with the flexibility of three independent phosphorylation sites to provide conformation stability.

Protein kinases are known to have a high degree of plasticity allowing for the adoption of different conformations to promote activity (Huse and Kuriyan, 2002). The D836 residue appears to allow for at least partial bypassing of phosphorylation of the a-loop of Ire1 in *S. cerevisiae*. The method by which this is achieved may be through mimicry or assistance in the facilitation of conformational changes promoting RNase activation and hence endoribonuclease activity resulting in activation of the UPR.

The final question of how the other phosphorylation residues within the a-loop are linked to RNase activity and UPR activation may be answered in part by the theory outlined above regarding the role of D836. It has already been documented that the S840, S841 and T844 residues are involved in the formation and stabilisation of the crucial IF3[c] through the formation of intramolecular salt bridges. In their phosphorylated state, the position of the phosphates of these three residues are arranged in such away the promote the

oligomerisation compatible conformation thought to be required for RNase activity (Korennykh et al., 2009). S837 and S850 appear to be involved in ER stress signal transduction (Fig. 11 and Fig. 15). There are two anchor points for the activation segment of Ire1, the N-terminal anchor and C-terminal anchor (Nolen et al., 2004). In many kinases the conformation of an inactive a-loop disrupts the N-terminal anchor, distorting the Mg^{2+} binding loop, (Nolen et al., 2004; Xie et al., 1998; Yang et al., 2002). This distortion may contribute to reduced activity by preventing the correct positioning of ATP (Nolen et al., 2004). This also may explain the contradiction in the models whereby a low level of kinase activity seems to be required to initiate the *trans*-autophosphorylation of Ire1 in the outset (see section 6.5). The Mg^{2+} binding loop and the β10 sections (Fig 2.) form the N-terminal anchor. The C-terminal anchor begins near the middle of the P + 1 loop and extends towards the APE conserved region. This anchor is critical in the interaction between the substrate and the kinase (Madhusudan et al., 1994). The S837 is located nine amino acids downstream from the DFG motif, which is at the N-terminal end of the N-terminal anchor. S850 is located nine amino acids upstream from the APE conserved motif at the C-terminal end of the C-terminal anchor. As the DFG and APE motifs are highly conserved (Fig. 2) (Mannan et al., 2013) and phosphorylation is believed to stabilise a-loop conformations, it may be the case that the S837 and S850 residues are placed in such a way to provide stability through interaction with activation segment anchors.

9.2 *Inclusion of D836A to phospho-acceptor site mutants reduces cell survivability in ER stress conditions*

It is evolutionarily encoded in cells to promote cell death when under excessive and stress from protein accumulation from which the cell is unable to recover. The UPR is a mechanism by which the cell processes accumulated proteins in the ER, should this system be unable to achieve this, then the cells suffer a reduction in survivability of ER stress (Chen and Brandizzi, 2013; Hetz, 2012; Jäger et al., 2012; Lin et al., 2007; Merksamer and Papa, 2010; Shore et al., 2011). PWY260 cells have shown a reduction in survivability when transformed with a-loop mutations preventing phosphorylation. Furthermore, the addition of the D836A mutation to these mutants further reduced cell tolerance to ER stress (Fig. 13).

Fig. 13 suggests that the idea that D836 allows for the role of phosphorylation to be partially bypassed is occurring *in vivo*. In phospho-mutants cell survival is reduced but not as detrimentally to the levels seen in the empty vector control. The addition of the D836A

mutation to phospho-mutants decreases survivability further, to the levels seen in the empty vector (-) control (Fig. 13). This suggests that D836 plays a role in facilitating activation of the UPR and hence promoting cell survival in phospho-mutants. ER stress induced by DTT effects D836A inclusive phospho-mutants at lower concentrations of DTT than cells with the native D836. Three other interesting questions were raised by the spotting assay results, however. Firstly, when ER stress was induced by tunicamycin the D836A mutant appeared to have improved stress tolerance. Secondly, the S850A mutation improved stress tolerance in both DTT and Tn induced ER stress when compared to the WT in Y01907 cells. Finally, that the single point mutations of the Q-A mutant (S840A, S841A, T844A and S850A), were able to tolerate ER stress much more readily than their multipoint mutant counterparts.

Addressing the first question, of increased survival of ER stress in the D836A mutant when compared to WT. This result was not expected and has not previously been reported in the literature. As discussed in section 8.3.3, WT *S. cerevisiae* cells should be able to tolerate concentrations of Tn used in this work (Lee et al., 2008; Schröder et al., 2003). This could mean that either the PWY260 cells are much more sensitive to Tn stress than Y01907 or an error in Tn concentrations used. Repetition of the D836A mutant alongside the WT on lower concentrations of plates using both PWY260 and Y01907 strains could help in understanding a definitive reason for this phenotype. The data collected in this work shows no increase in Ire1 expression in D836A mutants, no increase in β-galactosidase reporter activity and no Ire1 clustering phenotype when reviewed in fluorescence microscopy. *HAC1* mRNA splicing assays would allow for the investigation into the RNase activity levels of the D836A mutant whilst under Tn induced ER stress would also shed light on any link between RNase activity and increased ER stress tolerance in D836A mutants. This experiment should be carried out using DTT and Tn as ER stressors to understand the apparent Tn-specific phenotype.

Considering the second question of why does the S850A mutant in Y01907 show a phenotype of improved ER stress tolerance induced using DTT and Tn it must be considered the role S850 could play in the activation loop of Ire1. The idea that Ire1 function is not reduced by the mutation of S850 has been observed previously (Lee et al., 2008), where a S850A Ire1 mutant behaved as in the WT in terms of ER stress tolerance (assessed by spotting assays grown on Tn). However, the phenotype characterised by improved growth under ER stress has not been observed. Residues providing regulator

function is not unprecedented in Ire1, D828 in the kinase domain has been suggested to be important in the deactivation of Ire1 RNase activity (Chawla et al., 2011), perhaps S850 plays a similar regulatory role? As discussed in section 9.2 above, the S850 residue is located just outside the a-loop in the P+1 loop (Fig. 2). This loop was originally identified due to its involvement in contacting the P+1 residue structure of the kinase PKA with bound peptide inhibitor, and is found at a critical interaction between substrate and the kinase (Madhusudan et al., 1994; Nolen et al., 2004). This activity of the P+1 loop and position of the S850 residue within the loop might hint at the result of increased tolerance of ER stress. If the S850 residue is mutated, then the interaction between the P+1 loop and the kinase may be prevented. This may leave the Ire1 a-loop "active" due to the proximity of the S850 residue to the C-terminal anchor causing unregulated nucleotide binding resulting in RNase activity, as the anchors of the a-loop are important for conformation (Nolen et al., 2004). The subsequent increased UPR activation could result in increased ER stress survival compared to the WT.

Finally, is the observation that the constituent single point mutations of Q-A (S840A, S841A, T844A and S850A), seem to retain a higher level of ER stress tolerance than that exhibited by the combined Q-A mutant. This may highlight the role phosphorylation is playing in the activation of the Ire1 RNase activity, not involving the D836 residue. Comparing the multi-point mutant Q-A to its constituent single point mutants it can be seen that the Q-A mutant suffers from a lack of ER stress tolerance at lower concentrations of DTT than in the single point mutants (Figs. 13 and 15). Data shows that the S841A and T844A mutants show the largest sensitivity to DTT stress at 4 mM, similar to the levels of the Q-A mutant. It was noted that these residues were of particular importance in phosphorylation mediated Ire1 activation previously (Shamu and Walter, 1996). The S840A single mutant tolerates stress better than the Q-A mutant at 4 mM of DTT and the S850A has improved tolerance even compared to the WT (as discussed). The observation that the inclusion of multiple phosphorylation site mutations results in reduce ER stress survival in the Q-A mutant supports the β-galactosidase reporter data that the more extensive mutations result in an accumulative effect on ER stress tolerance (Fig. 11), as the single point mutants all tolerate ER stress either at around the same level or better than in the Q-A mutant. As S841A is believed to be a primary phosphorylation site and critical to RNase activation and Ire1 activity (Korennykh et al., 2009; Shamu and Walter, 1996), it would be expected that any mutant (such as Q-A) would suffer in a lack of effective UPR

activation by the presence of a S841A mutant. The S840 residue is believed to act in tandem with S841 (Shamu and Walter, 1996) compounding the reduction in ER stress signalling in Q-A and P-A mutants illustrating the effects of more extensive phosphorylation-site mutation. These spotting assays also indicate the role of S837 in UPR activation. The P-A mutant again shows reduced ER stress tolerance, exhibited by lack of growth at lower DTT concentrations, when compared to the Q-A mutant (Fig. 13). The only residue that the Q-A mutant possesses that the P-A does not is the S837 suggesting that it is indeed a functioning residue in the activation of Ire1.

9.3 Mutations in the activation loop do not produce an Ire1 clustering arrangement phenotype

As mentioned previously (section 6.2), there is much debate over the mechanics of how the lumenal domain of Ire1 detects unfolded protein accumulation. Regardless, once activated the process of lumenal domain dimerisation or oligomerisation allows for the formation of *foci* sites along the ER when unfolded protein accumulation stress is induced with DTT (Anshu et al., 2015). These *foci* suggest that Ire1 can still cluster when ER stress is induced despite the modifications made to its amino acid sequence. The lack of an Ire1 clustering phenotype in all mutants when compared to the wild type confirms that the lack of RNase activity and hence UPR activation is not a result of a reduced ability for Ire1 to form clusters. These data support the idea that clustering of Ire1 is believed to be a prerequisite of downstream signalling (Aragón et al., 2009; Kimata et al., 2007), however show that the clustering alone is not enough to activate Ire1. This is shown by D836A-containing phospho-mutants such as such as D836A-S840A-S841A, which still cluster under DTT-induced ER stress, yet have no UPR activity (Fig. 5, Fig. 12 B and Fig.20). This suggests that the phosphorylation (or mimicry of phosphorylation by D836) is important to the activation of Ire1. In all mutants, the Ire1 forms clusters. In the case of the D836A-phospho-mutnats, there is a complete attenuation of *β*-galactosidase reporter activity (Fig. 11 B) and in spotting assays these same mutants suffer in terms of ER stress tolerance (Fig 13). This suggests that the role of phosphorylation or D836 is to promote the active conformation requited from RNase activity after clustering (Korennykh et al., 2009; Lee et al., 2008; Nolen et al., 2004; Shamu and Walter, 1996), as without phosphorylation or the compensatory response of D836, Ire1 activation appears to stop at the stage of clustering.

10.0 Conclusions and Future Interests

10.1 Summary of findings and conclusions

This work has shown that the D836 residue of Ire1 appears to allow for a partial bypassing of phosphorylation. However, this maximising of the effect of D836-mediated bypassing is reliant on the phosphorylation sites of S837, T844 or S850 residues for the maximum retention of UPR activation by D836 in Ire1. This indicates that there may be a form of hierarchy in the phosphorylation sites in that, the S841, working in tandem with the S840 act as primary phosphorylation sites. T844 as a secondary and the roles of S837 and S850 perhaps being important in the conformation stability of the phosphorylated a-loop promoting efficient nucleotide binding. The D836 residue appears to have its maximum potential for retention of RNase activity in the presence of phosphorylation on S837, T844 and S850. The stabilisation of the a-loop in a conformation permissive of kinase activity has been suggested to be facilitated by phosphorylation and the resulting kinase activity actives the RNase domain (Lee et al., 2008; Nolen et al., 2004). Alternatively, initial oligomerisation may promote kinase activity which allows for a-loop phosphorylation and the formation of higher-order oligomers which activates the RNase domain (Korennykh et al., 2009). In both cases the activation of Ire1 appears to involve phosphorylation of the a-loop permitting a stable conformation resulting in RNase activation. Data presented in this thesis suggests that phosphorylation is dispensable due to the retention of Ire1 activity in mutants with no phospho-acceptor capability in the a-loop. This retention of Ire1 activity appears to be facilitated by D836. However, this retention is maximised by the phosphorylation of residues in the a-loop, namely S837, T844 and S850 shown in this work. This suggests a new model for the role of phosphorylation of Ire1 in its regulation of Ire1 RNase activity. Ire1 appears to not be dependent on total phosphorylation of it's a-loop, but possesses the ability to retain levels of RNase activity, utilising additional, non-phosphorylation, sites within the a-loop, namely D836. In the event of partial loss of phosphorylation one of two events may occur. Should phosphorylation be lost from a primary site (S840 or S841) then the D836 residue would mimic the a-loop conformational changes normally associated with phosphorylation and this conformation would be stabilised by phosphorylation of the secondary phosphorylation residues S837, T844 and S850. Should complete phosphorylation capability of the a-loop be lost then D836 can still provide a limited level of ER stress signal response mimicking a-loop phosphorylation but without the secondary residues being phosphorylated this response would appear to be

limited. This model would explain the phosphorylation of residues in the a-loop observed my mass spectroscopy (Lee et al., 2008), as well as the importance of the S841 residue working with S840 (Shamu and Walter, 1996). Additionally it is supported by the first experimental evidence of the role of S837 in ER stress signal transduction first theorised in the 90s (Shamu and Walter, 1996). The work presented here suggests that the conformation of the a-loop and kinase domain may be the driving factor in the regulation of RNase activity in Ire1, with phosphorylation playing, in part, a dispensable role.

10.2 Future interests

10.2.1 Characterising the role of individual phosphorylation sites within the a-loop

More data on the how much each of the phosphorylation residues impacts upon Ire1 activation would provide an improved understanding of the possible phosphorylation site hierarchy. The data presented here suggests that D836 relies on particular residues to allow for the retention of Ire1 stress signalling (S837, T844 and S850). *HAC1* mRNA and *KAR2* mRNA analysis via northern blot using single point mutants that make up the D836A-P-A mutants (D836A, S837A, S840A, S841A, T844A and S850A) would allow for the effect of phosphorylation at each of these residues to be assessed in terms of RNase activity. This would be of great interest as the S850A mutant in Y01907 strain possessing the S850A mutation shows increased survivability of ER stress and any increase in *HAC1* mRNA should become apparent in the northern blot data. To test this further, mutants possessing increasing a-loop phosphorylation sites and containing a S850A mutation in some cases and not in others could be investigated using the same methodology as presented in this thesis. This would allow an investigation into if S850 is providing a level of Ire1 activation control dependent on phosphorylation. This is of interest, as with the D836A mutants increased survivability, as it may have commercial applications such as in development of therapeutics to allow cells to survive under higher protein accumulation stress such as that seen in neurodegenerative diseases or in recombinant protein production.

10.2.2 What is the active conformation of the Ire1 phospho-acceptor mutants?

The examination of the conformational changes facilitated by both nucleotide binding to the NBP resulting from both phosphorylation of the a-loop and by D836 with lack of phosphorylation by protein crystallography would be of great interest. This would confirm if it is indeed a conformational change that is occurring or another process follows nucleotide binding promoting RNase activity of Ire1. Furthermore, this investigation of

conformational change could include an increasing number of phosphorylation site mutants to determine if there is a preferential order to phosphorylation and if this infers a tighter conformation of the RNase domain under ER stress conditions. Alongside this, mutations to the anchor points of the activation segment may allow for the role of these points and possible interactions with phosphorylation residues to be investigated.

10.2.3 Nucleotide binding by Ire1 mutants

The rates with which Ire1 a-loop mutants can bind ADP and ATP under stress conditions would also be interesting. This would provide information on how much of an impact the a-loop phosphorylation state has on nucleotide binding efficiency. Furthermore, the investigation of the rates of hydrolysis of ATP would allow a better understanding between the phosphorylation state of the a-loop and its effect on kinase activity.

11.0 References

Anken, E. van, Pincus, D., Coyle, S., Aragón, T., Osman, C., Lari, F., Puerta, S.G., Korennykh, A.V., and Walter, P. (2014). Specificity in endoplasmic reticulum-stress signaling in yeast entails a step-wise engagement of HAC1 mRNA to clusters of the stress sensor Ire1. eLife 3, e05031.

Ansari, N. and Khodagholi F. (2013) Molecular mechanism aspect of ER stress in Alzheimer's disease: current approaches and future strategies. Curr Drug Targets, 14, 114 – 122.

Anshu, A., Mannan, M.A., Chakraborty, A., Chakrabarti, S., and Dey, M. (2015). A Novel Role for Protein Kinase Kin2 in Regulating HAC1 mRNA Translocation, Splicing, and Translation. Mol. Cell. Biol. 35, 199–210.

Aragón, T., van Anken, E., Pincus, D., Serafimova, I.M., Korennykh, A.V., Rubio, C.A., and Walter, P. (2009). mRNA Targeting to ER Stress Signaling Sites. Nature 457, 736–740.

Bertolottie, A. and Ron, D. (2001) 'Alterations in an IRE1-RNA complex in the mammalian unfolded protein response', J Cell Science, 114, 3207 – 3212.

Chawla, A., Chakrabarti, S., Ghosh, G., and Niwa, M. (2011). Attenuation of yeast UPR is essential for survival and is mediated by IRE1 kinase. J. Cell Biol. 193, 41–50.

Chen, Y., and Brandizzi, F. (2013). IRE1: ER stress sensor and cell fate executor. Trends Cell Biol. 23.

Cominacini, L., Mozzini, C., Garbin, U., Pasini, A., Stranieri, C., Solaieri, E., Vallerio, P., Tinelli, I.A. and Fratta Pasini, A. (2015) 'Endoplasmic recticulum stress and Nrf2 signaling in cardiovascular diseases' Free radical biology & medicine, 88(B), 233 – 242.

Cox, J.S. and Walter, P. (1996) A Novel Mechanism for Regulating Activity of a Transcription Factor That Controls the Unfolded Protein Response, Cell, 87(3), 391 – 404.

Cox, J.S., Shamu, C.E., and Walter, P. (1993). Transcriptional induction of genes encoding endoplasmic reticulum resident proteins requires a transmembrane protein kinase. Cell 73, 1197–1206.

Credle, J.J., Finer-Moore, J.S., Papa, F.R., Stroud, R.M., and Walter, P. (2005). On the mechanism of sensing unfolded protein in the endoplasmic reticulum. Proc. Natl. Acad. Sci. U. S. A. 102, 18773–18784.

Fang, Z., Kuang, X., Zhang, Y., Shi, P. and Huang, Z. (2015) 'A novel HAC1-based dual-luciferase reporter vector for detecting endoplasmic reticulum stress and unfolded protein response in yeast Saccharomyces cerevisiae', Plasmid, 79,. 48 – 53.

Gething, M.-J., and Sambrook, J. (1992). Protein folding in the cell. Nature 355, 33–45.

Ghaemmaghami, S., Huh, W.-K., Bower, K., Howson, R.W., Belle, A., Dephoure, N., O'Shea, E.K., and Weissman, J.S. (2003). Global analysis of protein expression in yeast. Nature 425, 737–741.

Gietz, R.D., and Schiestl, R.H. (2007). High-efficiency yeast transformation using the LiAc/SS carrier DNA/PEG method. Nat. Protoc. 2, 31–34.

Hetz, C. (2012). The unfolded protein response: controlling cell fate decisions under ER stress and beyond. Nat. Rev. Mol. Cell Biol. 13, 89–102.

Hodgson, D.R.W. and Schröder, M. (2011) 'Chemical approaches towards unravelling kinase-mediated signalling pathways', Chemical Society Reviews, 40, 1211 – 1223.

Huse, M., and Kuriyan, J. (2002). The Conformational Plasticity of Protein Kinases. Cell 109, 275–282.

Jäger, R., Bertrand, M.J.M., Gorman, A.M., Vandenabeele, P., and Samali, A. (2012). The unfolded protein response at the crossroads of cellular life and death during endoplasmic reticulum stress. Biol. Cell 104, 259–270.

Johnson, L.N., Noble, M.E.M., and Owen, D.J. (1996). Active and Inactive Protein Kinases: Structural Basis for Regulation. Cell 85, 149–158.

Joshi, A., Newbatt, Y., McAndrew, P.C., Stubbs, M., Burke, R., Richards, M.W., Bhatia, C., Caldwell, J.J., McHardy, T., Collins, I. and Bayliss, R. (2015) 'Molecular mechanisms of human IRE1 activation through dimerization and ligand binding', Oncotarget, 6, 13019 – 13035.

Joshi, A., Newbatt, Y., McAndrew, P.C., Stubbs, M., Burke, R., Richards, M.W., Bhatia, C., Caldwell, J.J., McHardy, T., Collins, I. and Bayliss, R. (2015) Molecular mechanisms of human IRE1 activation through dimerization and ligand binding, Oncotarget, 6(15), 13019 – 13035.

Kimata, Y., Ishiwata-Kimata, Y., Ito, T., Hirata, A., Suzuki, T., Oikawa, D., Takeuchi, M., and Kohno, K. (2007). Two regulatory steps of ER-stress sensor Ire1 involving its cluster formation and interaction with unfolded proteins. J. Cell Biol. 179, 75–86.

Kimata, Y., Kimata, Y.I., Shimizu, Y., Abe, H., Farcasanu, I.C., Takeuchi, M., Rose, M.D., and Kohno, K. (2003). Genetic Evidence for a Role of BiP/Kar2 That Regulates Ire1 in Response to Accumulation of Unfolded Proteins. Mol. Biol. Cell 14, 2559–2569.

Knighton, D.R., Zheng, J.H., Eyck, L.T., Ashford, V.A., Xuong, N.H., Taylor, S.S., and Sowadski, J.M. (1991). Crystal structure of the catalytic subunit of cyclic adenosine monophosphate-dependent protein kinase. Science 253, 407–414.

Kohno, K., Normington, K., Sambrook, J., Gething, M.J., and Mori, K. (1993). The promoter region of the yeast KAR2 (BiP) gene contains a regulatory domain that responds to the presence of unfolded proteins in the endoplasmic reticulum. Mol. Cell. Biol. 13, 877–890.

Korennykh, A.V., Egea, P.F., Korostelev, A.A., Finer-Moore, J., Stroud, R.M., Zhang, C., Shokat, K.M., and Walter, P. (2011). Cofactor-mediated conformational control in the bifunctional kinase/RNase Ire1. BMC Biol. 9, 48.

Korennykh, A.V., Egea, P.F., Korostelev, A.A., Finer-Moore, J., Zhang, C., Shokat, K.M., Stroud, R.M., and Walter, P. (2009). The unfolded protein response signals through high-order assembly of Ire1. Nature 457, 687–693.

Laemmli, U.K. (1970). Cleavage of structural proteins during the assembly of the head of bacteriophage T4. Nature 227, 680–685.

Lee, K.P.K., Dey, M., Neculai, D., Cao, C., Dever, T.E., and Sicheri, F. (2008). Structure of the dual enzyme Ire1 reveals the basis for catalysis and regulation in non-conventional RNA splicing. Cell 132, 89–100.

Lin, J.H., Li, H., Yasumura, D., Cohen, H.R., Zhang, C., Panning, B., Shokat, K.M., Lavail, M.M., and Walter, P. (2007). IRE1 signaling affects cell fate during the unfolded protein response. Science 318, 944–949.

Liu, C.Y., Schröder, M., and Kaufman, R.J. (2000). Ligand-independent Dimerization Activates the Stress Response Kinases IRE1 and PERK in the Lumen of the Endoplasmic Reticulum. J. Biol. Chem. 275, 24881–24885.

Madhusudan, Trafny, E.A., Xuong, N.H., Adams, J.A., Ten Eyck, L.F., Taylor, S.S., and Sowadski, J.M. (1994). cAMP-dependent protein kinase: crystallographic insights into substrate recognition and phosphotransfer. Protein Sci. Publ. Protein Soc. 3, 176–187.

Mannan, M.A., Shadrick, W.R., Biener, G., Shin, B.-S., Anshu, A., Raicu, V., Frick, D.N., and Dey, M. (2013). An Ire1–Phk1 Chimera Reveals a Dispensable Role of Autokinase Activity in Endoplasmic Reticulum Stress Response. J. Mol. Biol. 425, 2083–2099.

Mathuranyanon, R., Tsukamoto, T., Takeuchi, A., Ishiwata-Kimata, Y., Tsuchiya, Y., Kohno, K., and Kimata, Y. (2015). Tight regulation of the unfolded protein sensor Ire1 by its intramolecularly antagonizing subdomain. J. Cell Sci. 128, 1762–1772.

Merksamer, P.I., and Papa, F.R. (2010). The UPR and cell fate at a glance. J. Cell Sci. 123, 1003–1006.

Miller, J. 1972. Experiments in Molecular Genetics, p. 352-355. Cold Spring Harbor Laboratory, NY

Montenegro-Montero, A., Goity, A., and Larrondo, L.F. (2015). The bZIP Transcription Factor HAC-1 Is Involved in the Unfolded Protein Response and Is Necessary for Growth on Cellulose in Neurospora crassa. PLoS ONE 10.

Mori, K. (2000) Tripartite Management of Unfolded Proteins in the Endoplasmic Reticulum, Cell, 101, 451 – 454.

Mori, K., Kawahara, T., Yoshida, H., Yanagi, H., and Yura, T. (1996). Signalling from endoplasmic reticulum to nucleus: transcription factor with a basic-leucine zipper motif is required for the unfolded protein-response pathway. Genes Cells 1, 803–817.

Mori, K., Sant, A., Kohno, K., Normington, K., Gething, M.J., and Sambrook, J.F. (1992). A 22 bp cis-acting element is necessary and sufficient for the induction of the yeast KAR2 (BiP) gene by unfolded proteins. EMBO J. 11, 2583–2593.

Morl, K., Ma, W., Gething, M.-J., and Sambrook, J. (1993). A transmembrane protein with a cdc2+CDC28-related kinase activity is required for signaling from the ER to the nucleus. Cell 74, 743–756.

Nishitoh, H., Matsuzawa, A., Tobiume, K., Saegusa, K., Takeda, K., Inoue, K., Hori, S., Kakizuka, A. and Ichijo, H. (2002). ASK1 is essential for endoplasmic reticulum stress-induced neuronal cell death triggered by expanded polyglutamine repeats. Genes Dev 16, 1345-1355.

Nolen, B., Taylor, S., and Ghosh, G. (2004). Regulation of Protein Kinases. Mol. Cell 15, 661–675.

Özcan, U., Cao, Q., Yilmaz, E., Lee, A-H., Iwakoshi, N.N., Ozdelen, E., Tuncman, G., Görgün, C., Glimcher, L.H. and Hotamisligil, G.S. (2004). Endoplasmic reticulum stress links obesity, insulin action, and type 2 diabetes. Science 306, 457-461.

Papa, F.R., Zhang, C., Shokat, K., and Walter, P. (2003). Bypassing a Kinase Activity with an ATP-Competitive Drug. Science 302, 1533–1537.

Pike, A.C.W., Rellos, P., Niesen, F.H., Turnbull, A., Oliver, A.W., Parker, S.A., Turk, B.E., Pearl, L.H., and Knapp, S. (2008). Activation segment dimerization: a

mechanism for kinase autophosphorylation of non-consensus sites. EMBO J. 27, 704–714.

Pincus, D., Chevalier, M.W., Aragón, T., van Anken, E., Vidal, S.E., El-Samad, H., and Walter, P. (2010). BiP Binding to the ER-Stress Sensor Ire1 Tunes the Homeostatic Behavior of the Unfolded Protein Response. PLoS Biol. 8.

Pirruccello, M., Sondermann, H., Pelton, J.G., Pellicena, P., Hoelz, A., Chernoff, J., Wemmer, D.E., and Kuriyan, J. (2006). A Dimeric Kinase Assembly Underlying Autophosphorylation in the p21 Activated Kinases. J. Mol. Biol. 361, 312–326.

Prinz, W.A., Grzyb, L., Veenhuis, M., Kahana, J.A., Silver, P.A., and Rapoport, T.A. (2000). Mutants Affecting the Structure of the Cortical Endoplasmic Reticulum in Saccharomyces cerevisiae. J. Cell Biol. 150, 461–474.

Prischi, F., Nowak, P.R., Carrara, M., and Ali, M.M.U. (2014). Phosphoregulation of Ire1 RNase splicing activity. Nat. Commun. 5.

Rubio, C., Pincus, D., Korennykh, A., Schuck, S., El-Samad, H., and Walter, P. (2011). Homeostatic adaptation to endoplasmic reticulum stress depends on Ire1 kinase activity. J. Cell Biol. 193, 171–184.

Rüegsegger, U., Leber, J.H., and Walter, P. (2001). Block of HAC1 mRNA Translation by Long-Range Base Pairing Is Released by Cytoplasmic Splicing upon Induction of the Unfolded Protein Response. Cell 107, 103–114.

Sathe, L., Bolinger, C., Mannan, M.A., Dever, T.E., and Dey, M. (2015). Evidence That Base-pairing Interaction between Intron and mRNA Leader Sequences Inhibits Initiation of HAC1 mRNA Translation in Yeast. J. Biol. Chem. 290, 21821–21832.

Schenborn, E. and Goiffon, V. (1993) Promega Notes 41, 11–3

Schneppenheim, R., Budde, U., Dahlmann, N., and Rautenberg, P. (1991). Luminography – a new, highly sensitive visualization method for electrophoresis. ELECTROPHORESIS 12, 367–372.

Schröder, M., Chang, J.S. and Kaufman, R.J. (2000) The unfolded protein response represses nitrogen-starvation induced developmental differentiation in yeast, Genes and Development, 14, 2962 – 75.

Schröder, M., Chang, J.S., and Kaufman, R.J. (2000). The unfolded protein response represses nitrogen-starvation induced developmental differentiation in yeast. Genes Dev. 14, 2962–2975.

Schröder, M., Clark, R., and Kaufman, R.J. (2003). IRE1- and HAC1-independent transcriptional regulation in the unfolded protein response of yeast. Mol. Microbiol. 49, 591–606.

Schröder, M., Clark, R., Liu, C.Y. and Kaufman, R.J. (2004) The unfolded protein response represses differentiation through the RPD3-SIN3 histone deacetylase. EMBO, 23, 2281 – 22 92.

Shamu, C.E., and Walter, P. (1996). Oligomerization and phosphorylation of the Ire1p kinase during intracellular signaling from the endoplasmic reticulum to the nucleus. EMBO J. 15, 3028–3039.

Shore, G.C., Papa, F.R., and Oakes, S.A. (2011). Signaling Cell Death from the Endoplasmic Reticulum Stress Response. Curr. Opin. Cell Biol. 23, 143–149.

Sidhu, A., Miller, J.R., Tripathi, A., Garshott, D.M., Brownell, A.L., Chiego, D.J., Arevang, C., Zeng, Q., Jackson, L.C., Bechler, S.A., Callaghan, M.U., Yoo, G.H., Sethi, S., Lin, H.S., Callaghan, J.H., Tamayo-Castillo, G., Sherman, D.H., Kaufman, R.J. and Fribley, A.M. (2015) Borrelidin Induces the Unfolded Protein Response in Oral Cancer Cells and Chop-Dependent Apoptosis. J. Am. Che. Soc. 6, 1122 – 1127.

Sidrauski, C., and Walter, P. (1997). The Transmembrane Kinase Ire1p Is a Site-Specific Endonuclease That Initiates mRNA Splicing in the Unfolded Protein Response. Cell 90, 1031–1039.

Smith, M.H., Ploegh, H.L., and Weissman, J.S. (2011). Road to Ruin: Targeting Proteins for Degradation in the Endoplasmic Reticulum. Science 334.

Smith, P.K., Krohn, R.I., Hermanson, G.T., Mallia, A.K., Gartner, F.H., Provenzano, M.D., Fujimoto, E.K., Goeke, N.M., Olson, B.J., and Klenk, D.C. (1985). Measurement of protein using bicinchoninic acid. Anal. Biochem. 150, 76–85.

Snapp, E.L. (2012). Unfolded Protein Responses with or Without Unfolded Proteins? Cells 1, 926–950.

Stevens, F.J., and Argon, Y. (1999). Protein folding in the ER. Semin. Cell Dev. Biol. 10, 443–454.

Tanaka, M., Shintani, T., and Gomi, K. (2015). Unfolded protein response is required for Aspergillus oryzae growth under conditions inducing secretory hydrolytic enzyme production. Fungal Genet. Biol. 85, 1–6.

Towbin, H., Staehelin, T., and Gordon, J. (1979). Electrophoretic transfer of proteins from polyacrylamide gels to nitrocellulose sheets: procedure and some applications. Proc. Natl. Acad. Sci. U. S. A. 76, 4350–4354.

Travers, K.J., Patil, C.K., Wodicka, L., Lockhart, D.J., Weissman, J.S., and Walter, P. (2000). Functional and Genomic Analyses Reveal an Essential Coordination between the Unfolded Protein Response and ER-Associated Degradation. Cell 101, 249–258.

Voeltz, G.K., Prinz, W.A., Shibata, Y., Rist, J.M., and Rapoport, T.A. (2006). A Class of Membrane Proteins Shaping the Tubular Endoplasmic Reticulum. Cell 124, 573–586.

Walter, P., and Ron, D. (2011). The unfolded protein response: from stress pathway to homeostatic regulation. Science 334, 1081–1086.

Welihinda, A.A., and Kaufman, R.J. (1996). The Unfolded Protein Response Pathway in Saccharomyces cerevisiae oligomerization and trans-phosphorylation of Ire1p (Ern1p) are required for kinase activation. J. Biol. Chem. 271, 18181–18187.

Winzeler, E.A., Richards, D.R., Conway, A.R., Goldstein, A.L., Kalman, S., McCullough, M.J., McCusker, J.H., Stevens, D.A., Wodicka, L., Lockhart, D.J., et al. (1998). Direct allelic variation scanning of the yeast genome. Science 281, 1194–1197.

Wiseman, R.L., Zhang, Y., Lee, K.P.K., Harding, H.P., Haynes, C.M., Price, J., Sicheri, F., and Ron, D. (2010). Flavonol activation defines an unanticipated ligand binding site in the kinase-RNase domain of IRE1. Mol. Cell 38, 291–304.

Xie, X., Gu, Y., Fox, T., Coll, J.T., Fleming, M.A., Markland, W., Caron, P.R., Wilson, K.P., and Su, M.S.-S. (1998). Crystal structure of JNK3: a kinase implicated in neuronal apoptosis. Structure 6, 983–991.

Yang, J., Cron, P., Thompson, V., Good, V.M., Hess, D., Hemmings, B.A., and Barford, D. (2002). Molecular Mechanism for the Regulation of Protein Kinase B/Akt by Hydrophobic Motif Phosphorylation. Mol. Cell 9, 1227–1240.

Zhang, L., Zhang, C., and Wang, A. (2016). Divergence and Conservation of the Major UPR Branch IRE1-bZIP Signaling Pathway across Eukaryotes. Sci. Rep. 6.

Zhou, J., Liu, C.Y., Back, S.H., Clark, R.L., Peisach, D., Xu, Z., and Kaufman, R.J. (2006). The crystal structure of human IRE1 luminal domain reveals a conserved dimerization interface required for activation of the unfolded protein response. Proc. Natl. Acad. Sci. U. S. A. 103, 14343–14348.